AMRL-TR-68-130




# DEVELOPMENT OF A LABORATORY MODEL GAS ANALYZER USING EMISSION TECHNIQUES

*E. L. GROVE*

*IIT Research Institute*

APRIL 1969



AEROSPACE MEDICAL RESEARCH LABORATORY
AEROSPACE MEDICAL DIVISION
AIR FORCE SYSTEMS COMMAND
WRIGHT-PATTERSON AIR FORCE BASE, OHIO

## NOTICES

When US Government drawings, specifications, or other data are used for any purpose other than a definitely related Government procurement operation, the Government thereby incurs no responsibility nor any obligation whatsoever, and the fact that the Government may have formulated, furnished, or in any way supplied the said drawings, specifications, or other data, is not to be regarded by implication or otherwise, as in any manner licensing the holder or any other person or corporation, or conveying any rights or permission to manufacture, use, or sell any patented invention that may in any way be related thereto.

Federal Government agencies and their contractors registered with Defense Documentation Center (DDC) should direct requests for copies of this report to:

DDC
Cameron Station
Alexandria, Virginia 22314

Non-DDC users may purchase copies of this report from:

Chief, Storage and Dissemination Section
Clearinghouse for Federal Scientific & Technical Information (CFSTI)
Sills Building
5285 Port Royal Road
Springfield, Virginia 22151

Organizations and individuals receiving reports via the Aerospace Medical Research Laboratories' automatic mailing lists should submit the addressograph plate stamp on the report envelope or refer to the code number when corresponding about change of address or cancellation.

Do not return this copy. Retain or destroy.

600 - July 1969 - CO455 - 84-1878

AMRL-TR-68-130

# DEVELOPMENT OF A LABORATORY MODEL GAS ANALYZER USING EMISSION TECHNIQUES

*E. L. GROVE*

*IIT Research Institute*

## FOREWORD

The research described was conducted by IIT Research Institute, 10 W. 35th St., Chicago, Illinois 60616, under Contract No. AF 33(615)-3271 and in support of Project 6373, "Equipment for Life Support in Aerospace," and Task 637302, "Respiratory Support Equipment." The work was performed during the period of 1 November 1965 to 25 August 1967. Mr. Ints Kaleps, Biotechnology Branch, Life Support Division, Biomedical Laboratory, Aerospace Medical Research Laboratories, was contract monitor. IITRI has assigned this work Project No. U-6033.

Personnel who contributed to the project were W. A. Loseke and Dr. E. L. Grove.

This technical report has been reviewed and is approved.

## ABSTRACT

An instrument using emission spectroscopic techniques was designed and developed for monitoring the major components in air-type atmospheres. The essential components consist of a hollow cathode excitation source, four interference filters mounted in a filter wheel rotating at 300 rpm, a single photomultiplier tube and an electronic circuit, controlled by switching diodes to trigger the gating circuit, which continuously records the response for each gas on individual meters. Hollow cathode excitation was selected because of the spectral intensities of the higher energy species associated with the negative and cathode glows, the lack of lower energy species associated with the positive column discharge and relatively low power requirements. Aluminum cathodes rapidly lost sensitivity and did not excite the 2883 Å and the 2896 Å $CO_2^+$ bands. Gold, which does not form an oxide, was satisfactory, so gold foil linings were used for both the cathode and anode. The region from about 2900 to 6000 Å was very dense with nitrogen and related band spectra which did not permit the selection of any wavelength without interference. The region toward the red was much more free of bands. Since the 6562.8 Å line is the only one suitable for hydrogen, the others selected in this region were the oxygen, 8446.4 Å, nitrogen, 8216.5 Å and carbon for carbon dioxide, 9094.9 Å lines. The influence of power, pressure and other gases were studied. Satisfactory responses were obtained in the 2-watt range. Wide concentrations of gases, such as oxygen and nitrogen, have little influence on each other. However, gases with wide differences in excitation potentials do have an influence on the excitation of each other. The excitation of helium, in the presence of oxygen, is somewhat suppressed at its lower concentrations. This effect is much less than for thermal modes of excitation. In helium, the line intensities for oxygen and hydrogen increased as the concentration of these gases decreased. At the same time the line intensities increased for helium as its concentration increased. Other gases were studied.

TABLE OF CONTENTS

TABLE OF CONTENTS (cont.)

LIST OF FIGURES

LIST OF FIGURES (cont.)

LIST OF FIGURES (cont.)

LIST OF FIGURES (cont.)

LIST OF FIGURES (cont.)

LIST OF TABLES

# DEVELOPMENT OF A LABORATORY MODEL GAS ANALYZER UTILIZING EMISSION TECHNIQUES

## SECTION I

## INTRODUCTION

The overall objective of the program was to study the emission spectra of air, then design, fabricate and evaluate an analyzer based on emission spectra to monitor the major components in a cabin atmosphere.

More specifically, the objectives are as follows:

- Evaluate flow discharge type sources as a means of monitoring oxygen, nitrogen, hydrogen and carbon dioxide by emission spectrometry.
- Evaluate the selected excitation source with respect to character of line and band spectra, emission requirements, and physical size. Select the best emission lines or bands with respect to sensitivity and freedom from spectral interference for monitoring the major atmospheric gases.
- Design, fabricate and evaluate an emission type laboratory model to monitor these gases.

## SECTION II

## EXPERIMENTAL STUDIES OF SPECTRAL PARAMETERS

### EXPERIMENTAL EQUIPMENT

The design of the gas analyzer utilizing emission techniques began with the study of the nature of the spectra from the hollow cathode excitation of air and the mixture of gases simulating the major cabin atmosphere components. The nature of the spectra, their isolation, as well as the influence of changing design and operating parameters on the spectra was studied with light diffraction instruments (the spectrograph and spectrometer) and with selected interference filters.

#### Spectrometers

During the initial phase of the program, a Jarrell-Ash 3.4-meter Ebert mount spectrograph, Model JA-7102, was used. This instrument's diffraction unit is a 15,000 line per inch plane grating blazed for 4000 Å in the first order. Reciprocal dispersion for the instrument is 5.2 Å/mm. The Jarrell-Ash comparator-microphotometer, Model 2100, was used for line intensity measurements on the photographic plates. This instrument has high resolution but is relatively slow. It was used chiefly to study the emission lines and bands associated with the gas mixtures, nitrogen, oxygen, hydrogen and carbon dioxide, for spectral and background interferences and to tentatively select the particular lines and bands that were suitable for monitoring. The photographic emulsions used were the I-N, 6500-8800 Å, I-F, 4500-6800 Å, and the 103-O, 2100-5000 Å. Some special sensitized M plates were used to study the carbon lines in the 9094-Å region.

Because the above 3.4-meter spectrograph is optically quite slow, it was used for only the initial work. Additional studies were performed with a Jarrell-Ash 1-meter Czerny-Turner Model 78-466 scanning monochromator and a Spex 3/4-meter Czerny-Turner Model 1800 spectrograph.

The 1-meter Czerny-Turner instrument is equipped for two plane gratings with kinematic interchanger. Both gratings have 30,000 lines per inch, blazed in the first order, one with maximum reflection at 3000 Å and the other at 7500 Å. The reciprocal dispersion is 8.1 Å/mm and the effective aperture is f/8.7. This instrument is also equipped so that 4 x 4 inch photographic plates may be used.

The 3/4-meter Czerny-Turner instrument was designed for use as a small spectrograph or spectrometer. The grating is a 30,000 line per inch unit blazed in the first order with the energy maximum at 5000 Å. This instrument has a reciprocal dispersion of 10 Å/mm and an optical speed of f/6.3. A removable photomultiplier tube holder was designed for mounting in the plate holder so this instrument was also used as a single channel scanning instrument. The interference filters were evaluated with this instrument.

## Readout Equipment

The S-20 and S-1 response EMI and RCA photomultiplier tubes were used. For the earlier work d-c amplification was used, but throughout the major portion of the program amplification was a-c, i.e., pulsed d-c, achieved by chopping the input light signal. Readout was by means of Hewlett-Packard Model 400 HR vacuum tube voltmeters and Model 425 AR microvoltammeters. The Hewlett-Packard Model 132A dual-beam oscilloscope was used to monitor signal quality.

## Interference Filter Photometers

Following the initial study of the line and band spectra with the spectrometer, an interference filter photometer readout device was designed and built.

The schematic layout for the initial interference filter photometer, fig. 1, used d-c amplification of the signal from the photomultiplier tube. The chamber was designed to fit the filter holders from an old Fisher filter photometer. Each filter was mounted in a separate

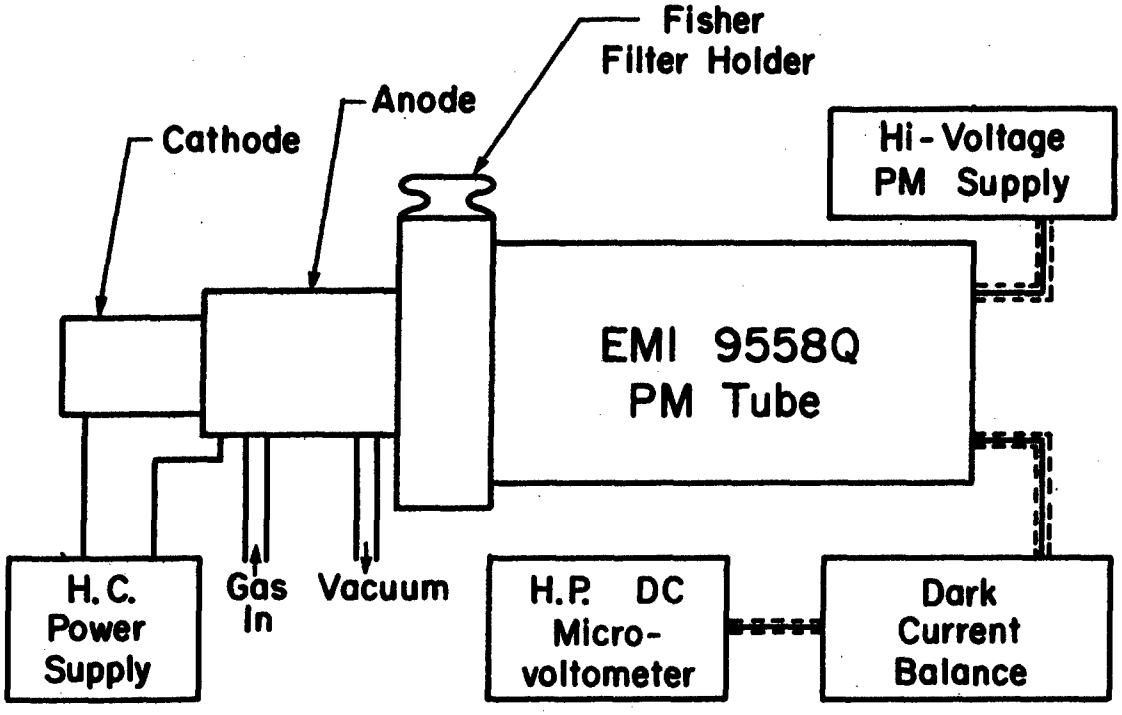


Figure 1. DIRECT READING HOLLOW CATHODE DEVICE

filter holder which allowed an easy, rapid exchange of wavelength.

This initial photometer was modified for pulsed d-c (a-c) amplification that included a chopper and a dark slide. An exploded view is shown in fig. 2. The dark slide makes possible more rapid filter change because it protects the photomultiplier tube that does not have to be shut off each time a filter is changed. The hollow cathode sources could also be changed quickly in this unit. Figure 3 shows an instrumental layout when a source was being evaluated on the relatively long runs.

In these extended stability runs the cathode emission was passed through a 300-rpm synchronous-driven, four-blade chopper wheel, thence through the 2-in. 7771 oxygen interference filter, and a 40% T neutral density filter to impinge on the face of the PM tube. This tube is a 14-stage, S-20 response RCA 7265. Output signal is hooked in parallel with a 1-meg resistor, a 390 K resistor, a Tetronics Type 503 oscilloscope, and a Tetronics Type 122 Low Level Preamplifier. A Tetronics Type 125 Power Supply supplied the Type 122 Preamplifier. Output signal of the preamplifier was rectified by a diode rectifier circuit and fed to an Esterline Angus Model AW galvanometer type recorder. Calibration was possible by removing the PM lead and connecting a Hewlett-Packard Model 200 AB Audio Oscillator. The PM tube was supplied by the Kepco Regulated d-c Supply used in most previous electronic readout work.

The cathode unit was driven by a voltage regulated power supply. Cathode voltage was obtained from a Rustrak 100 $\mu$A d-c recorder in series with a 5.1 meq resistor hooked across the anode and cathode. Cathode current measurements were made by amplifying the voltage drop across a 50-ohm resistor in the cathode lead with a Rustrak Amplifier and displaying on a 1 ma d-c Rustrak recorder.

Figure 4 illustrates a later model, the prototype, under test. In this model, the chopper wheel has been replaced by a four-channel filter wheel. Supplemental readout and response was followed with the oscilloscope. In this model the dark slide was replaced with a combination dark slide and angle mirror so that when it was in

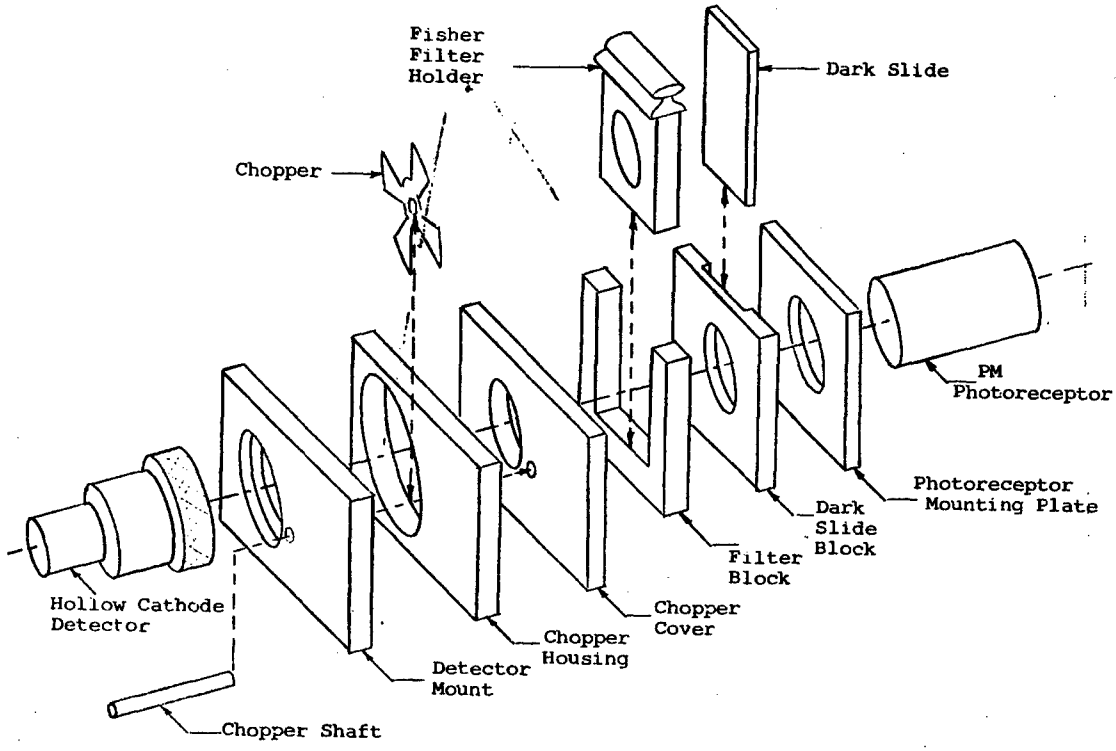


Figure 2. IMPROVED DIRECT READING HOLLOW CATHODE DEVICE

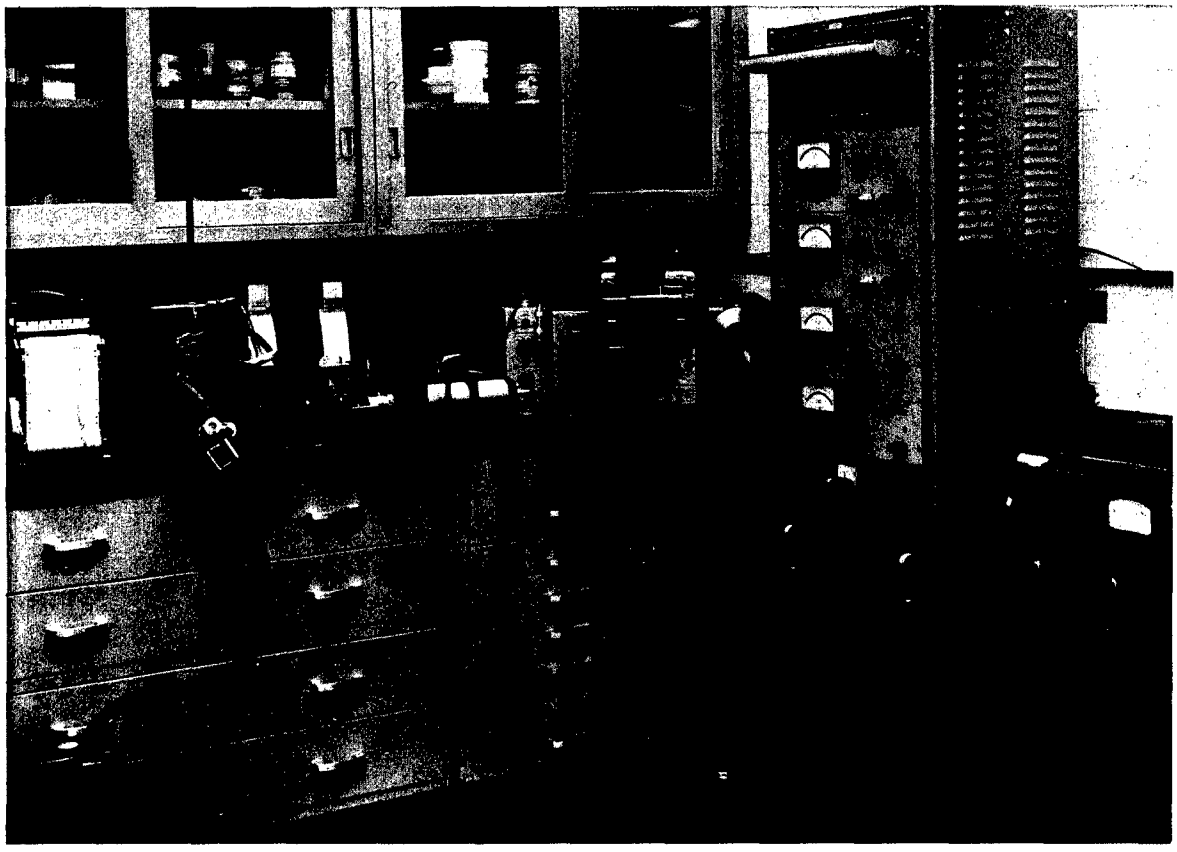

Figure 3. EXPERIMENTAL LAYOUT FOR HOLLOW CATHODE WITH READOUT SYSTEM FOR CHOPPED SIGNAL

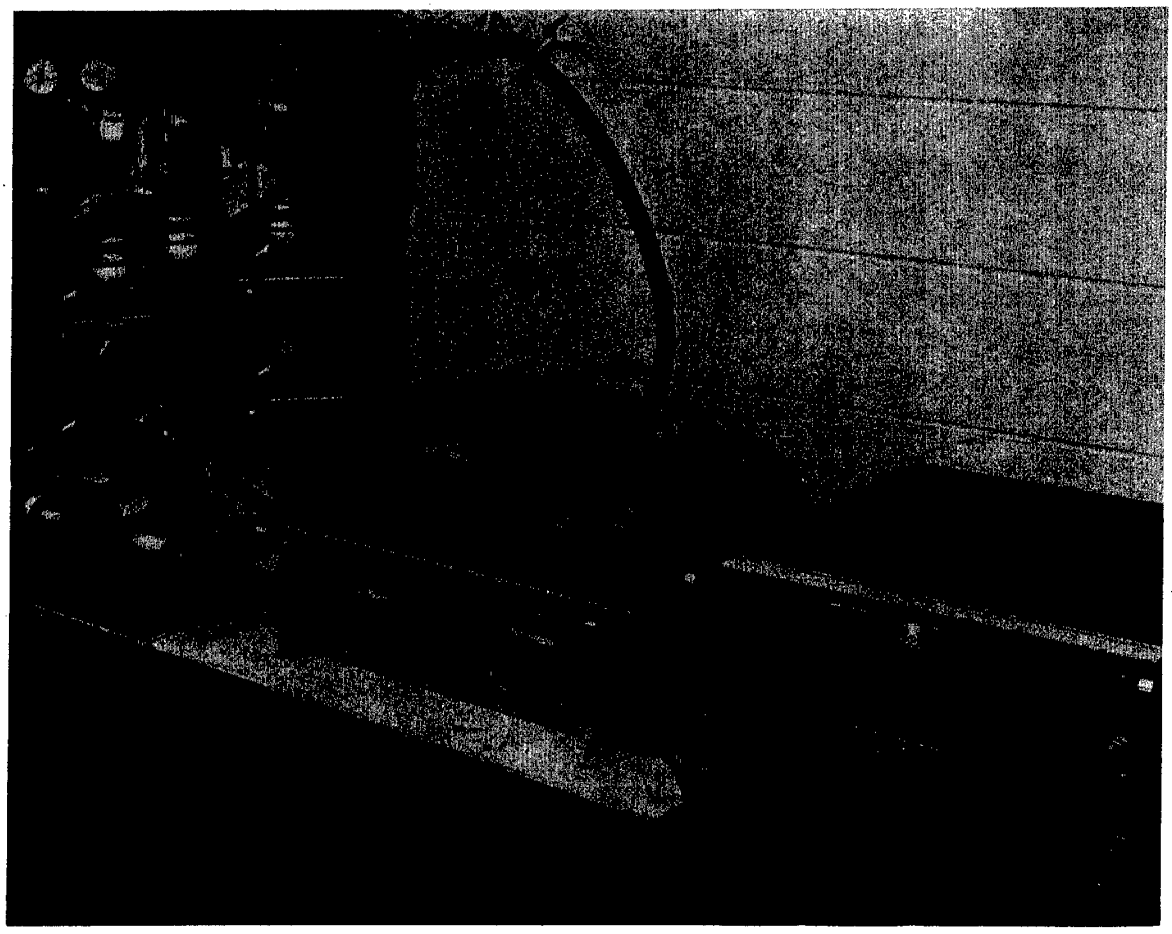

**Figure 4. INSTRUMENTATION FOR MECHANICAL COMPONENTS CHECKOUT**

the down position, the inside of the source could be observed during operation. Figure 4 illustrates the slide in the up or monitoring position. The chassis rack carrying the vacuum tube voltmeters is to the right of the picture. The power supply is a Harrison Model 6521 Å voltage regulated-current regulated unit.

## Standard Gases

The simulated atmosphere, fixed specific mixtures of oxygen, hydrogen, carbon dioxide and nitrogen, were used throughout much of the program. Four selected concentrations in Matheson size C bottles were purchased, fig. 4, for spectral response and calibration studies. These initial concentrations are given in table I. The oxygen, nitrogen and other gases were high grade, comparable to "zero" grade gas.

Table I

PERCENT COMPOSITION OF GAS MIXTURES

| Tank | % Oxygen | % Nitrogen | % Hydrogen | % $CO_2$ |
|---|---|---|---|---|
| 1 | 7 | 87 | 3.5 | 1 |
| 2 | 15 | 88.5 | 3 | 2 |
| 3 | 30 | 65 | 2 | 3 |
| 4 | 50 | 44 | 1 | 5 |
| | 100 | 0 | 0 | 0 |
| | | 100 | 0 | 0 |

## Gas Metering System

To obtain a more versatile range of concentrations, binary, ternary and quaternary mixtures, as well as other gases such as helium were used. This required a gas metering device. The schematic layout is illustrated in fig. 5 for one that we designed and fabricated. The stainless capillary tubing with good pressure gauges ($\pm$ 1/4% F.S. accuracy) and needle valve controls provided a good

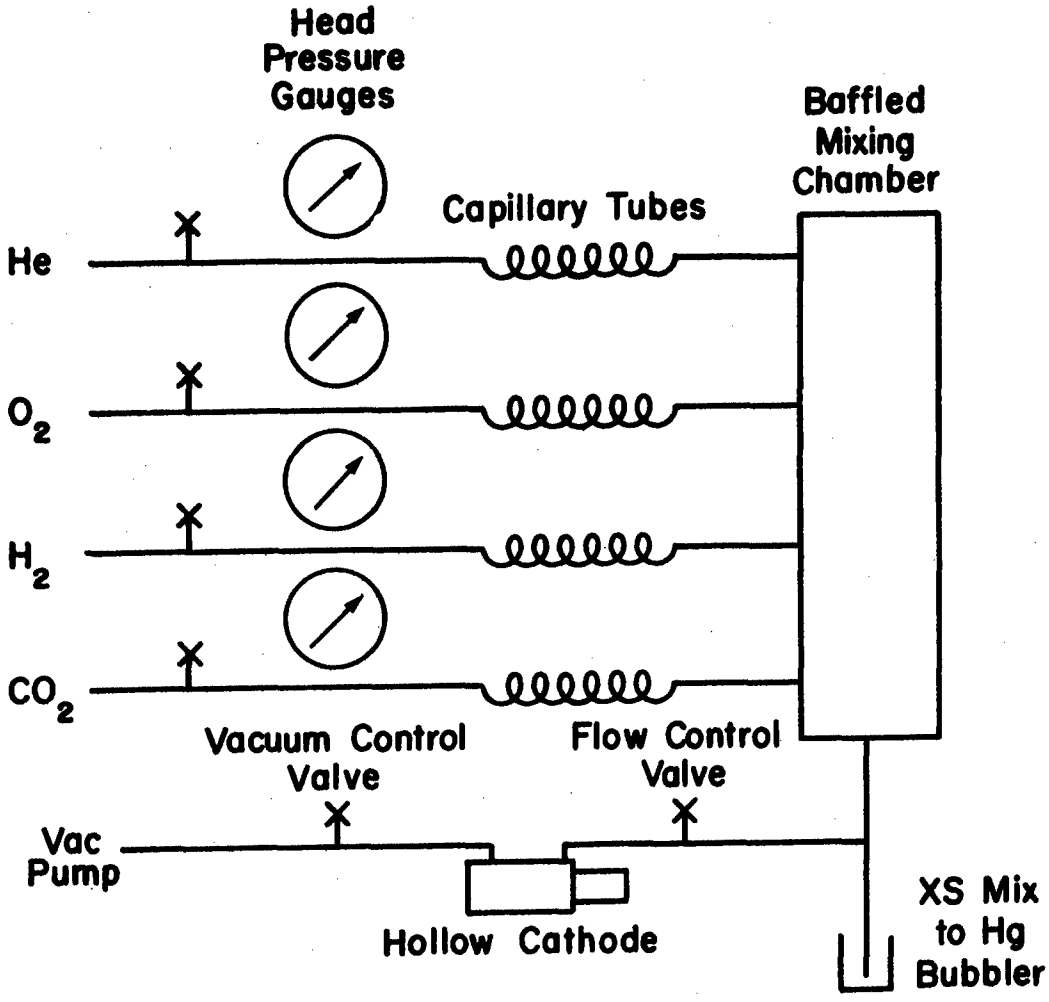


Figure 5. GAS MIXING SYSTEM

means of metering small flows of gases. The total flow is dependent on the gas, the pressure and the diameter and length of the capillary. For example, the hydrogen flow through a specific coil at a given pressure will be much greater than that of carbon dioxide, since flow rates are primarily a function of gas viscosity rather than atomic weight. Each channel must be calibrated. An example of a calibration curve is shown in fig. 6. The gas mixing chamber, fig. 7, was designed so that the greatest gas flows, in this case $N_2$ and $O_2$ entered first and carried the lower concentration along with its flow. This initial mixer, 2 in. x 1 ft, was found to be too large and at low flow rates; the gas took too long to cover the 3-ft mixing distance. It was replaced by a much smaller single tube that was found to be satisfactory.

## INITIAL STUDY OF SPECTRA

Very little work has been reported in the literature concerning the spectra from the discharge excitation of air. Most of the work pertains to pure elements or compounds. For this reason the initial work was carried out with a 3.4-meter Ebert mount spectrograph with good reciprocal dispersion and resolution in order to study the line and band spectra. An aluminum hollow cathode was used during these studies.

Based on the spectra recorded and its discussion in standard references for band structure, such as Herzberg (ref. 1), "Spectra of Diatomic Molecules" and Pearse and Gaydon (ref. 2), "The Identification of Molecular Spectra," a tentative group of band spectra was selected and their relative position shown on a focal curve for a proposed multichannel spectrometer. Based on past experience (ref. 3-5), the 6562.8-Å line is the only good choice for hydrogen, and the only good oxygen lines in this region are the 7771.9 Å oxygen triplet. All recorded bandheads in the near vicinity of these lines degradated from R → V, that is away from these lines so the tail of the band would not build up and become a spectral interference or were sufficiently far away and weak so there was no spectral interference. Emission spectra at other wavelengths for the nitrogen and carbon dioxide that appeared to be free of interferences were $N_2$, 6544.8 Å, R → V; CO,

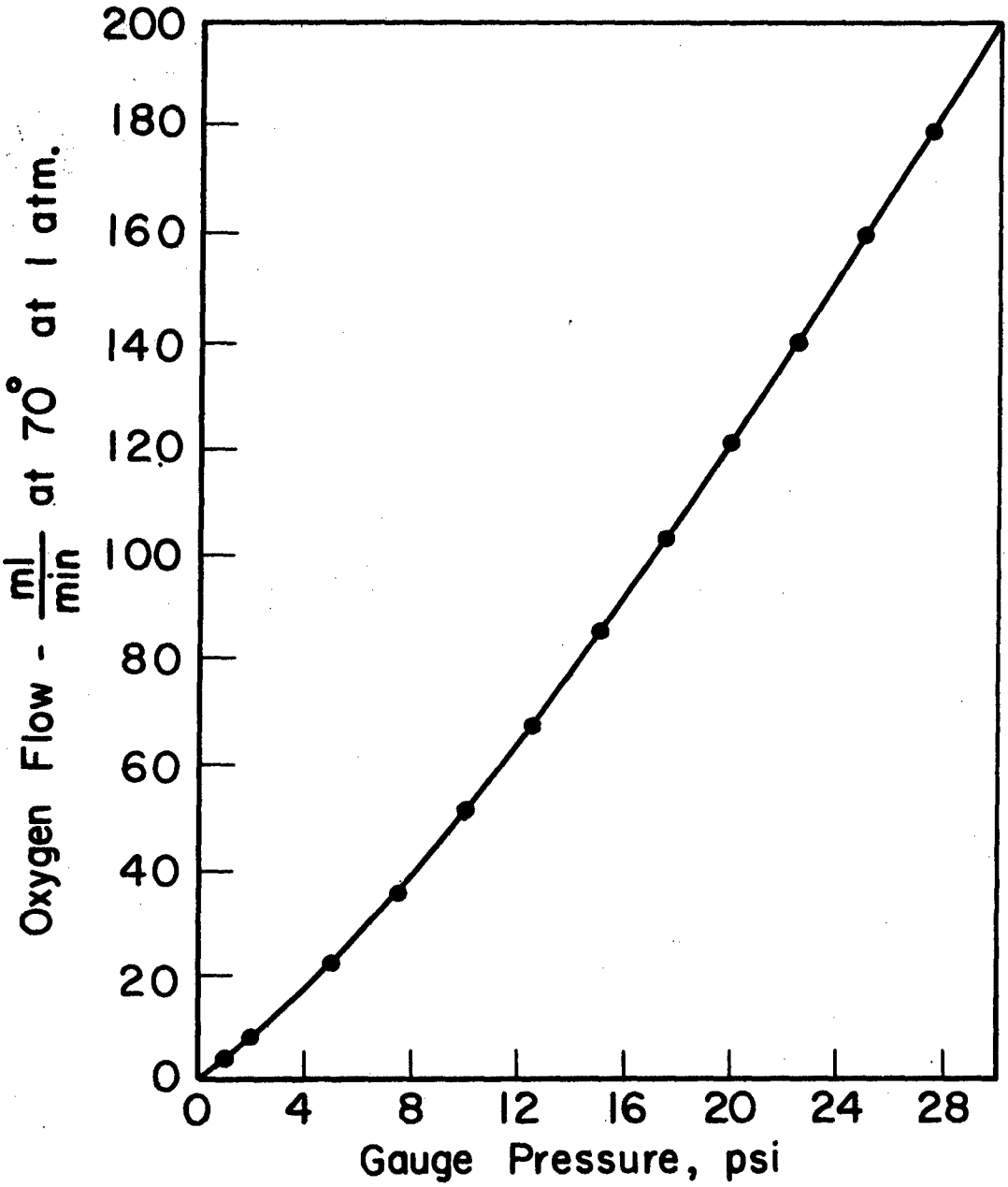


Figure 6. CALIBRATION CURVE FOR OXYGEN

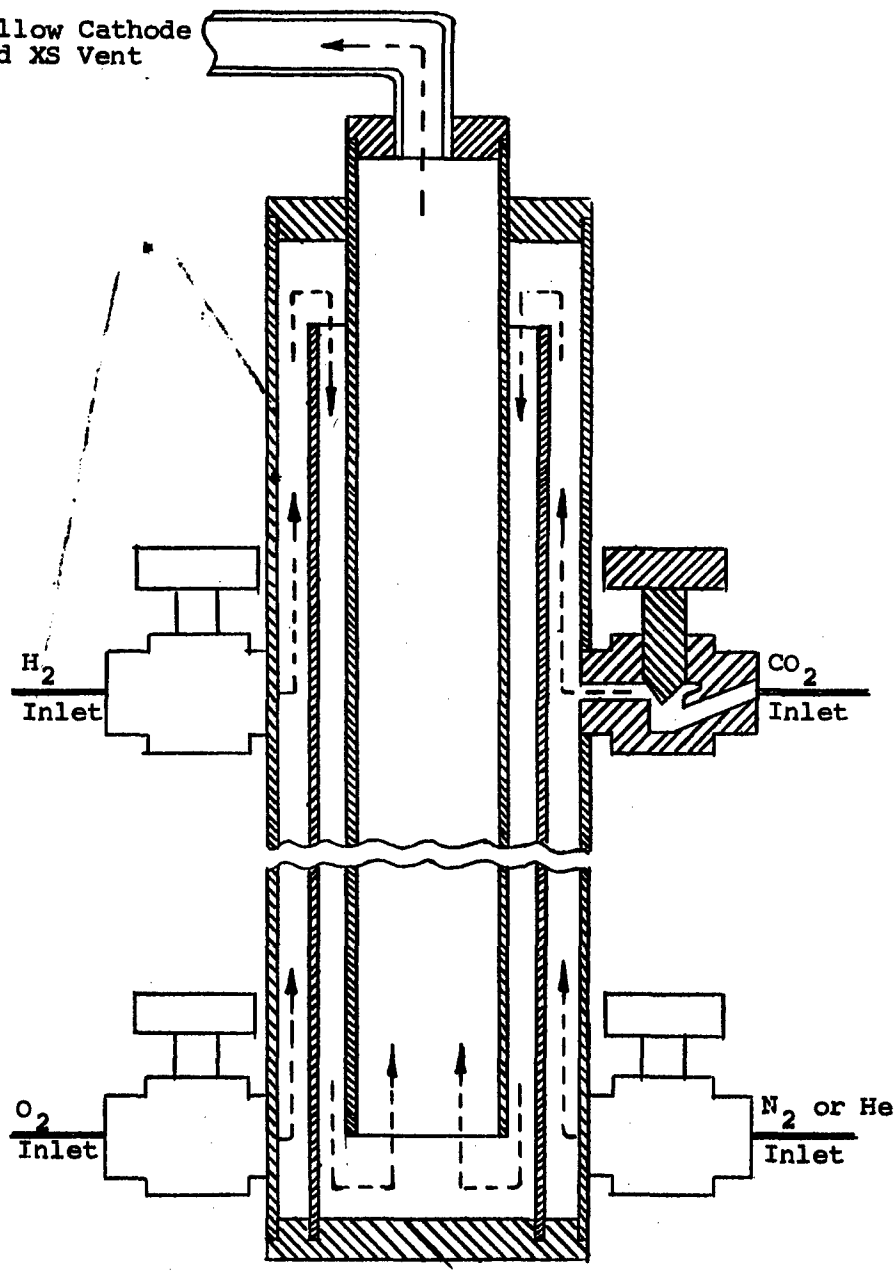


Figure 7. SECTION VIEW, MIXING CHAMBER
OF GAS MIXING DEVICE

5198.2 Å, R → V; $N_2$, 4151.4 Å, R → V; and the strong line for N at 4109.9 Å. In addition there are the two strong and persistent bands for $CO_2^+$ at 2883 and 2896 Å reasonably close to the relatively strong 2478.6 Å carbon line. On the basis of design planning, these wavelengths are quite far from the only available hydrogen and oxygen lines.

The purpose of the initial study was to evaluate the air emission spectra to see if the deductions based on the literature were valid.

The separate gases in an inert atmosphere were briefly studied using an aluminum hollow cathode with the 3.4-meter spectrograph to see if band structures for each gas appeared. For oxygen and hydrogen, the hydrogen 6562.8-Å line and the oxygen 7771.9-Å triplet and 8446-Å singlet were quite intense. No specific diatomic bands were observed. The spectra for carbon dioxide did not show the expected 2883-Å and 2896-Å bands that are reported in the literature. The 2478.6-Å carbon line from carbon dioxide was quite strong and it was also detected in air. In the longer wavelength the oxygen 7771.9-Å triplet and 8446.4-Å singlet showed strongly. The weak carbon 8335.2-Å line was faintly visible and was considered too weak to monitor $CO_2$. Contrary to expectation, the supposedly strong bands for $CO_2$ and CO in the 3900- to 6200-Å region were too weak and poorly defined for quantitative monitoring.

The emission spectra for air was very complex and dense in the 2900- to 6000-Å region. From a cursory examination these bands appeared to belong chiefly to the CN, $N_2$ and $N_2^+$ band systems, however, since the region was entirely too complex to monitor any specific line or bandhead without appreciable spectral interference, no attempt was made to identify the bandheads. The 2300- to 2800-Å region had relatively simple spectra and the 6200- to 8800-Å region was quite clear of any background and band spectra.

A group of moderately strong atomic carbon lines exist at 9094.9 Å and nearby wavelengths. These lines came out reasonably strong using the hypersensitized 1-M emulsion. The type 1-M emulsion is only about 1/10 as

sensitive as the 1-N so this line appears to be a good line for monitoring, since it is also in the wavelength range of reasonably good sensitivity for the S-1 phosphor.

Based on the above work the wavelengths selected for further study were as follows: oxygen, 8446.4 Å and the 7771.9-Å triplet; hydrogen 6562.7 Å; nitrogen 8216.5 Å and the carbon 9094.9 Å. None of the intense and well defined bands of the four gases were sufficiently free from spectral interference for quantitative measurements. The $N_2$ and $N_2^+$ band systems are complex, then the addition of the complex NO system results in a very complex system with many overlapping band spectra. The spectral bands that were initially selected were heavily masked. Since the two supposedly strong $CO_2^+$ bands at 2883 Å and 2896 Å did not develop and since all the other possible choices, until at about 6000 Å, appeared to be plagued with spectral interferences, the sensitive atomic lines 6000- to 9000-Å region held the most promise for quantitative monitoring of the several components.

## BASIC INSTRUMENT DESIGN

There are two approaches for the instrument design. One is the use of a diffraction element, i.e., a prism or grating and the other is the use of interference filters. Since the atomic lines listed above can all be monitored with the same S-1 response phosphor, it was agreed to use the single photomultiplier with electronic switching and the interference filters approach.

## SPECTRAL RESPONSE STUDIES

### Spectrograph and 50Å Half-Power Bandwidth Filters

The spectral response for oxygen, 7771.9 Å, hydrogen 6562 Å, and nitrogen 7468.8 Å lines using the four prepared gases and aluminum hollow cathode excitation with the 3.4-meter spectrograph were quite encouraging, fig. 8, 9, and 10. These calibration curves are quite linear and are based on direct densitometer readings from the photographic plates and not ratios based on an internal standard.

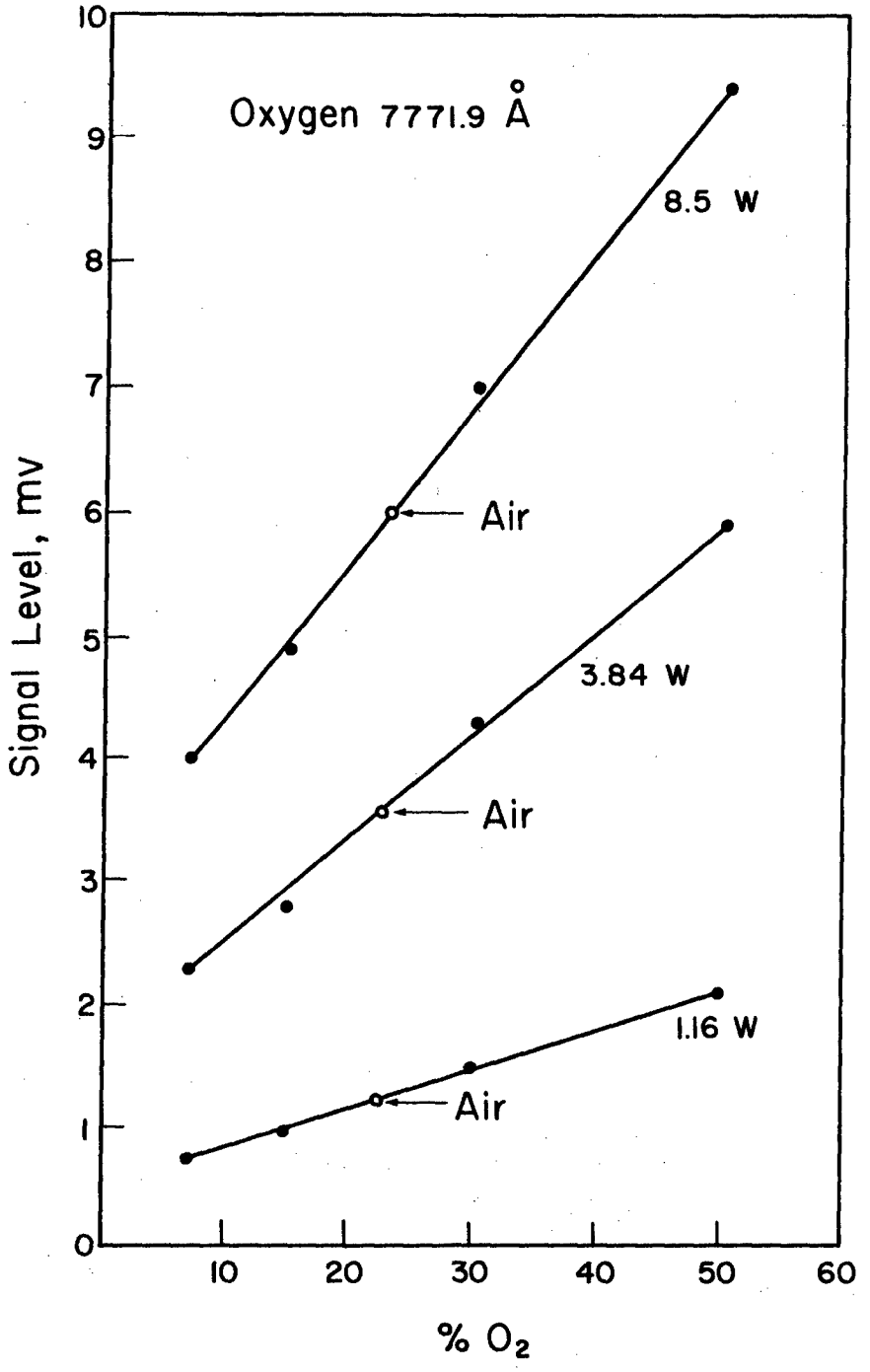


Figure 8. CALIBRATION CURVE FOR OXYGEN WITH 3.4-METER SPECTROGRAPH

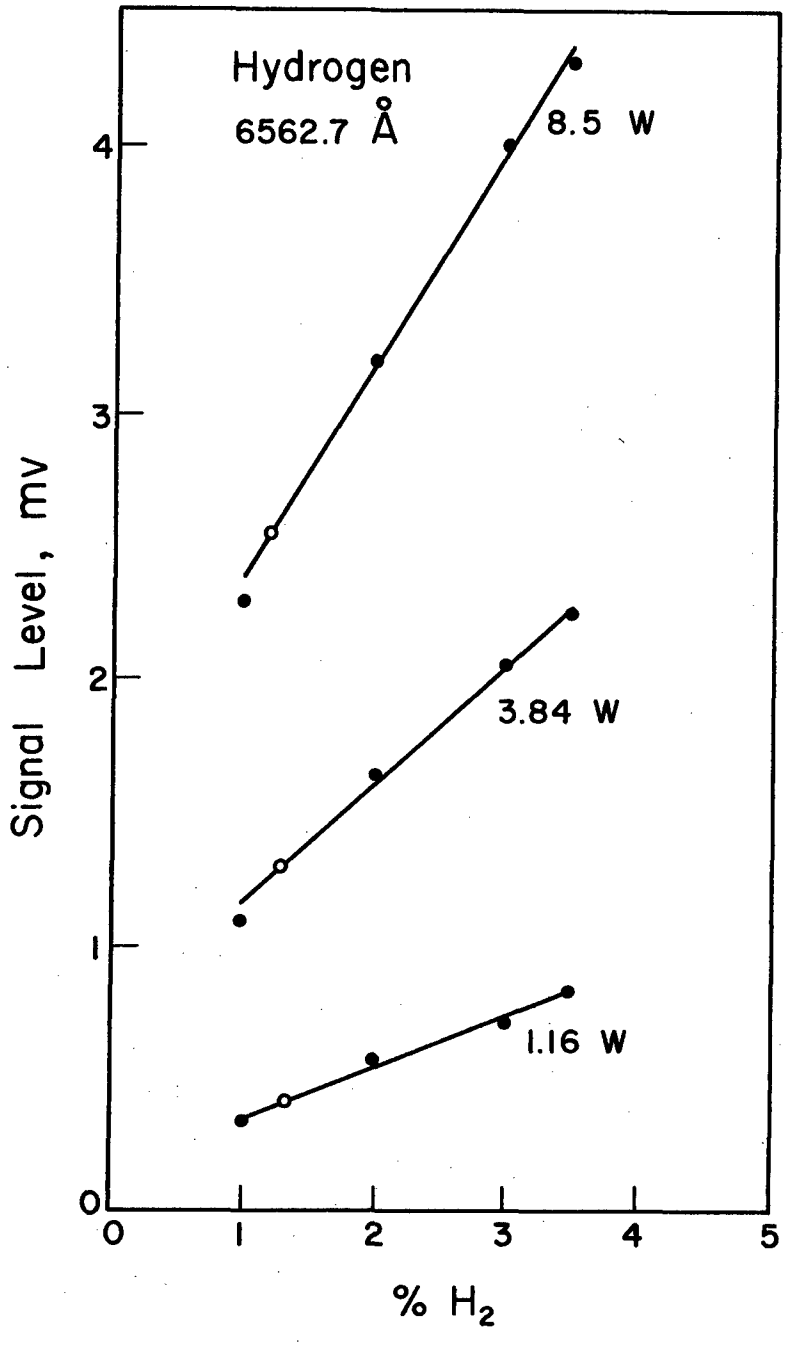


Figure 9. CALIBRATION CURVE FOR HYDROGEN WITH 3.4-METER SPECTROGRAPH

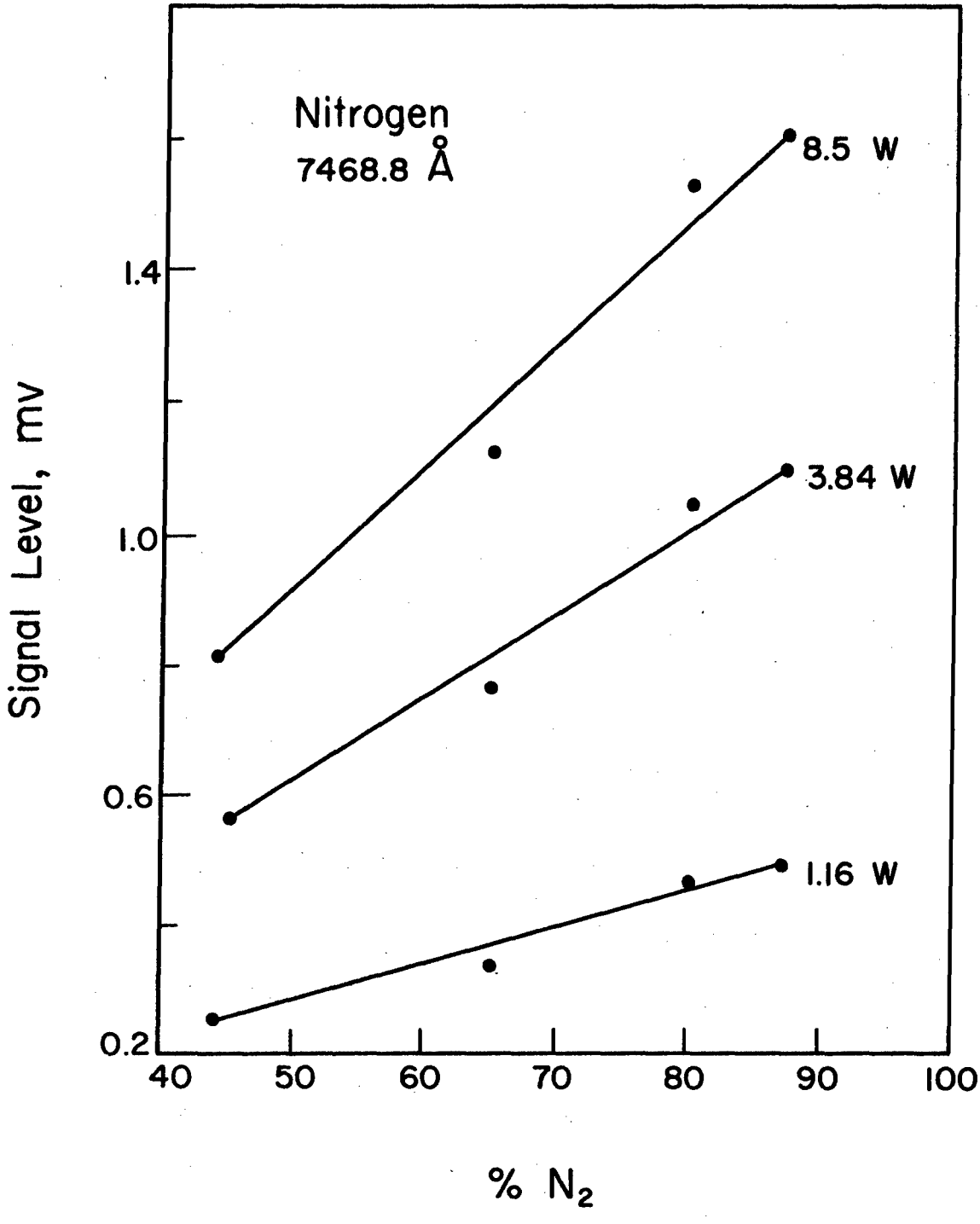


Figure 10. CALIBRATION CURVE FOR NITROGEN WITH 3.4-METER SPECTROGRAPH

No spectral interferences are indicated.

The effect of the applied voltage is indicated by the slopes of these curves.

The same responses were measured, except N 8216.4 was used in place of N 7468.8 Å, using interference filters instead of the spectrometer to isolate the wavelengths. The direct readout device, fig. 1, designed for use with filters was used. These were 50 Å half-power bandwidth filters supplied by Capt. William Thornton of Brooks Air Force Base.

The response curve using the 7771.9 Å filter was the opposite of that expected, fig. 11. The output signal decreased as the concentration of the oxygen was increased. This would indicate that this filter is not correct or there is very great spectral interference. The response curves were rerun with the 3.4-meter spectrograph with and without the filter in the optical path ahead of the slit. The normal response, approximate linear function of concentration, fig. 12, indicated that the filter wavelength was correct. The response for hydrogen was that expected, fig. 13, but the response for nitrogen showed a strong positive curve, fig. 14.

The oxygen response curves were the first obtained, so considerable time was used rechecking electronic circuitry since the initial studies using spectrographic plates did not show any interferences.

To further check this possibility of spectral interference, a very long exposure, 8 hours, was made using the 3.4-meter spectrograph, operating the hollow cathode at 9.6 watts using the 7% $O_2$-88.5% $N_2$ mixture. A very light band structure was found on each side of the relatively very strong 6562-Å hydrogen line. There appeared to be no background on the long wavelength or red side of the 7771 Å oxygen triplet. However, on the shorter wavelength, violet side, the rather weak bandhead at 7753 Å did develop, this band degrades to the violet. This bandhead was within the half-power bandwidth of this filter.

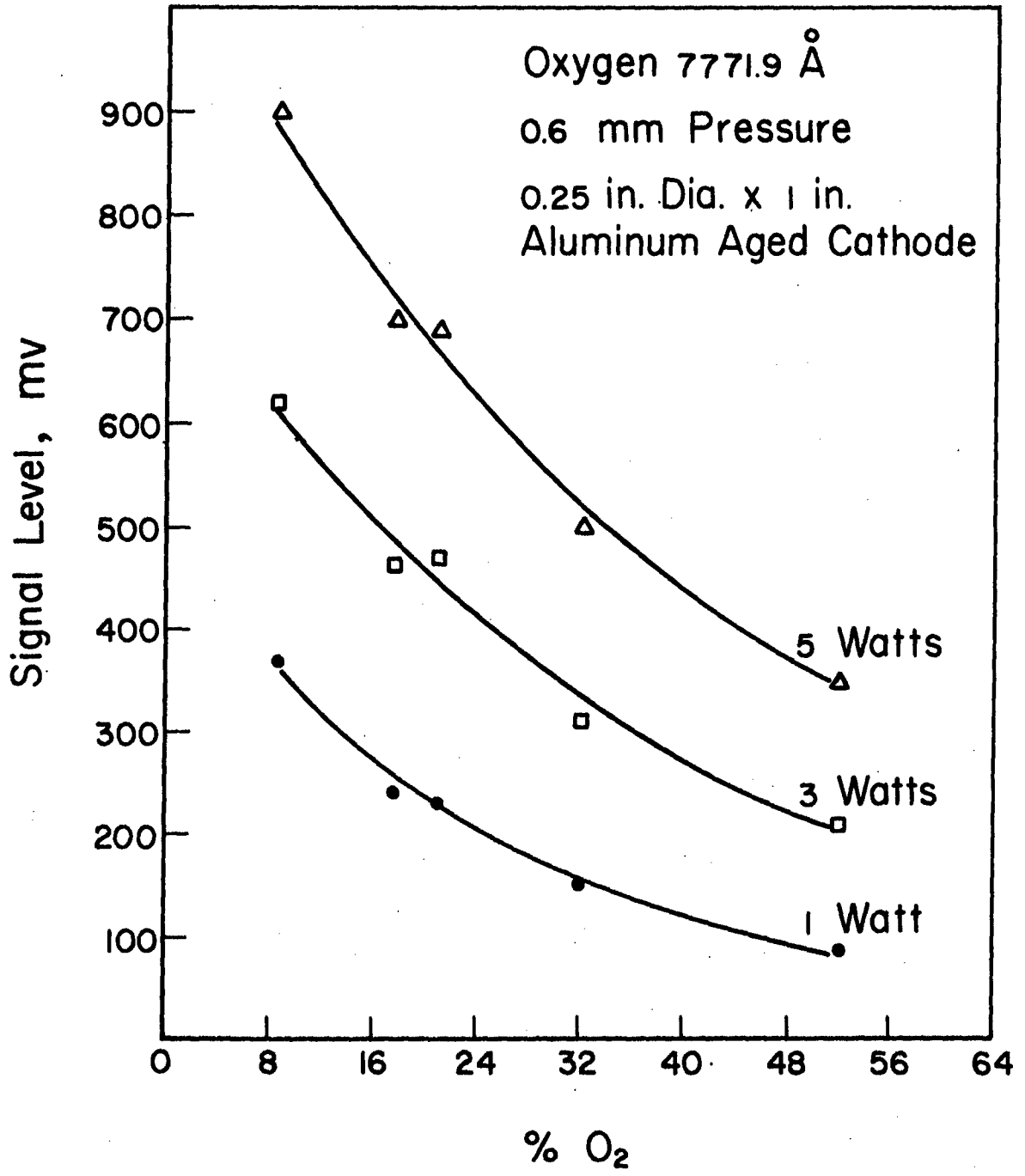


Figure 11. RESPONSE FOR OXYGEN; 50 Å HALF-POWER BANDWIDTH FILTER

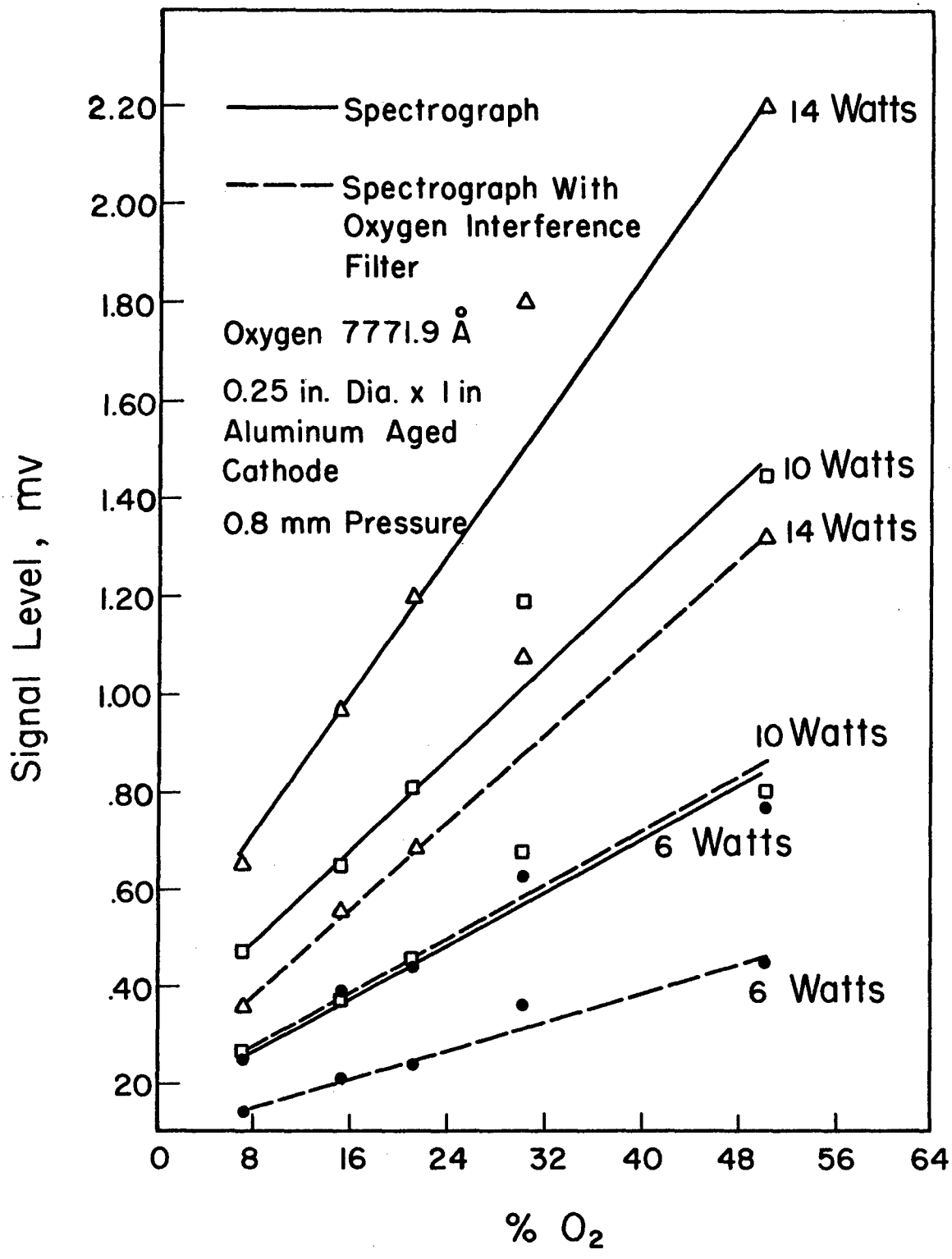


Figure 12. INFLUENCE OF INTERFERENCE FILTER IN LIGHT PATH ON SPECTROGRAPHIC RESPONSE

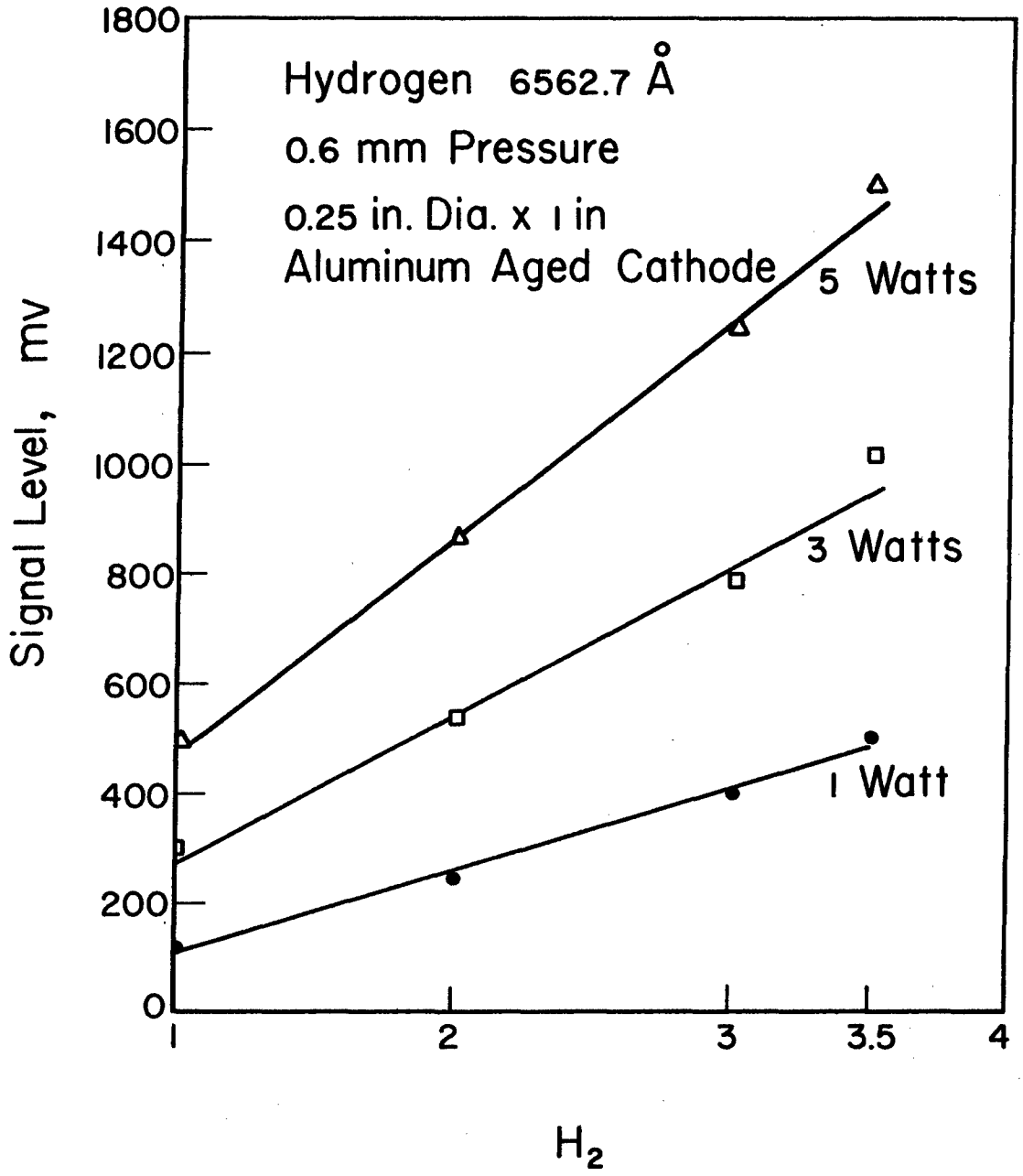


Figure 13. RESPONSE FOR HYDROGEN; 50 Å HALF-POWER BANDWIDTH FILTER

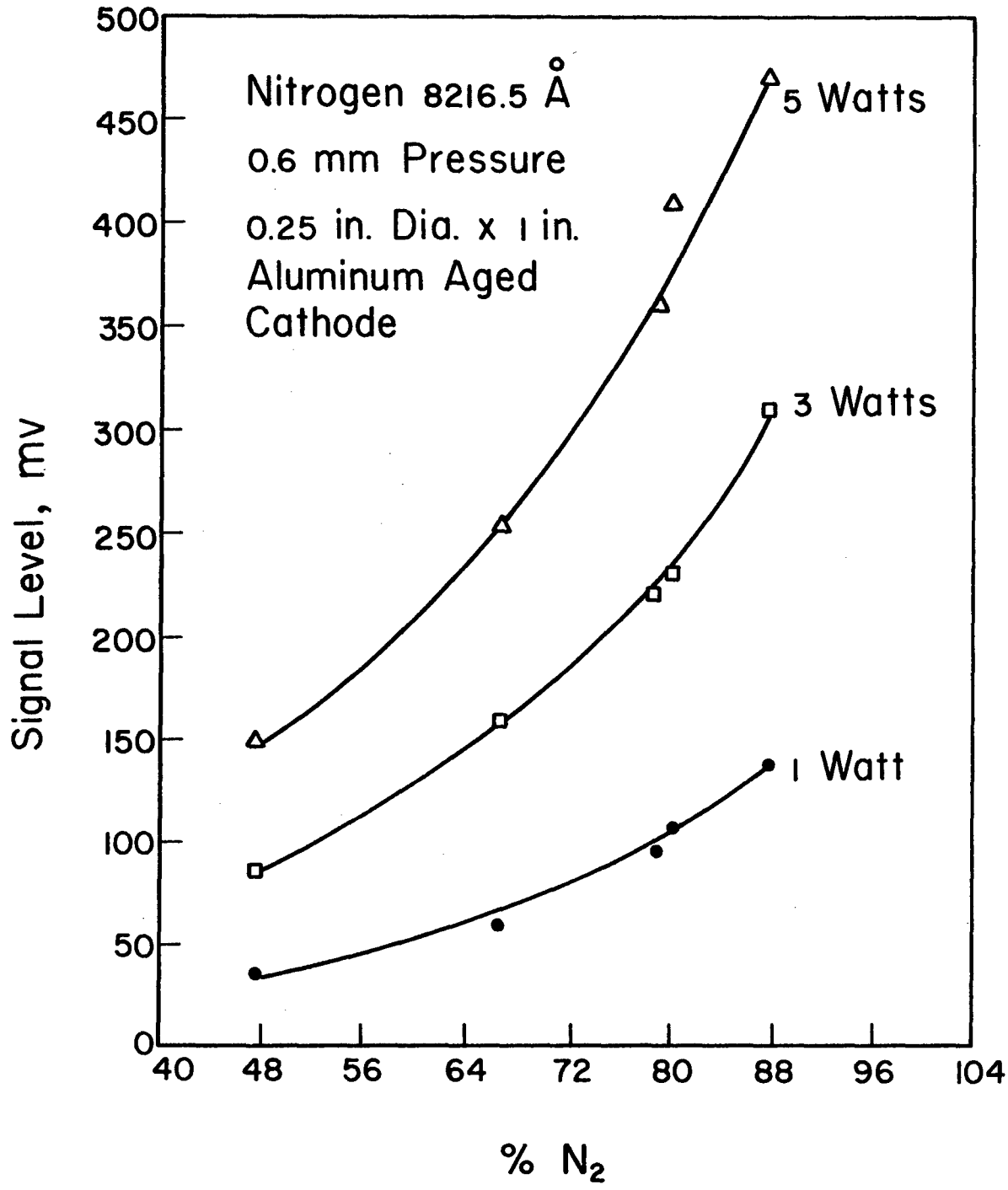


Figure 14. RESPONSE FOR NITROGEN;
50 Å HALF-POWER BANDWIDTH FILTER

Since the PM output followed the changes of the nitrogen concentration instead of that for oxygen, this band which did appear through the interference filter apparently supplied sufficient radiation so that its influence was greater than that for the oxygen 7771 Å triplet. The concentration of nitrogen in the bottles was high when the oxygen was low, table I. This would account for the decreasing response as the oxygen concentration was increasing, fig. 11.

A reexamination of spectrograms prepared earlier with shorter exposure periods revealed that this band did appear very weakly in some cases. The reason it did not appear in all cases could be due to emulsion inertia. The high nitrogen concentration was used to bring out the poorest conditions that could be expected.

## Filter Selection and Evaluation

No background could be seen at the 8446.4 Å oxygen line so this intense line was considered worthy of further investigation. Background also was not observable to the eye from the use of a hand lens at the 8216.5 Å nitrogen line.

These observations, data from the use of the 50 Å half-power bandwidth filters, efficiency and cost considerations were the basis for the half-power bandwidths selected for the filters used in the remainder of the studies. These are listed in table II. The 7771.9 Å filter was measured and found to be 6 Å half-power bandwidth.

The maximum for 7771.9 Å wavelength filter was requested to be on the red side to avoid any 7753 Å nitrogen background. On the long side, i.e., at the 7772 and 7773 Å lines, there appeared to be no background. The wider halfwidth was used for the carbon 9094.9 Å line because this range had only recently become available.

Table II

HALF-POWER BANDWIDTH FILTERS SELECTED

| Element | Wavelength, Å | Half-Power Bandwidth | |
|---|---|---|---|
| Oxygen | 8446.38 | 20 A | |
| Oxygen | 7771.93 | 10 A | 6 Å* |
| Nitrogen | 8216.46 | 20 A | |
| Hydrogen | 6562.72 | 10 A | |
| Carbon | 9094.89 | 30 A | |

*Measured

These filters were also evaluated by the direct readout device, fig. 2. Readout was by the chopped direct current method using the RCA 7102 S-1 response tube since longer wavelengths were involved. The power levels were the same as those used previously, 3 and 5 watts.

The response for hydrogen and nitrogen increased as a function of concentration, however, the slope of the response curves for oxygen 7771.9 Å and for carbon 9094.9 Å lines were negative, indicating that the response was largely due to nitrogen interference. The response for the oxygen 8446.4 Å line increased as a function of concentration.

Because these relatively narrow half-power bandwidth filters had been expected to eliminate the spectral interferences, additional spectrograph studies were made with the new 3/4-meter f6.3 Czerny-Turner spectrograph. A full spectrum exposure was made to show all lines and bands for reference purposes. This was followed by separate exposures through the different interference filters. Due to the speed of the spectrograph, the full spectrum exposure required only 10 minutes on 1-N plates which was doubled for interference filter exposures. This short time is in contrast to 8 hours required for the 3.4 meter, ~f30 Ebert spectrograph. Carbon 9094.9 Å required 30 and 60 minutes, respectively, on hypersensitized 1-M plates. The results are shown in fig. 15. The spectra numbered 1, 2, 3, 7, 8, and 9 were prepared with the 7% $O_2$ -

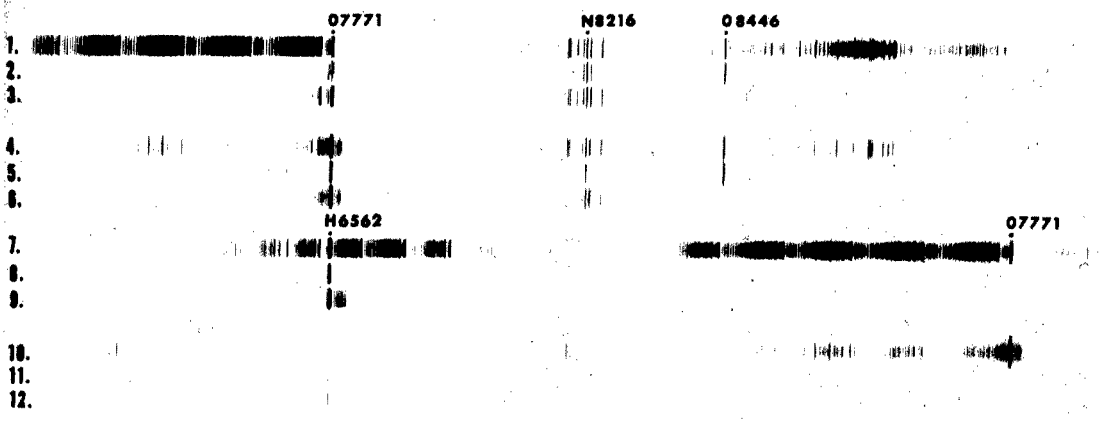


No. 1. Complete Spectrum for 7% $O_2$, 88% $N_2$
2. O - 7771 Å, 10 Å Half-Power Bandwidth, N - 8216 Å, 20 Å Half-Power Bandwidth, O - 8446 Å, 20 Å Half-Power Bandwidth
3. O - 7771 Å; N - 8216 Å; 50 Å Half-Power Bandwidth
4. Complete Spectrum for 50% $O_2$, 44% $N_2$
5. Same as No. 2
6. Same as No. 3
7. Complete Spectrum for 3.5% $H_2$, 7% $O_2$
8. H - 6562 Å, 10 Å Half-Power Bandwidth
9. H - 6562 Å, 50 Å Half-Power Bandwidth
10. Complete Spectrum for 1% $H_2$, 50% $O_2$
11. Same as No. 8
12. Same as No. 9

Figure 15. SPECTROGRAM SHOWING TRANSMISSION CHARACTERISTICS OF THE VARIOUS INTERFERENCE FILTERS

88% $N_2$ - 3.5% $H_2$ while the numbers 4, 5, and 6 were prepared with the 50% $O_2$ - 44% $N_2$ - 1% $H_2$ gas mixture. Spectra 1, 4, and 7 were taken with no filter and show the complete spectra, including the band spectra. Spectra No. 3 shows the band spectra being transmitted by the 50 Å half-power bandwidth, both the oxygen 7771 Å and the nitrogen 8216 Å regions. The oxygen filter passes the 7771 Å oxygen triplet, the nitrogen 7753 Å bandhead and an additional weak band at 7738 Å. A portion of the band, that we attribute to nitrogen, on the short wavelength side of the oxygen 7771 Å line is transmitted through the new filter, spectra No. 2, even though its half-power bandwidth was measured to be 6 Å. The order requested that the maximum for this filter be on the red side of the 7771.9 Å line. In this way part of the 7771.9 Å line would be transmitted as well as the 7774.1 and 7775.4 Å lines that show no nitrogen band structure or heavy background. However, the maximum was slightly on the violet side which transmitted the 7753 nitrogen bandhead and excluded most of the 7774.1 and 7775.4 Å lines. This is quite clearly shown in spectrum No. 2 of fig. 15.

The full spectrum exposure adjacent to the 8446 Å oxygen line shows extremely weak bands but these are not passed by the interference filter. The nitrogen 8216 Å region appears to be clean. The interference filter transmits the 8216 Å nitrogen as well as the 8210 and 8223 Å nitrogen lines. Spectra No. 2 and 3 illustrate the additional nitrogen lines in the 8216 Å group that is transmitted by the 50 Å as compared to the 20 Å half-power bandwidth filter.

The No. 7 spectrogram shows the fine band structure previously observed on each side of the 6562 Å hydrogen line. The spectra No. 9 shows the band transmitted by the hydrogen 50 Å filter and No. 8 shows that very little, if any, of the band structure is passed by the 10 Å filter.

The difference in the influence of the nitrogen concentration is clearly shown in spectra No. 2 and 5. The concentration of nitrogen for No. 5 was 44%, one-half that for No. 2, and no band is visible through the oxygen 7771 Å filter.

Evaluation of carbon 9094 Å line was performed using the mixture containing the 5% carbon dioxide. The full spectrum exposure shows fine structure to either side as well as four nitrogen lines some 30 Å distant. The interference filter passed all this emission. Although the nitrogen lines were at greatly reduced intensity they are still sufficiently strong to produce a negative response. These extra lines or background were not observed on any of the previous spectrographic studies with the larger spectrograph and were not listed in the regular wavelength atlases.

The curvilinear response, such as illustrated in fig. 14, was not expected and is not as desirable as the more linear response exhibited from the spectrometer recordings. It was found that pure nitrogen as well as pure argon produced substantial signals through each of the interference filters.

It is possible for some interference filters to transmit as much as 1/2% of the incident wavelengths outside of the desired passband. If this were the case, then the integrated intensities of all the strong nitrogen bands present could easily exceed a weak signal of an analyte gas through the passband. Then the filter approach to the monitor is not desirable. As an initial check on the blocking characteristics, the separate filters were run on the Cary Model 14 at maximum sensitivity, 10% transmission full scale. There was no transmission in the blocked regions as the base line was superimposed on a base line obtained with an opaque material in the light path. For further investigation of the passband characteristics, the Cary lacked sufficient sensitivity, and the transmission curves would not show which element emission was being transmitted. A better method would be to disperse the transmitted emission in order to analyze the various lines and bands. These additional studies were accomplished by using the 3/4-meter Czerny-Turner spectrograph fitted with a PM tube for electronic readout. The small spectrograph was fitted with an S-20 PM tube (the S-1 was of insufficient sensitivity) in place of the camera back, and a 125-micron exit slit inserted at the film plane to coincide with the wavelength counter. A variable speed d-c motor coupled to a variable speed transmission was used to very slowly drive the scanning

mechanism. The PM responses were displayed on an oscilloscope and photographed.

The recombination energies associated with pure argon is known to produce considerable background but the background seemed high for nitrogen.

Operating conditions for the hollow cathode unit was 280-microns pressure and 5-watts power input. The S-20 response photomultiplier tube was operated at 1500 volts. Motor speed was set to give a scan rate of 1 Å/second. The single sweep speed of the oscilloscope was set to 5 sec/cm. Thus it was possible to display a 50 Å scan during one traverse of the spot across the face of the cathode ray tube. Photographs were made in pairs, the first through a Corning CS2-61 red filter to eliminate second order lines, yet display the full spectrum in the 50-Å region. The second photograph was made by replacing the CS2-61 filter with the proper interference filter. The first 5 Å or 1 cm of the trace was made with the spectrometer shutter closed to establish a base line.

Several photographs of different gas and filter combinations were prepared. Figure 16 illustrates the photographs obtained for the hydrogen 6562 Å line using the gas containing 3-1/2% hydrogen. The upper photograph shows the normal spectrum, the small peaks being a weak band structure, and the large one due to the response for the 6562 Å hydrogen line. This band structure continues under the hydrogen peak, therefore the total signal contains a percentage of nitrogen band signal. The interference filter photograph on the bottom shows this structure as undulations in the wings which also exist under the hydrogen peak, and therefore adds to the signal. The short line at the left is a base line established by blocking the light to the spectrometer. These weak bands were visible at the 87% nitrogen, very faintly at 80% and not at the lower concentrations.

Photographs for the oxygen 7771 Å interference filter for the same gas mixture are shown in fig. 17. In the upper photograph the O-7771 triplet is the large off-scale peak followed by the fine structure and the 7753 $N_2^+$ bandhead to the right. The lower photograph shows quite clearly the transmission of the undesirable wavelengths.

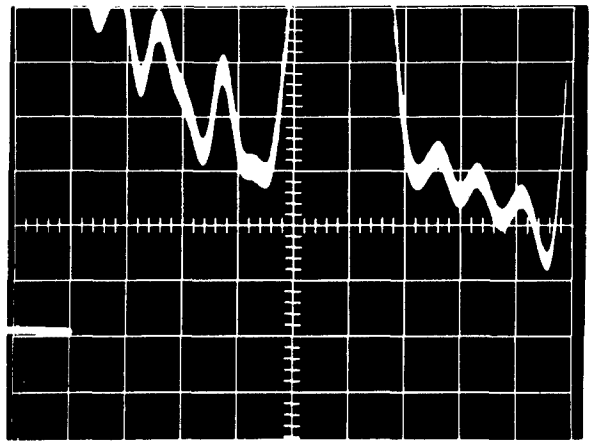

6590 6562 6537

Through CS2-61 Red Filter
10 mv/cm Sensitivity

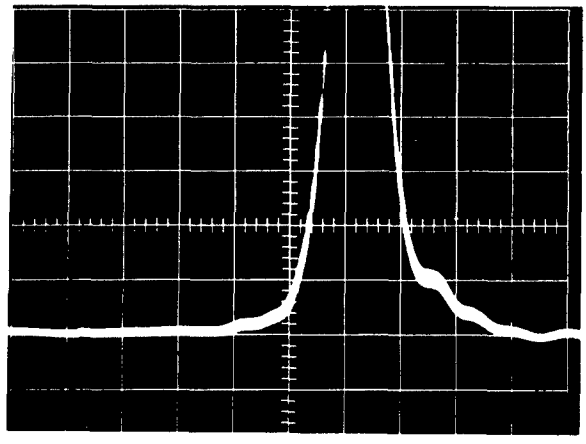

6590 6562 6545

Through H-6562 Interference Filter
10 mv/cm Sensitivity

Figure 16. INTERFERENCE AT THE HYDROGEN 6562 Å LINE PASSING THROUGH THE 10 Å HALF-POWER INTERFERENCE FILTER

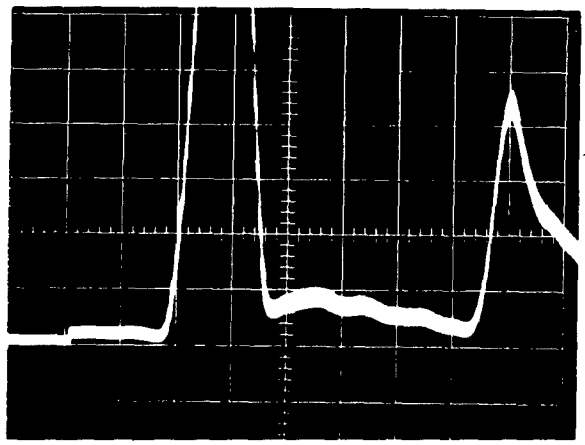

7790 7771 7753 7747

Through CS2-61 Red Filter
10 mv/cm Sensitivity

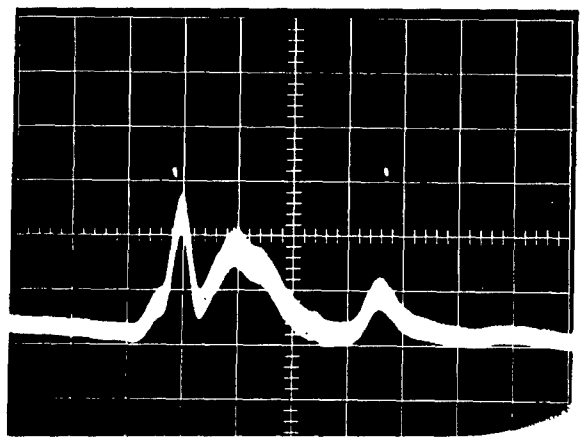

7790 7771 7753 7733

Through O-7771 Interference Filter
2 mv/cm Sensitivity

Figure 17. INTERFERENCE AT THE OXYGEN 7771 Å TRIPLET PASSING THROUGH THE 6 Å HALF-POWER INTERFERENCE FILTER

Scanning speed was somewhat higher in the lower photograph. This resulted in compression of the peaks. These two figures show graphically that much of the area under the curve is due to nitrogen, which explains the negative slope obtained for calibration curves with the oxygen 7771 Å filter. As the oxygen concentration increased, the nitrogen concentration decreased in these mixed gases and the greater signal was due to the nitrogen band emission. In this interference filter the peak is on the short side of the 7771,9 Å line, although in our order we specified that it be on the longer wavelength side in order to make use of the oxygen 7773 Å and 7775 Å lines and avoid nitrogen interference which was nearly zero on the red side. The 8446.4 Å oxygen line is stronger than the 7771.9 Å line, however, here it shows a weaker response, fig. 18, because this is near the end of the useful range for an S-20 response tube.

In contrast, fig. 18 shows the response for the oxygen 8446.4 Å line with the same gas mixture. The upper photograph shows a small amount of background. Additional photographs of the other gases showed this background to be greatest with 100% $N_2$ and to decrease with a decreasing nitrogen concentration, and finally vanishing completely with 100% $O_2$.

Figure 19 shows the 8216 Å nitrogen line group, again using the same gas. The two weaker lines at 8210 Å and 8223 Å also can be seen with the 8216.4 Å line although part of the 8223 Å line is lost.

The carbon 9094 Å line was not investigated because of the lack of sensitivity of the S-20 photomultiplier tube at that wavelength. The S-1 photomultiplier tube was tried initially but was abandoned because of the very slow signal-to-noise ratio.

The photographs of this series were intended to precisely show the amount and nature of the light being transmitted through the various interference filters. This includes the 1/2% or more of general background, plus any additional background due to stray light and the formation of weak bands. It was found that the background signal could be further reduced by screening out or blocking light from the anode glow and the positive column or ring area.

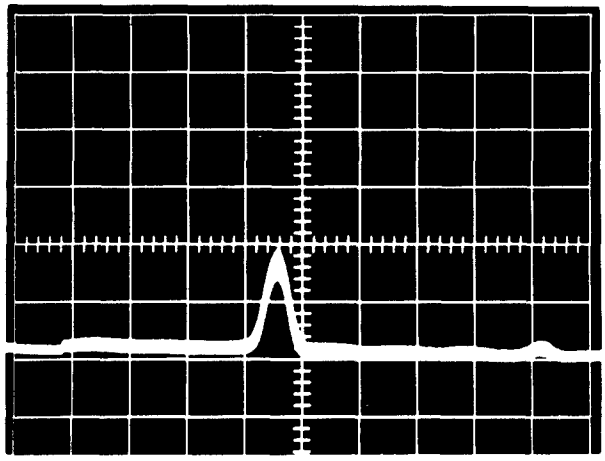

8470 8446 8420

Through CS2-61 Red Filter
5 mv/cm Sensitivity

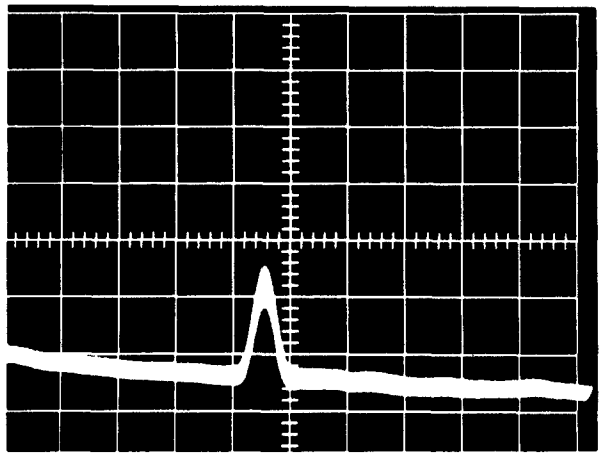

8470 8446 8420

Through O-8446 Interference Filter
2 mv/cm Sensitivity

Figure 18. INTERFERENCE AT THE OXYGEN 8446 Å LINE PASSING THROUGH THE 20 Å HALF-POWER INTERFERENCE FILTER

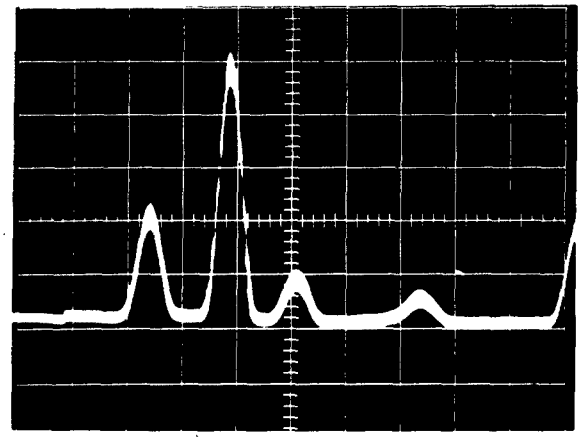

8235 8223 8216 8210 8200 8189

Through CS2-61 Red Filter
5 mv/cm Sensitivity

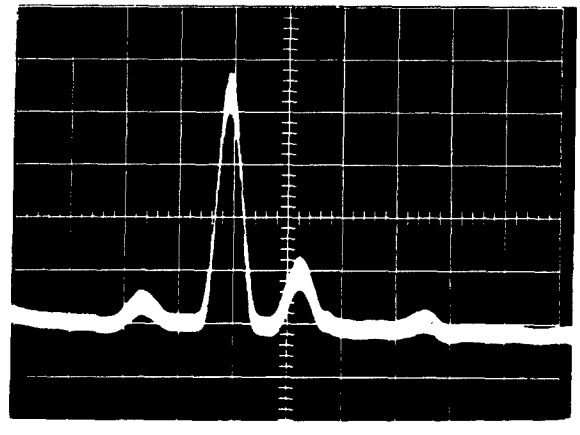

8235 8223 8216 8210 8200 8189

Through N-8216 Interference Filter
2 mv/cm Sensitivity

Figure 19. INTERFERENCE AT THE NITROGEN 8216 Å GROUP PASSING THROUGH THE 20 Å HALF-POWER INTERFERENCE FILTER

The break in the line to the left of the figures is the base line, the change in level represents background when the shield is removed.

The hollow cathode unit used in this work consisted of a 5/8-in. diameter gold-foil-lined anode section, a vycor separator with a 1/4-in. hole and a 3/8-in. x 1-in. gold-foil-lined cathode cavity. This was mounted in the direct reading device to provide for a ready interchange of filters and the whole positioned before the spectrometer. A 53-mm lens was used to focus a point approximately midway down the cathode cavity upon the 100-micron entrance slit.

Anode Glow

Visual studies of the interior of the excitation source indicated a glow from the anode. This formed a ring and would correspond to the anode glow of the glow discharge tube. This glow appeared to expand, i.e., spread across the insulator toward the cathode at higher gas pressures and higher concentrations of nitrogen.

With pure oxygen and carbon dioxide the glow appeared to be coming from inside the hollow cathode. There was very little light from the anode glow. However, with pure nitrogen there was little visible glow from the hollow cathode but the glow from the anode ring was quite intense and this area of glow rapidly expanded as the gas pressure was increased. Thus it would appear, as previously expected, that the nitrogen band systems arise from the anode glow and positive column regions. When a neutral filter was used the response from increasing nitrogen concentration did not show a linear response, but one with a strong positive curvature. This would indicate that the output signal to a large extent was from the anode area since visual observations indicated that the anode glow not only became more intense but occupied more space as the nitrogen concentration increased. The response using the interference filter was very similar, fig. 20, which is not the atomic line response as indicated by fig. 10.

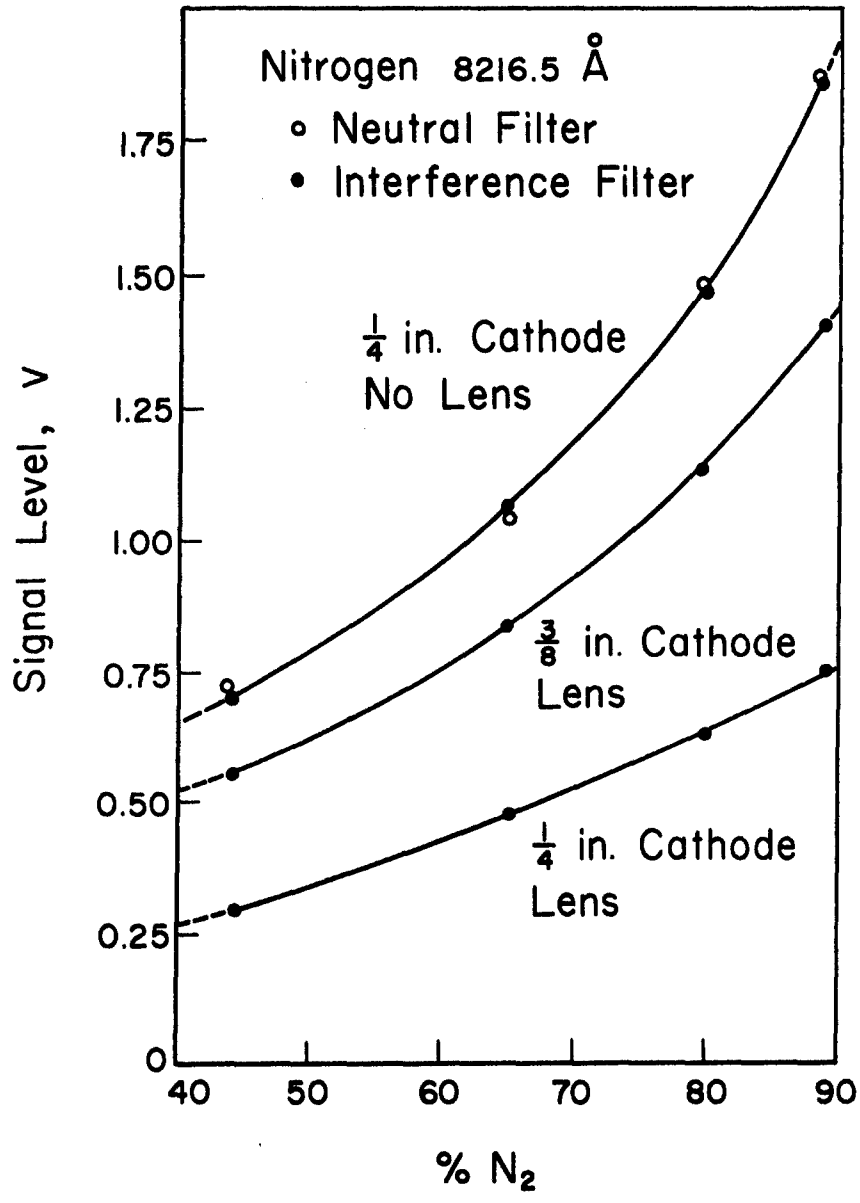


Figure 20. INFLUENCE OF NEUTRAL FILTER, INTERFERENCE FILTER AND FOCUSING LENS ON RESPONSE FOR NITROGEN

Further evidence that nitrogen is the major contributor of the light coming from the synthetic air mixtures is indicated from an experiment in which the response for the attenuated total light through a neutral filter was kept constant by adjusting the voltage supply to the PM tube and then measuring the line response, fig. 21. The response is quite linear for the hydrogen 6562.7 Å line and for both oxygen lines being studied while previously the oxygen-7771.9 Å line was negative. There is no real response for the nitrogen-8216.5 Å line.

The use of a lens and a mask was studied to remove or mask out the nitrogen band radiation. The effectiveness of the technique is shown in fig. 22. Without the lens and mask the influence of the nitrogen band was greater than that of the oxygen-7771.9 Å line, but with these present the response is more nearly what should be expected. The influence of the nitrogen band has been screened out, but apparently some background light is present. The lens also removes much of the radiation that influenced the response for the nitrogen 8216.5 Å line. The response is much more linear and the overall response is much less, fig. 20.

The use of the lens does reduce the light flux for a specific line reaching the PM tube, as is illustrated in fig. 20 for nitrogen, and in fig. 23 for oxygen.

The mask with a 5/16-in. opening was placed in front of the PM tube. The lens, 5/8-in. in diameter just fit in the opening ahead of the quartz window, fig. 24. The initial lens, 39-mm focal length, focused just inside the cathode. The purpose of the lens was to transmit the light gathered at or near its focal point through the mask opening. The position of the lens was such that it magnified the image somewhat so the anode and positive column glows were largely dispersed into a ring surrounding the mask opening. The use of two lenses was studied. These were what were on hand. The second was a 33-mm focal length lens that focused further down the cathode.

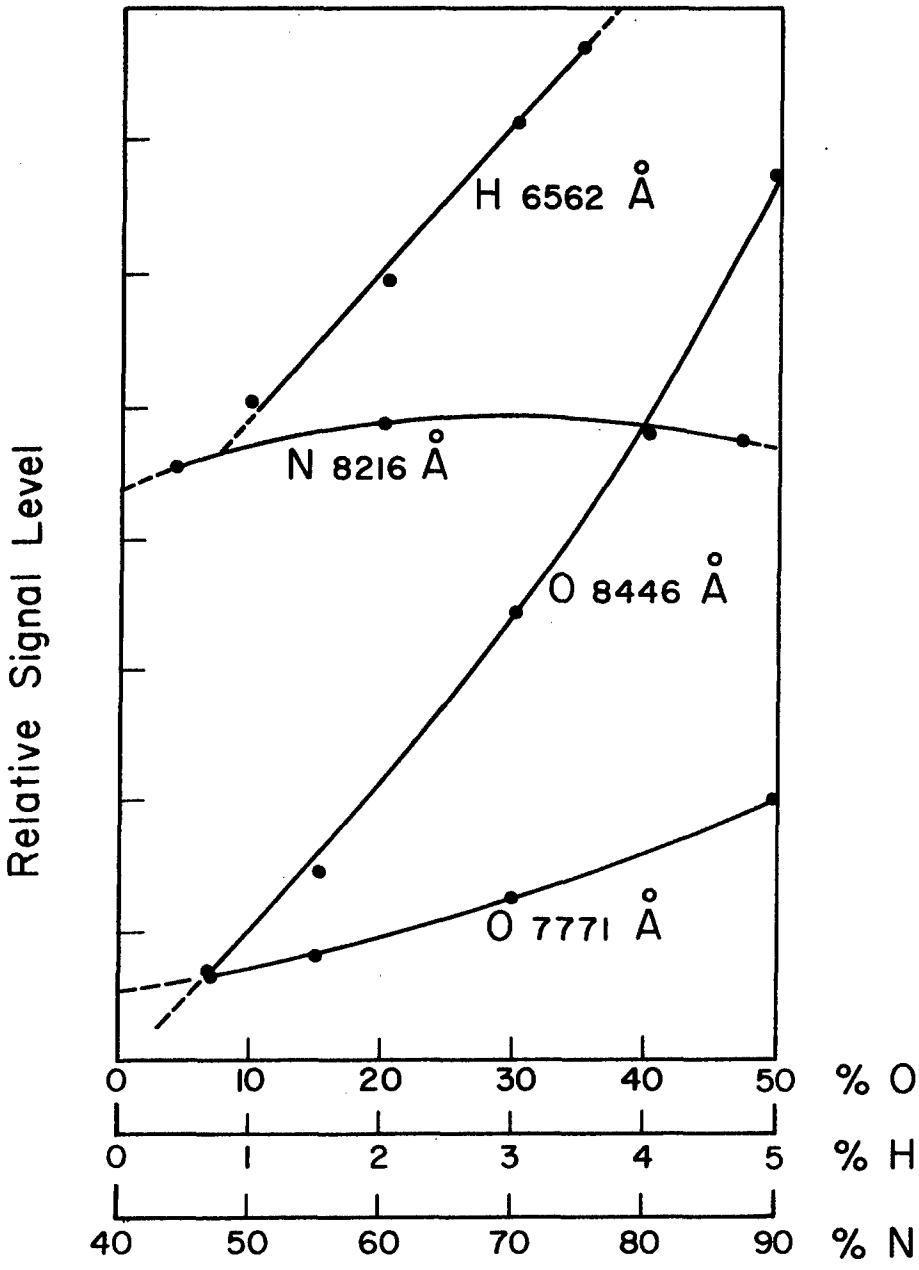


Figure 21. EFFECT OF KEEPING RESPONSE TO TOTAL LIGHT CONSTANT

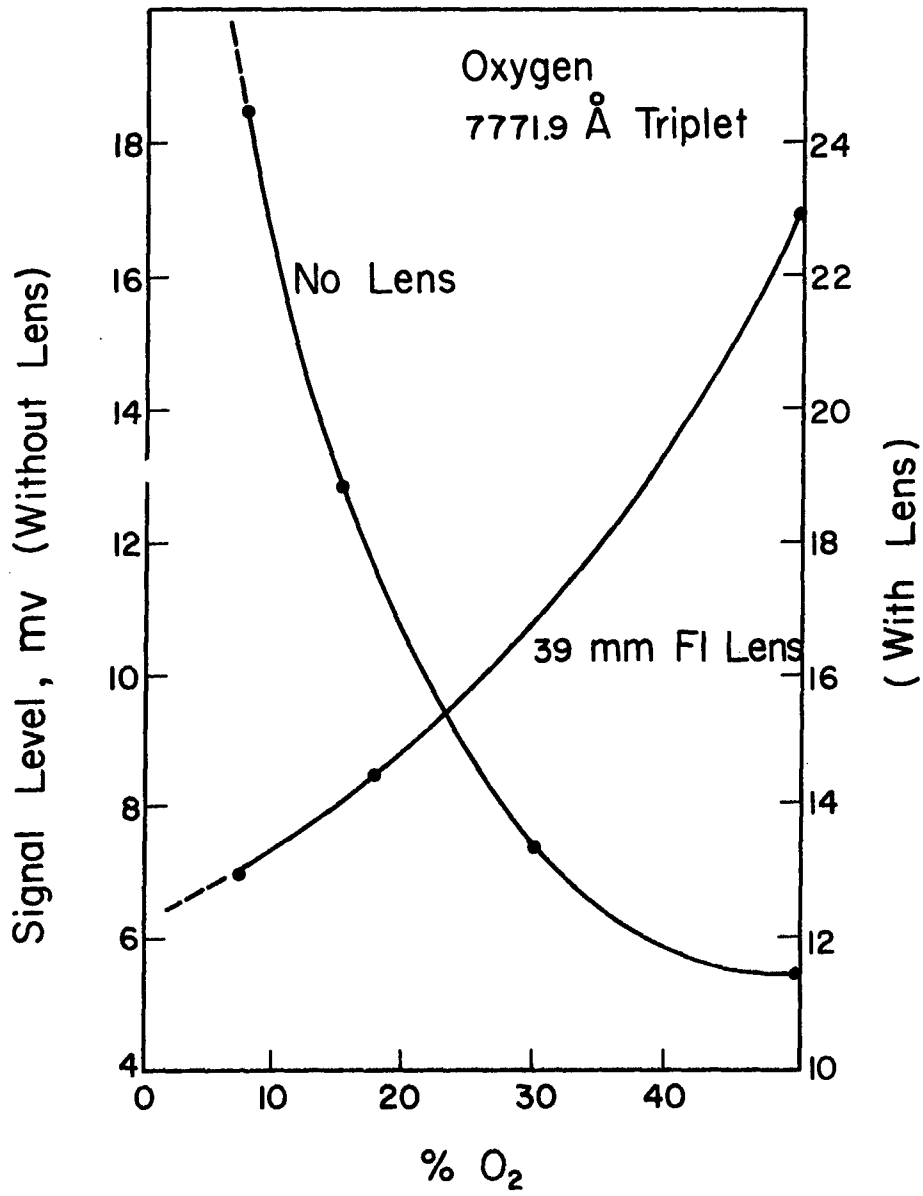


Figure 22. INFLUENCE OF LENS AND MASK ON RESPONSE FOR OXYGEN 7771.9 Å LINE

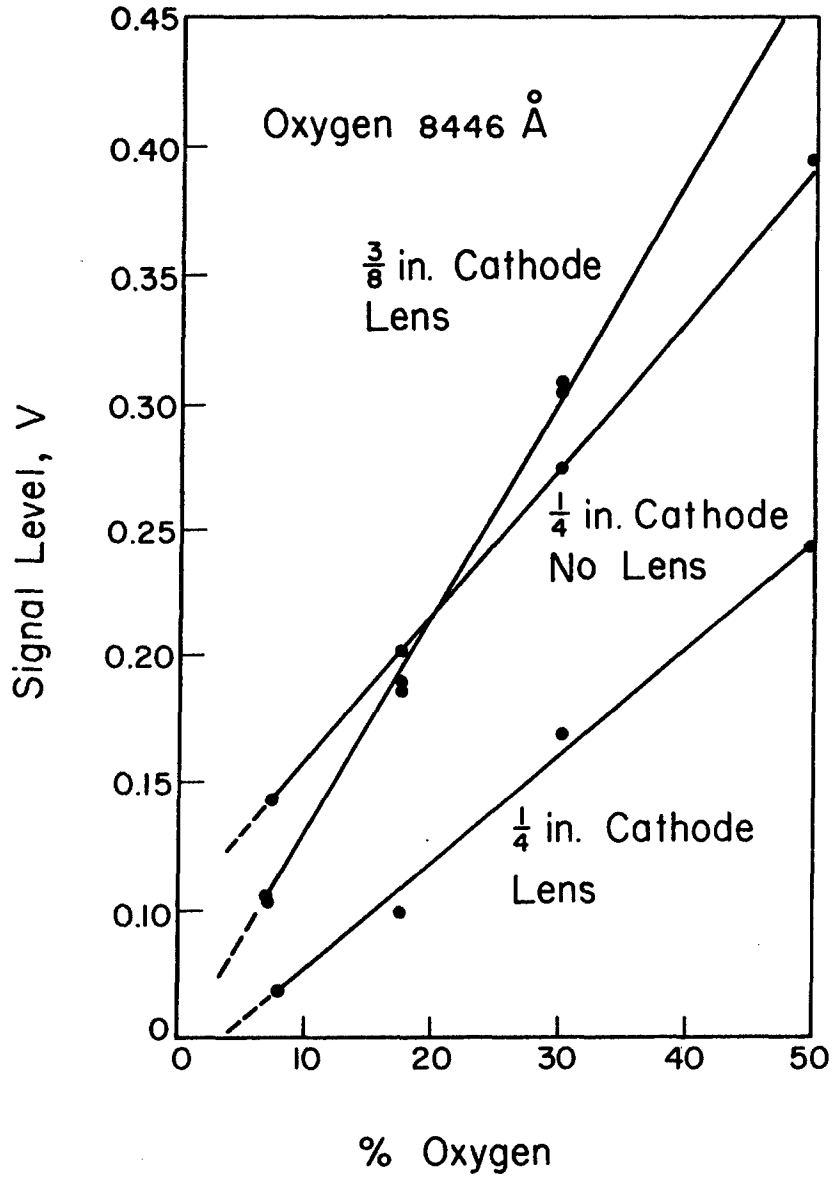


Figure 23. EFFECT OF CATHODE DIAMETER AND LENS ON LIGHT OUTPUT FOR 8446.4 Å OXYGEN LINE

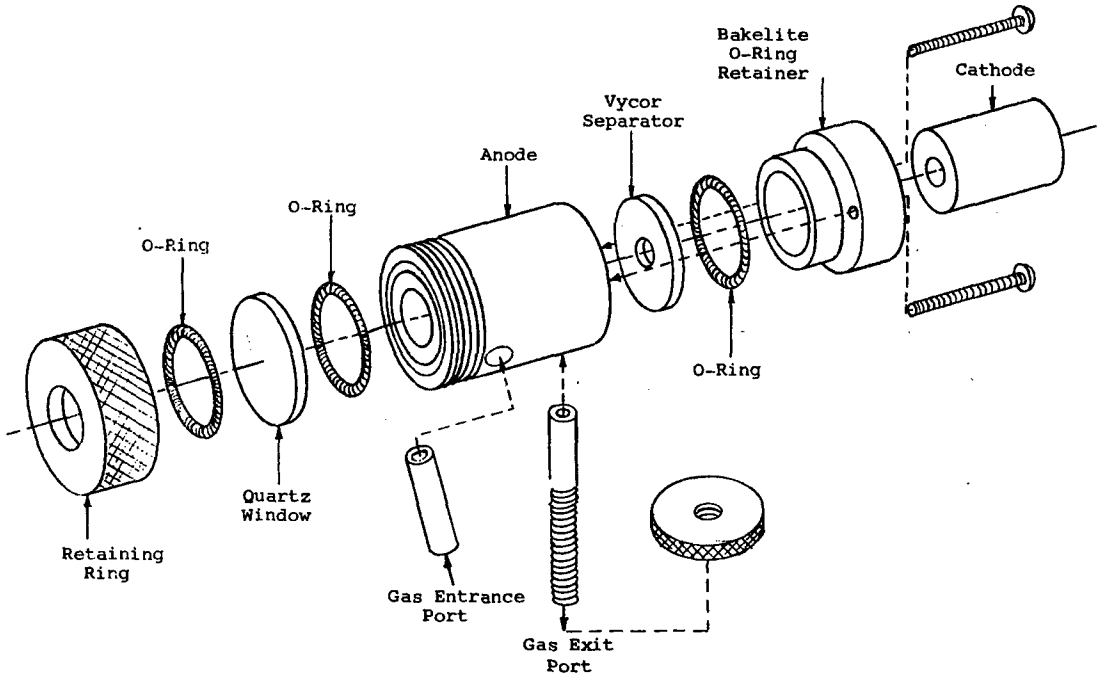


Figure 24. HOLLOW CATHODE UNIT
USED IN INITIAL STUDIES

### Subtraction of Nitrogen Response in $H_2$ and $CO_2$ Channels

It was not possible to effectively remove all the influence of the anode glow with the mask and the lens. For oxygen, this problem was bypassed by using the oxygen 8446.4 Å line. There was still some spectral interference at the hydrogen 6562.7 Å and carbon 9094.9 Å lines, fig. 31.* This interference increased proportionally with the increasing nitrogen concentration. It was decided to electronically subtract the proportional quantities from these two channels.

## HOLLOW CATHODE DESIGN

The general design of the source was similar to that by Werner et al. (ref. 6). The two major reasons for this selection was this unit's simplicity of construction and assembly, and that the writer had had a working contact with this unit while a Summer Participant at the Oak Ridge National Laboratory.

Since quite low power consumption was desired in this program and the light emission for the gaseous components is influenced by power, pressure and possibly other factors, this required an examination of design and operating parameters as well as materials of construction. The high concentration of oxygen created problems that previous workers, using only inert gases, had not experienced.

### Anode Design

The hollow cathode source used in the initial phase of this study had a brass anode chamber 1-in. in length and 5/8-in. in diameter. In various experimental runs it was found that the front window was becoming coated with sputtered metal. This chamber was replaced by a new anode 2 in. x 5/8 in.; the air was taken in at the front and flowed back toward and through or across the face of

---

*See page 68

the cathode. These two factors and the replacement of a resistor that had been removed when our power supply was on loan reduced window coating to a minimum. With the replacement of the resistance the discharge was much more even. An exploded view of a unit used in the initial phase of the program is illustrated in fig. 24.

At a later date the anode chamber of a new unit was heavily gold-plated since the anode was eroding, though not as rapidly as the cathode. This eroding was attributed to oxygen in the atmospheres being studied.

## Cathode Materials

### Aluminum

Aluminum metal is considered a good cathode material for hollow cathode materials because of its favorable normal cathode fall value, 229 V, as compared to the other elements.

During the course of the initial study, it was noticed that, although the same power and pressures were being used, there was a continued and relatively large decrease in emission line and band intensity. After 30 to 40 hours of operation, the inside of a cathode was found to be coated with a heavy layer of black powder. This was relatively thick, i.e., a sample was easily removed with a small spatula. Spectrographic analyses showed this finely divided metal or oxide to be mostly aluminum, the minor components being characteristic of brass. The process took place more rapidly if a higher wattage was used. A cathode was cleaned but not redrilled. Partial sensitivity was restored but the cathode again quite rapidly decreased in sensitivity and stabilized with the line and/or band intensity at only about 25% of the original intensity.

The result of a 72-hour run is summarized in fig. 25. A new aluminum cathode was used in which voltage, current, and emission intensity of the 7771 Å oxygen triplet was monitored. The gas used was 50% oxygen-50% nitrogen. As the source operated there was a steady increase in voltage, decrease in current and a corresponding decrease in

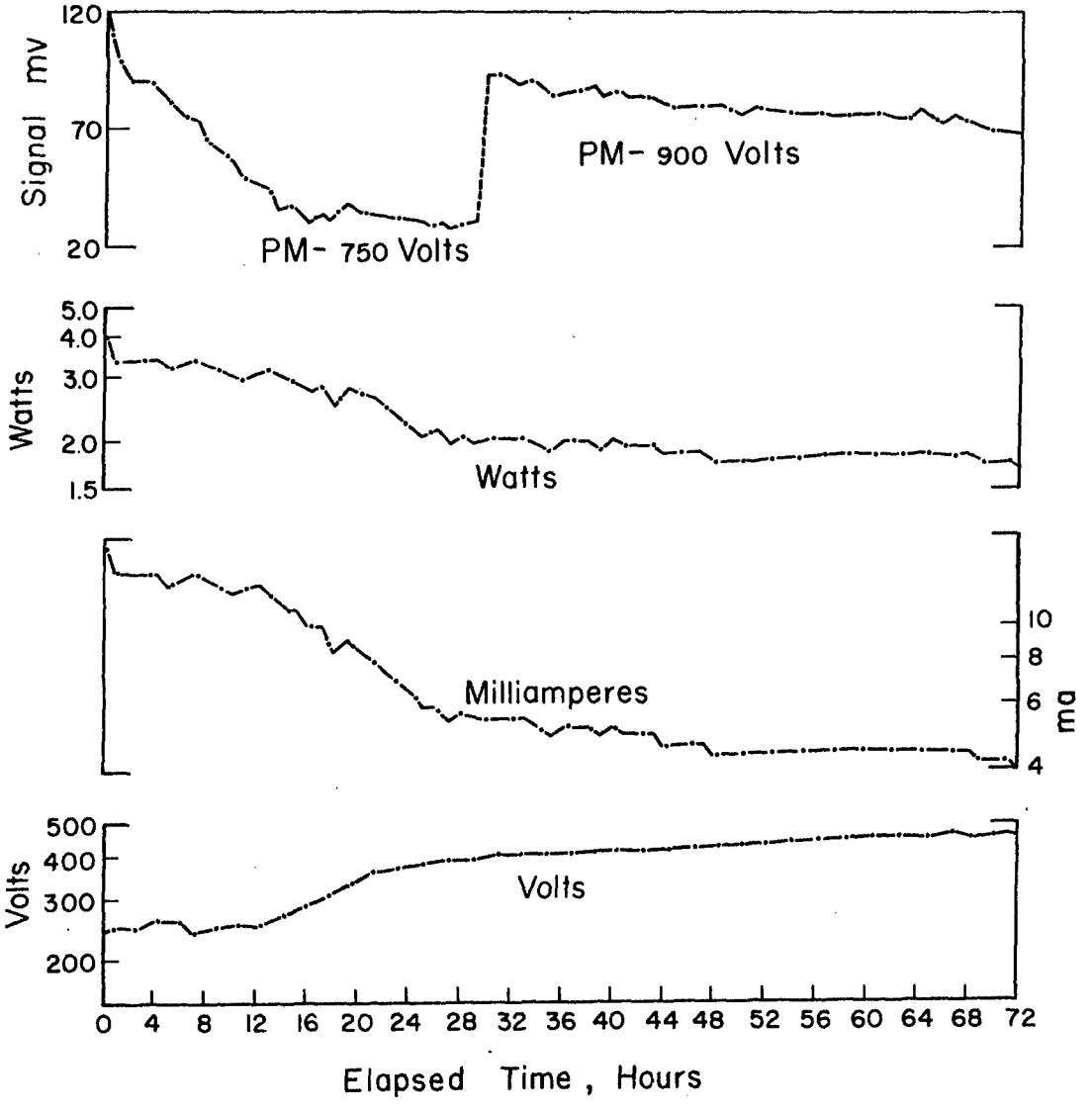


Figure 25. RESULTS FOR A 72-HOUR ALUMINUM CATHODE STABILITY RUN

power input. This was accompanied by a corresponding decrease in emission intensity. The above increase in voltage is apparently due to the buildup of the coating in the cathode. There is a close correlation with change in power and emission output at constant pressure and concentration.

Photographs were made of the oscilloscope traces of the PM output signal at various intervals throughout the run. The initial and final traces are shown in fig. 26. The final trace photograph, fig. 26b, shows the effect of the cathode sputtering and oxidation effects. Note that in figs. 25 and 26 that an increase in PM voltage was required to maintain sensitivity as the cathode operated. However, in fig. 26b, the sensitivity of the scope was decreased to keep the little specks of light on the screen.

During this period a thin coating of aluminum deposited on the window that resulted in a decrease in transmittance of 3.1% at 9094 Å to 4.8% at 6562 Å. Electronic stability was checked for a similar period so the variations observed were not due to equipment instability.

Gold Lined

Gold was selected for a new cathode material since its oxide does not form. Initial short runs and an overnight run using a cathode with a gold foil insert looked promising, so a new source was prepared from brass and was heavily gold plated. The result for the 17-hour run is shown in fig. 27. The stability was not as good as expected. However, it will be noted that the voltage remained very constant and that the drift of the current and power was small. Part of this variation appeared to be due to small fluctuations in pressure from the pressure reduction valves since there was appreciably less variation during a test period in which air was drawn from the surrounding atmosphere. The filter used at that time was the 7771 Å - 50 Å half-power interference filter which passed a high level of nitrogen radiation so the decrease in variation was not due to decreased oxygen radiation.

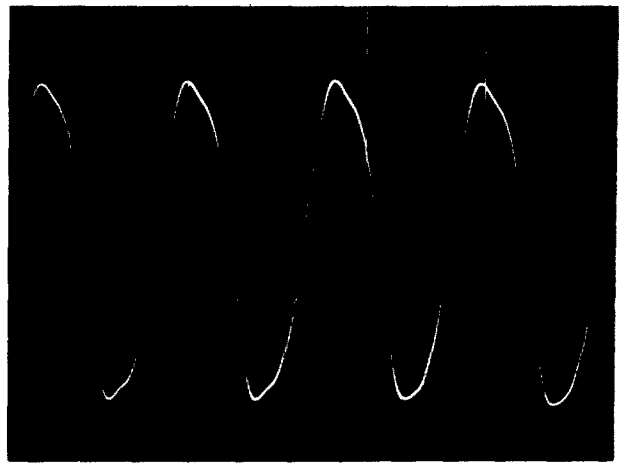

Initial Al Cathode Signal Trace
20-mv/cm PM Voltage 750

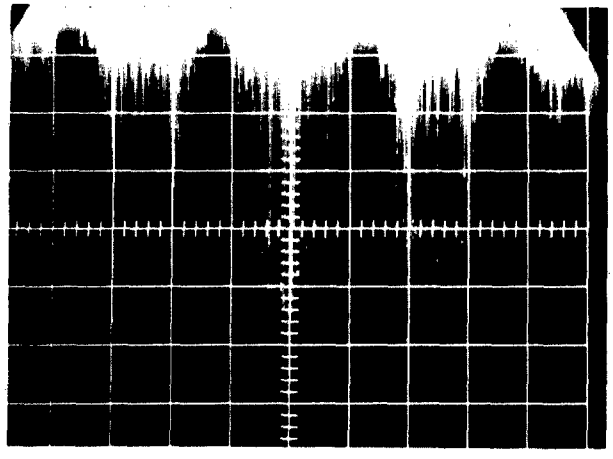

Final Al Cathode Signal Trace
Showing Effects of Cathode Sputtering
200 mv/cm PM Voltage 900

Figure 26. INITIAL AND FINAL SIGNAL TRACES FOR 72-HOUR ALUMINUM CATHODE RUN

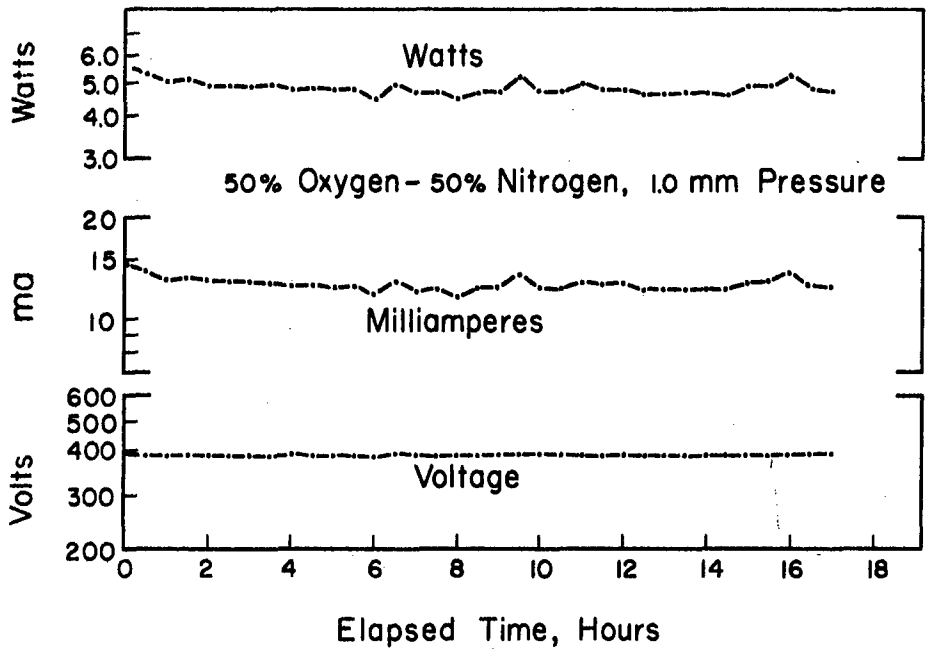


Figure 27. 17-HOUR GOLD-PLATED CATHODE STABILITY RUN

It was planned to run the gold-plated source continuously for a 30-day test period using the 50% oxygen-50% nitrogen and the same 50 Å half-power interference filter.

The oscilloscope response to the output signal is shown in fig. 28. On the sixth day the oscilloscope trace indicated a small decrease in signal output but nothing else unusual. However a visual examination of the discharge showed small irregularities in the glow, which appeared to be near the rear of the cathode. This was also observed at the end of the fifteenth day accompanied by an additional decrease in photomultiplier output, fig. 28c. This was interpreted to mean some degradation of the gold plate, although no sputtering effect was observed and the decrease was relatively small as compared to that for the aluminum cathode.

At this time the source was opened for visual examination. The gold-plated anode showed some darkening in rings but no appreciable corrosion. However the cathode was darkened throughout the cell with very small beads of gold scattered about on the surface. Near the insulator, corrosion had definitely taken place in a ring pattern.

During this run there was no increase in power to the hollow cathode or voltage to the photomultiplier to maintain sensitivity. In addition there was no loss of transmittance through the quartz window.

The hollow cathodes used from this point on were lined with a single layer of 0.005-in. gold foil. The foil is rolled on a mandril slightly less than 1/4-in. in diameter (different sizes for different cathodes), inserted into the hollow cathode, then fitted into place by simply reversing the mandril. Some cathodes were used with lining only with a press fit although it is better to silver solder the end, then the end surface was polished. These gold-foil-lined cathodes remain bright even after much use, resembling a polished surface. Some slight erosion could be seen after much use, for example, after a month or two.

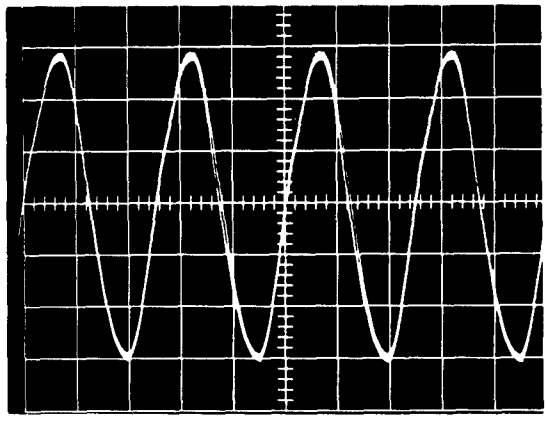

a. Beginning of Run

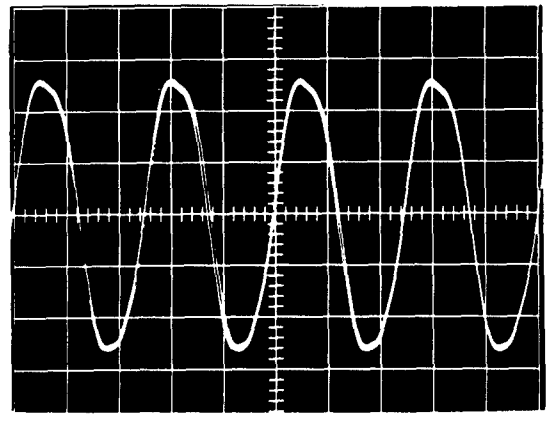

b. After 6 days of Operation

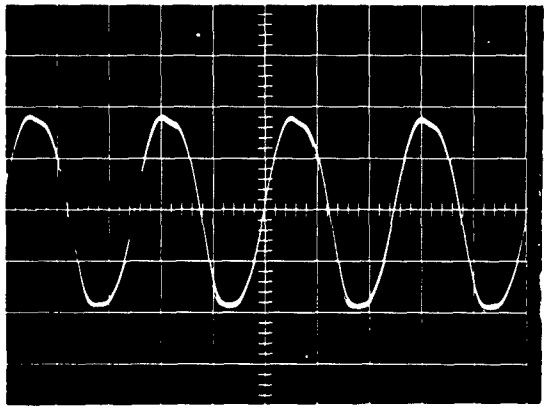

c. After 14 days

Figure 28. OSCILLOSCOPE RESPONSE TO SIGNAL FROM GOLD-PLATED HOLLOW-CATHODE SOURCE

## The $CO^+$ Bands

In the studies using aluminum cathode, the supposedly strong and persistent bands at 2883 Å and 2896 Å did not develop. Using the gold-lined cathode with the 3/4-meter Czerny-Turner spectrograph, this band pair developed strongly. Each band is composed of two strong lines, then a closely spaced group of lines to form the band. These two bands occur in a so-called window between intense nitrogen bands. However at this time the instrument design had been fixed and these bands were not used. A reexamination of the spectrographic plates taken earlier using the aluminum hollow cathode showed no trace of these bands in the 5% $CO_2$ range.

## Influence of Cathode Design Parameters

### Open End vs. Closed End Cathode

The initial plan was to use an open hollow cathode, i.e., one in which the air entered the anode chamber and was exhausted through the cathode. It was expected that this type would have a quicker and truer response to any change in composition since there would be no static air space as there would appear to be with a closed end cathode, fig. 24. It was found that the discharge did travel down the exhaust tube even though glass insulator tubes were inserted in the leads and the metal hollow cathode itself was connected directly to the negative pole of the power supply.

Routinely, air was used in a standard closed hollow cathode that had been set up for some experimental analyses of solids. In this type, air was taken in near the window and exhausted through a port close to the cathode, fig. 24. The intensity of the lines was surprisingly strong, much more than expected. Therefore a comparison of the signal level as a function of power with the two types of cathodes using the same pressures and cathode dimensions was made. The results, fig. 29, show the response to be much greater for the conventional cathode.

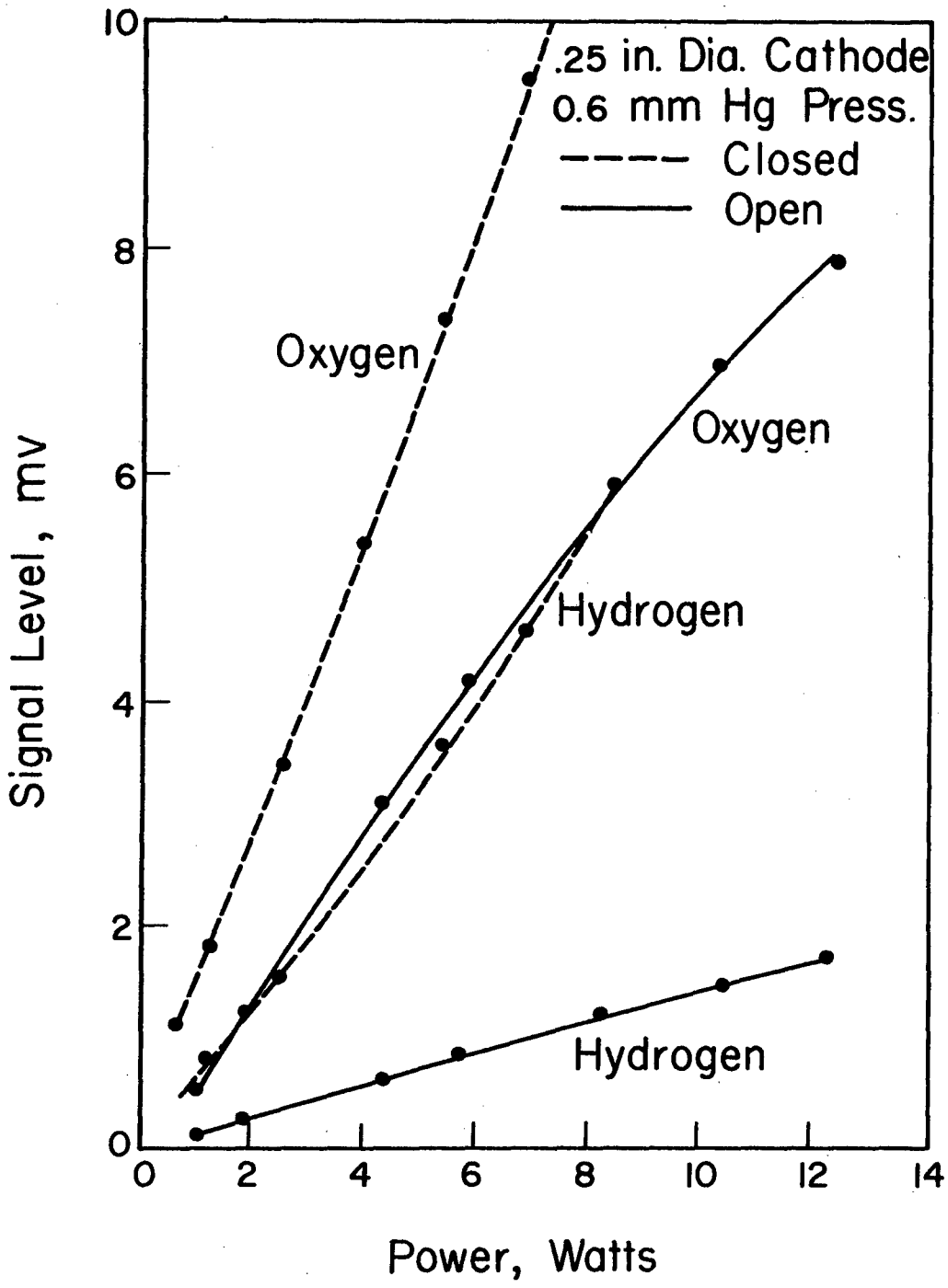


Figure 29. COMPARISON OF RESPONSE FOR OPEN AND CLOSED CATHODE

Experiments were then performed with the conventional cathodes to determine the drift and response since the so-called dead air space was not expected to immediately reflect with a change in air composition but to change slowly which would appear to be drift in the output signal. This was found not to be the case.

Cathode Diameter Larger than Insulator Opening

Dr. R. S. Braman (ref. 7) devised and briefly studied a cathode using an inside diameter larger than the opening in the dividing insulator and used helium as the carrier gas. This unit appeared to operate with an excellent collimated beam and appeared very stable. The size of the beam was the diameter of the opening in the insulator. Therefore a cathode was prepared for study using air as the gas for this program, fig. 30.

The results of this initial study using an aluminum cathode were quite disappointing. The spectra contained a great number of intense diatomic emission bands. The carbon 2478 Å line was completely masked though it was reasonably measurable in previous spectra from the conventional cathode. Weak bands were found in the vicinity of both the H-6562.7 Å and the O-7771.9 Å lines. In addition the intensity of these analytical lines were less for equivalent operating conditions.

After the value of the gold inserts was established, this concept was again explored. The spectral intensity was more satisfactory and the discharge appeared quite stable.

An 11-day stability run was made using 50% oxygen-50% nitrogen. The anode was the same as described previously. The cathode cavity was 3/8-in. diameter by 1-in. deep. The vycor insulator contained a 1/4-in. hole. Previous short runs, 8 hours, seemed to indicate that this configuration caused a pinch effect with a resultant signal enhancement. At a point, 100 hours into the run, it was observed that the insulator had cracked as well as becoming heavily gold plated. Resistance measurements from the front to the back side of the insulator were in the 15 ohm range. A new insulator with a 3/8-in. hole was installed and the run continued.

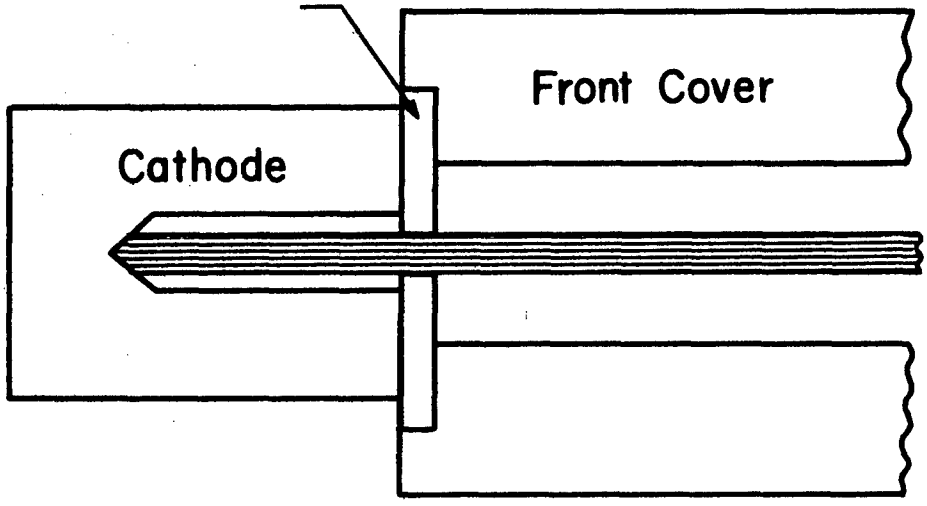


Figure 30. HOLLOW-CATHODE SOURCE
USING SMALL DIAMETER OPENING IN INSULATOR

The PM output was quite stable during most of the run, but during the middle part and again at the end a slow drift was observed accompanied by an increase in the noise level which corresponded to a variation of 1 to 2% of the reading. An examination of the cathode did not reveal a reason for these changes. However, it was observed at this time and again later that the insulator becomes coated with a layer of gold which would short the unit. No further experiments were performed with a reduced diameter insulator.

Final Cathode Design

The preceding hollow cathode as well as one using an insulator opening the same size as the cathode were found to be reasonably stable and would reproduce at a given pressure when a selected gas mixture was changed then returned to the original mixture. However, there was not sufficient reproducibility of data for different days although all the variables according to measurements were constant. This is illustrated in figs. 31 and 32, especially for oxygen and nitrogen. The variation in readout applied to a specific gas composition after a change in pressure or after restarting the discharge.

In a program presently in progress (ref. 8) we have shown good reproducibility with good pressure measurement instrumentation. At present we are using the MKS Baratron Type 90 pressure meter which is a very accurate and continual measurement device.

The flow-through type cathode was again examined but using a gold insert with the ends loosely folded to form a semi-closed cathode. Discharge was stable and the discharge was retained, i.e., it did not travel down the tube. However, sensitivity again was not good. The small openings in the end enlarged apparently due to sputtering which caused changes in readout.

A new design was developed in which the gas flowed through the opening in the vycor insulator to the conventional hollow cathode where it spreads to eight openings or exit tubes and is pumped from the rear of the cathode. This final design is shown in fig. 33. The narrow space between the cathode and insulator, 0.015 in., was offset

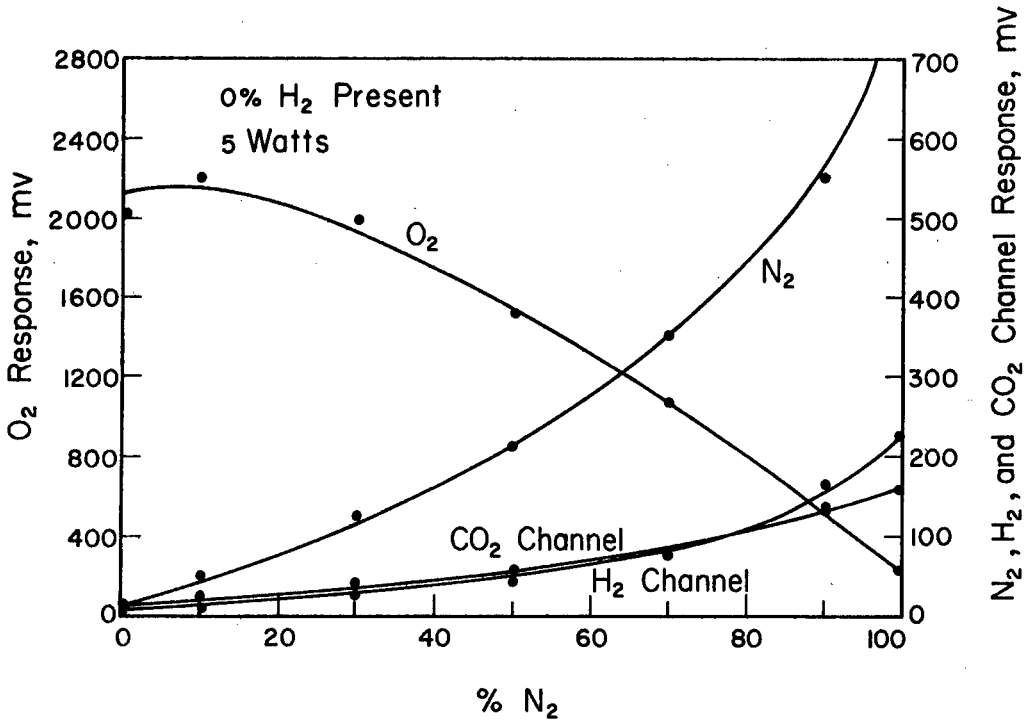


Figure 31. RESPONSE FOR $O_2$ AND $N_2$ AND INFLUENCE OF $N_2$ ON THE $H_2$ AND $CO_2$ CHANNELS

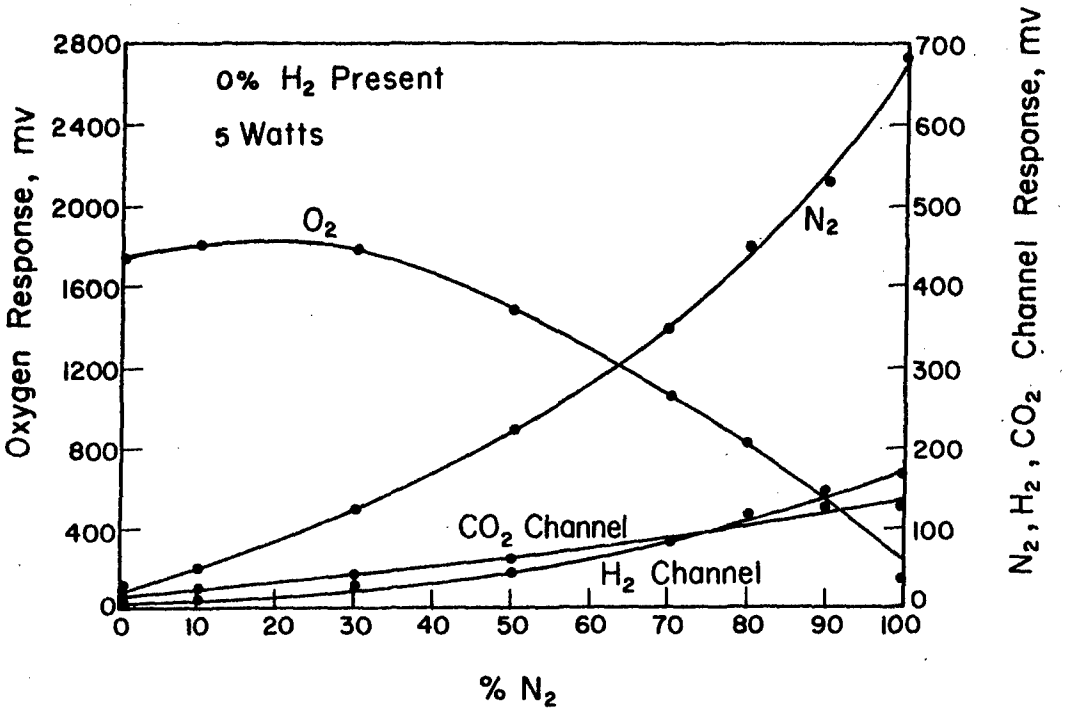


Figure 32. RESPONSE FOR $O_2$ AND $N_2$ AND INFLUENCE OF $N_2$ ON THE $H_2$ AND $CO_2$ CHANNELS

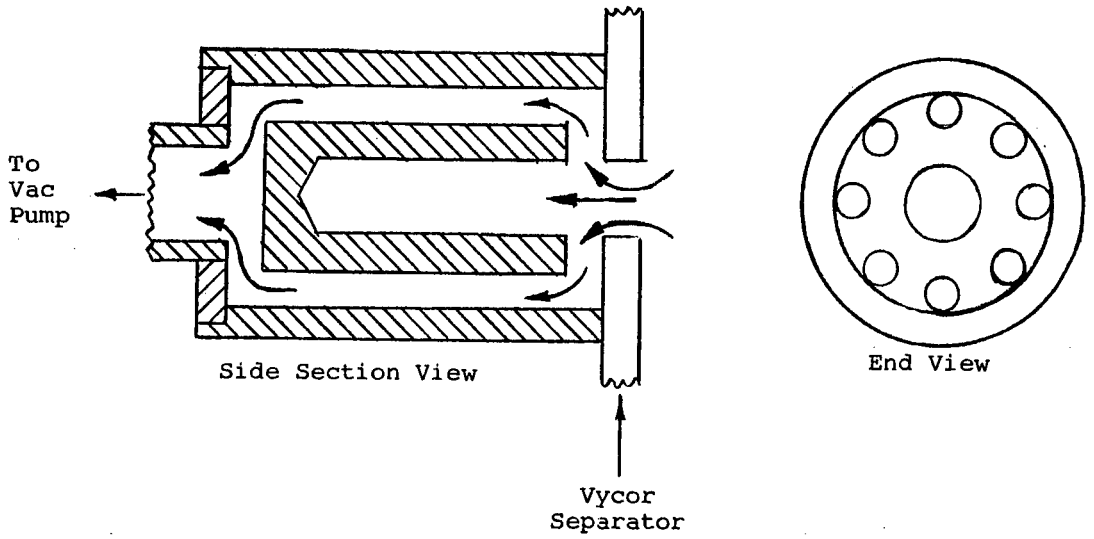


Figure 33. FINAL DESIGN OF HOLLOW CATHODE SOURCE

to permit air passage to the small exhaust tubes and was included to create a small pressure drop. This was to create a more stable discharge and to prevent the discharge from dropping back into the exhaust tubes which caused a change in discharge characteristics, i.e., a decrease in emission output. The last design included a cathode which was actually a reversible unit held in place by a press fit. Gold foil was again used as an insert. The resulting discharge was very stable. Based on a calculation that a 2% change in PM response represented one scale division on the recorder, variation was in the order of ± 1/2% for short runs and approximately ± 1% for the longer periods, such as 8 hours.

MODE OF POWER

The hollow cathode source can operate using three modes of power regulation, i.e., constant voltage, constant current and constant power.

Figures 34 and 35 show the response for oxygen 8446.4 Å and nitrogen 8216.5 Å lines for these modes of power regulation for the concentration range of the standard gases. In general, the response was more linear as a function of concentration with constant current so this mode was adopted for instrument operation.

If voltage is fixed and maintained constant, then the current and power varies as the gas composition varies in the excitation source at a given pressure. If the current is maintained constant the voltage varies in the same manner. If the input power is maintained constant, both the voltage and current vary as a function of the change in resistance due to the gas composition. Depending on the gases the voltage or current can have a wide range of changes. These variations are illustrated in table III.

In these experiments the gas concentrations cover a very wide range in order to see the influence on the mode of excitation. If more narrow ranges of gas concentrations were used, as in the practical situation, the variation in electrical parameters would be less. Also

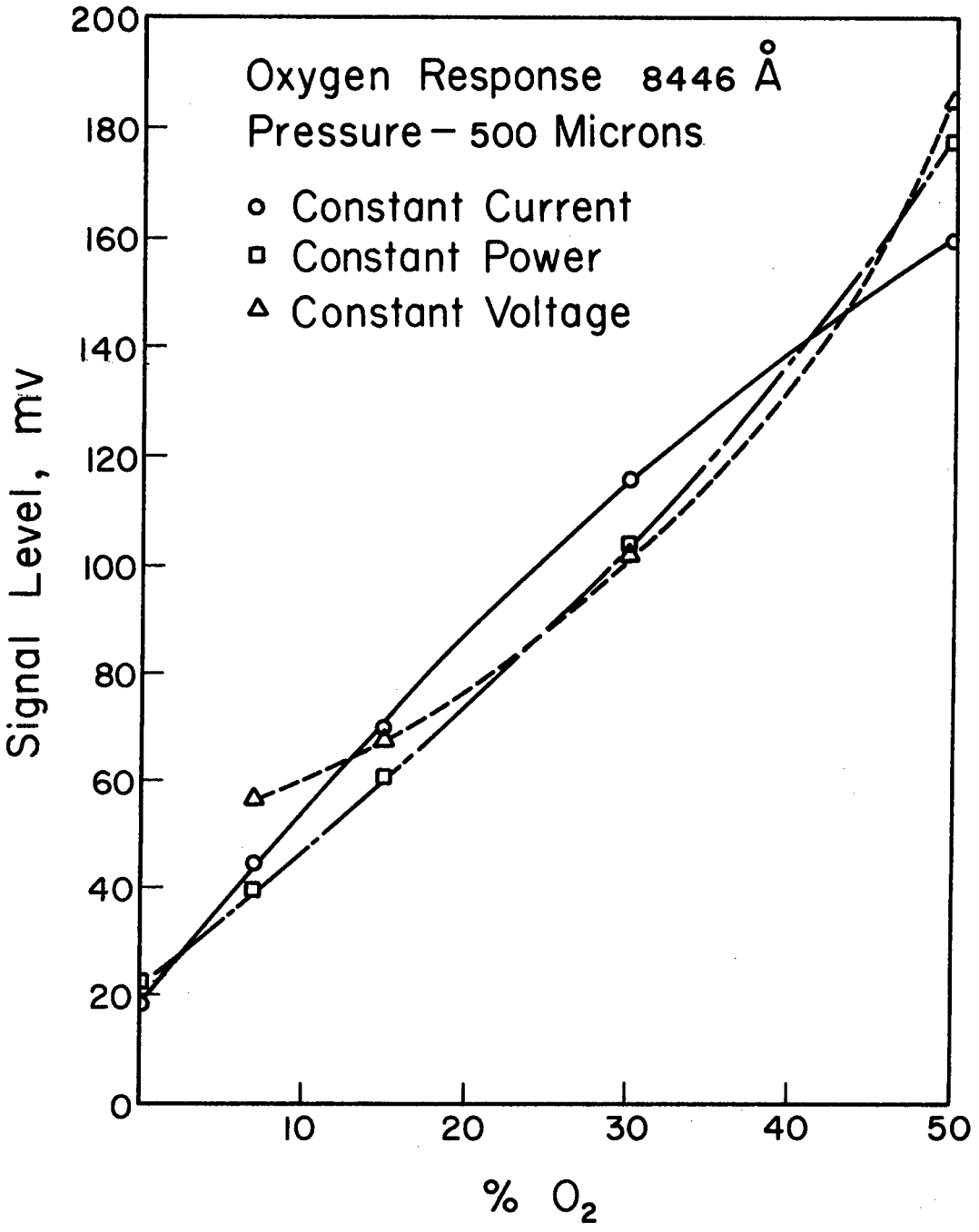


Figure 34. POWER MODE RESPONSE CURVES FOR OXYGEN

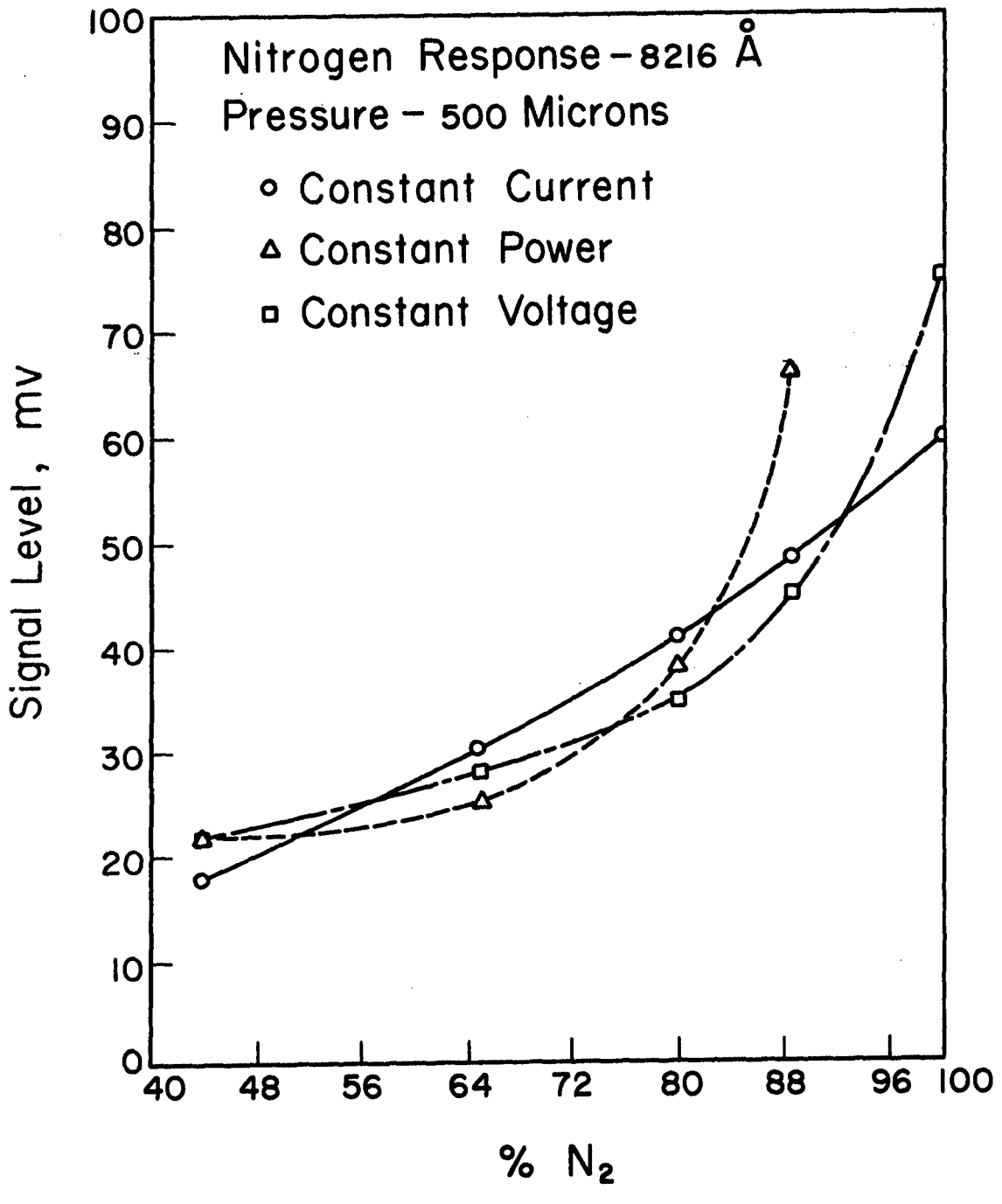


Figure 35. POWER MODE RESPONSE CURVES FOR NITROGEN

Table III. RESPONSES FOR HYDROGEN, OXYGEN AND NITROGEN CONCENTRATIONS

| % Conc. | | | Constant Current | | | | | | Constant Power | | | | | | Constant Voltage | | | | | |
|---|---|---|---|---|---|---|---|---|---|---|---|---|---|---|---|---|---|---|---|---|
| | | | | | | Response, mv | | | | | | Response, mv | | | | | | Response, mv | | |
| $H_2$ | $O_2$ | $N_2$ | Volt | ma* | Watt | $H_2$ | $O_2$ | $N_2$ | Volt | ma | Watt* | $H_2$ | $O_2$ | $N_2$ | Volt* | ma | Watt | $H_2$ | $O_2$ | $N_2$ |
| 1 | 50 | 44 | 372 | 5 | 1.86 | 9 | 160 | 17.8 | 374 | 5.4 | 2.0 | 12 | 178 | 22 | 378 | 6.0 | 2.3 | 11 | 185 | 22 |
| 2 | 30 | 65 | 387 | 5 | 1.94 | 21 | 116 | 30.5 | 386 | 5.2 | 2.0 | 20 | 104 | 28 | 378 | 4.2 | 1.6 | 21 | 102 | 25 |
| 3 | 15 | 80 | 383 | 5 | 1.92 | 47 | 70 | 41 | 384 | 5.2 | 2.0 | 40 | 61 | 35 | 378 | 4.8 | 1.8 | 44 | 68 | 38 |
| 3-1/2 | 7 | 88 | 368 | 5 | 1.84 | 73 | 45 | 48.5 | 370 | 5.4 | 2.0 | 66 | 40 | 45 | 378 | 6.3 | 2.4 | 90 | 57 | 66 |
| | | 100 | 329 | 5 | 1.64 | 36 | | 58 | 336 | 6.0 | 2.0 | 37 | | 75 | | | | | | |
| 100 | | | 912 | 5 | 4.57 | 550 | | | No Discharge | | | | | | | | | | | |
| 100% $CO_2$ | | | 472 | 5 | 2.36 | 10 | | 7 | 469 | 4.2 | 2.0 | 7 | | 5 | | | | | | |

*Value arbitrarily selected.

if gases with more similar excitation potentials were involved, this variation would be less.

The variation also takes place in the excitation of binary gases especially when one has a large and the other a relatively small excitation potential such as for helium and oxygen.

## FACTORS INFLUENCING RESPONSE

The size, shape, pressure, major gas and power are parameters that influenced the response from the hollow cathode.

### Closed End Cathode

The cathode in which the air was taken in through the anode chamber and exhausted through the cathode proved to have much less response, i.e., much less sensitive under equivalent condition of power and pressure than the conventional hollow cathode. In the latter case the sample entered near the front of the anode chamber and passed across in front of the cathode to the vacuum pumps, fig. 24.

### Pressure Power Response Curves

For a given cathode dimension the PM response is nearly a linear function of the input power at a given pressure. The response for the hydrogen 6562.7 Å and the oxygen 8446.4 Å lines are shown in figs. 36 and 37. The response was similar for other emission lines. The data was obtained by means of a chopped signal using a setup based on fig. 2 and the readout equipment from the panels in fig. 3.

The deflection shown at the low pressures and lower power levels appears to represent a shift in the mode of excitation. As gas pressure is increased the change takes place at lower power levels. From visual observations a weak glow seemed to appear at the face or opening of the cathode. As power was increased, the glow shifted

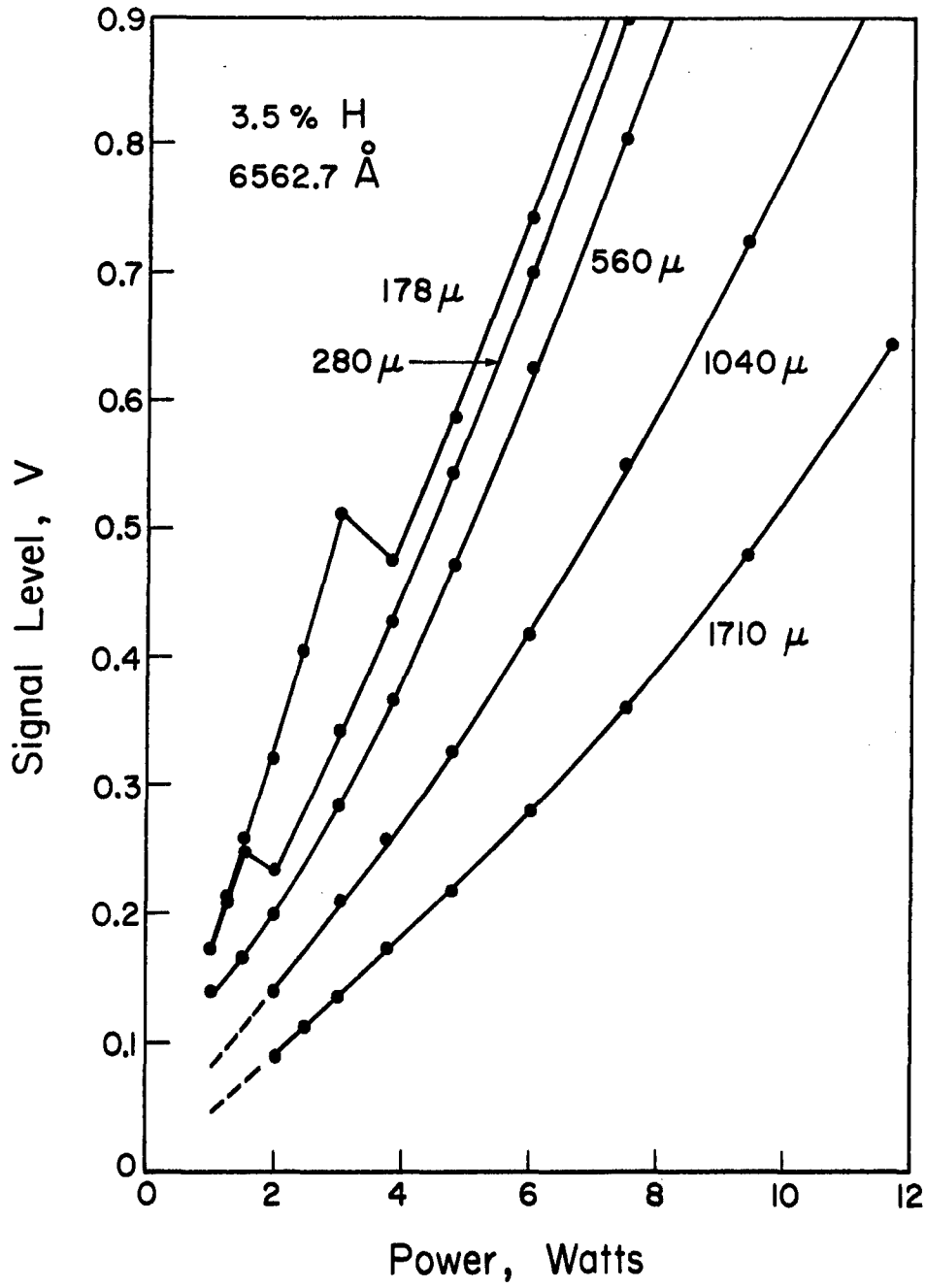


Figure 36. POWER-PRESSURE RESPONSE CURVES FOR HYDROGEN

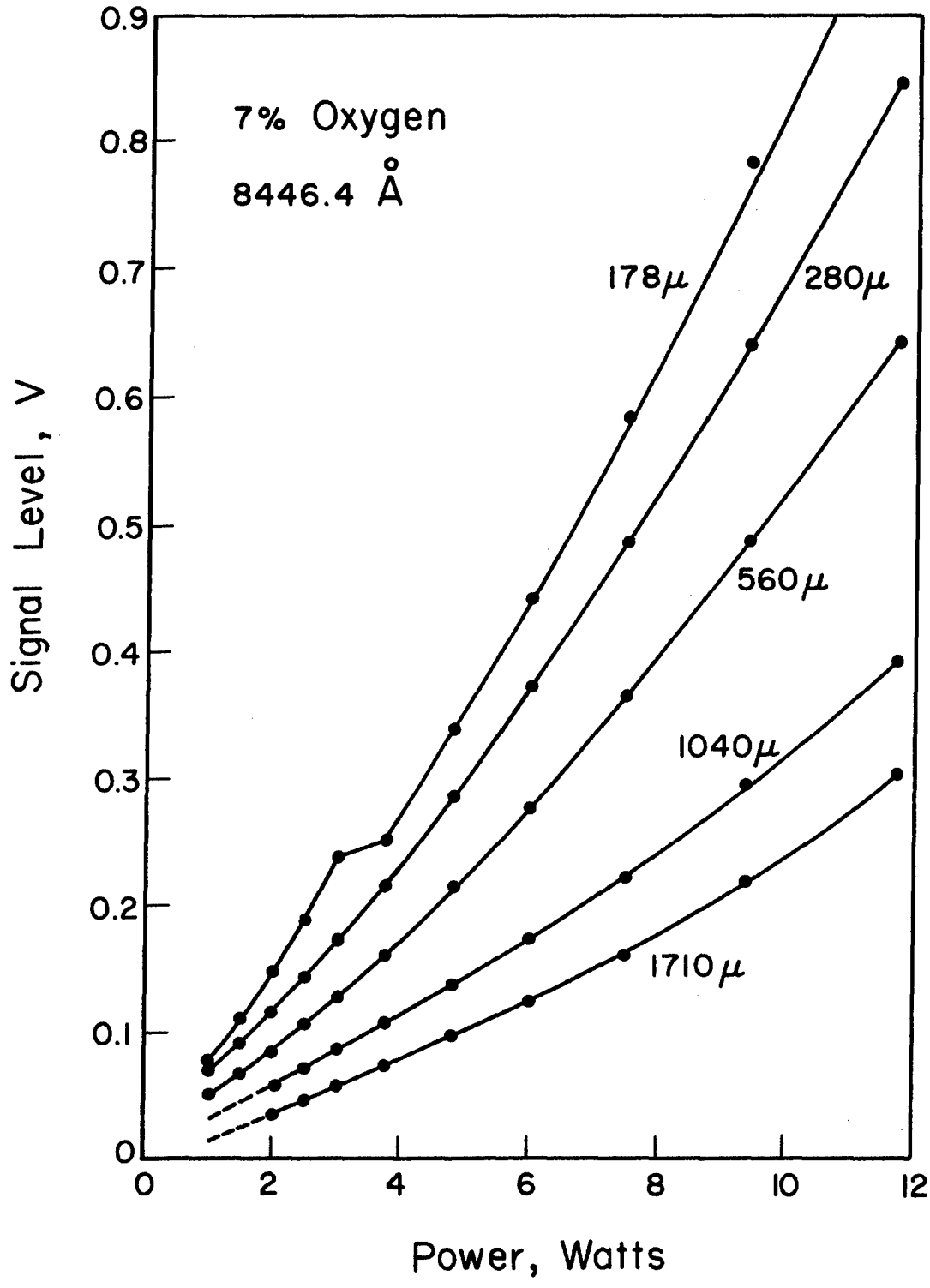


Figure 37. POWER-PRESSURE RESPONSE CURVES FOR OXYGEN

back into the cathode which at a given pressure level resulted in a deflection of the response curve. These experiments were performed with the conventional gold-lined cathode.

In the preliminary studies in which the aluminum cathodes were being used with the 3.4 Ebert spectrograph with photographic readout, this same effect in which the output was influenced by pressure at a constant gas composition was noticed to be quite pronounced for nitrogen and oxygen in natural air.

Cathode Dimensions

The dimensions of the hollow cathode influence the level of the selected line radiation. Figure 38 illustrates the response for the O-7771.9 Å line for different depths for a 1/4-in. diameter cathode. The 1/4-in. deep cathode produced a response for He slightly below that for the 1/2-in. depth, and the response for oxygen was erratic but at about the same level as for the 1/2-in. cathode.

The change in size has less effect on helium with its very high ionization potential than on oxygen with its lower ionization potential.

The 1/4-in. diameter cathode produced a greater spectral response at given conditions than the 3/8-in. cathode, fig. 39. This work, performed on the 3.4-meter Ebert spectrograph, was again confirmed on the 1-meter Czerny-Turner spectrometer. In this latter study, a 1/8-in. diameter cavity produced a still greater response than the 1/4-in., however, it was difficult to start and maintain especially with helium atmospheres. Figures 20 and 23 show that the larger diameter cathode cavity yields the greatest signal response. This is apparently due to the focus of the lens in the cathode and the mask over the PM tube.

A question was raised concerning the possible reflections from the rear of the hollow cathode. A 1/4-in. diameter piece of black Viton (rubber) was inserted to the back of the cathode. Response data indicated that

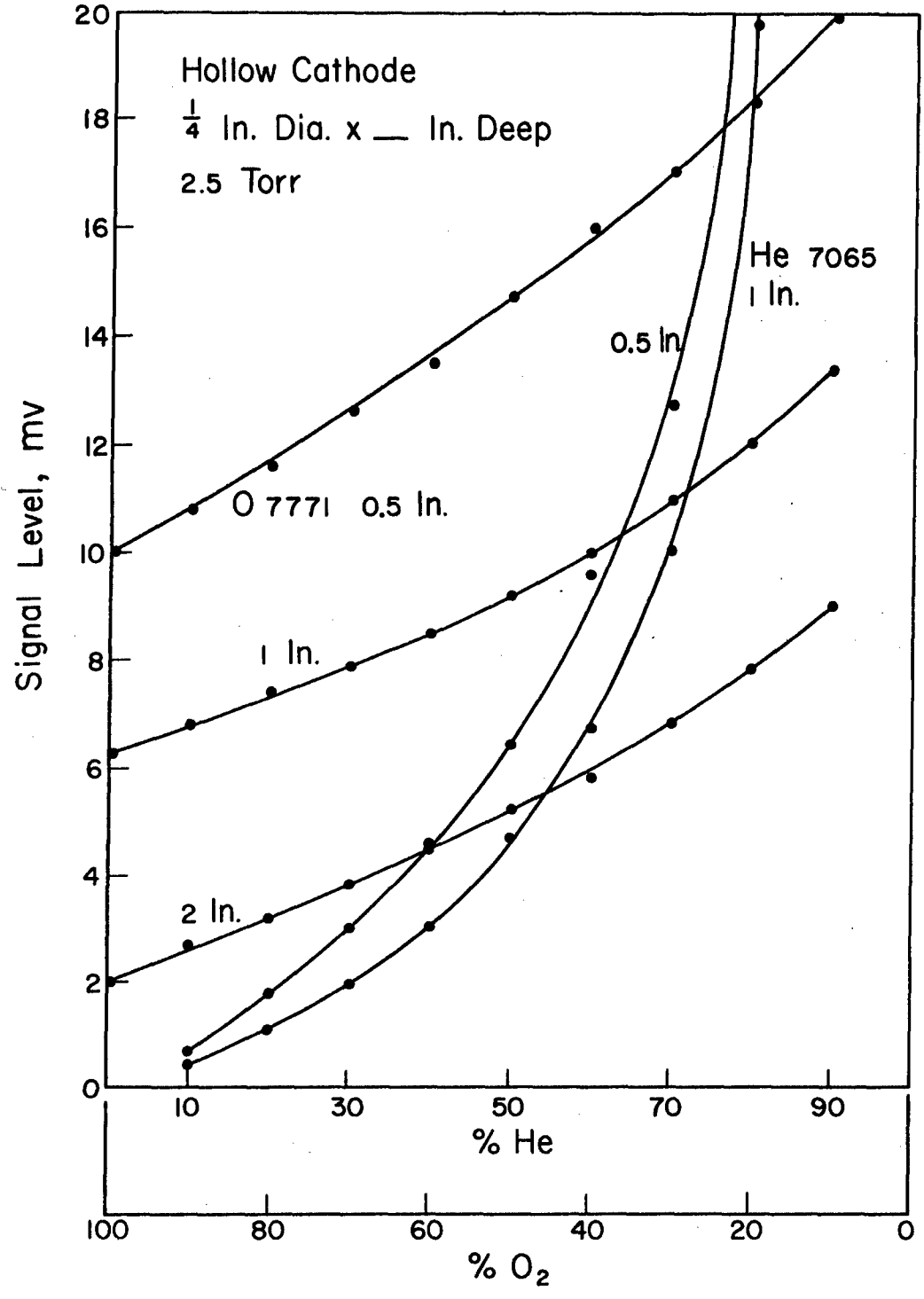


Figure 38. EFFECT OF CATHODE CAVITY LENGTH ON SPECTRAL RESPONSE

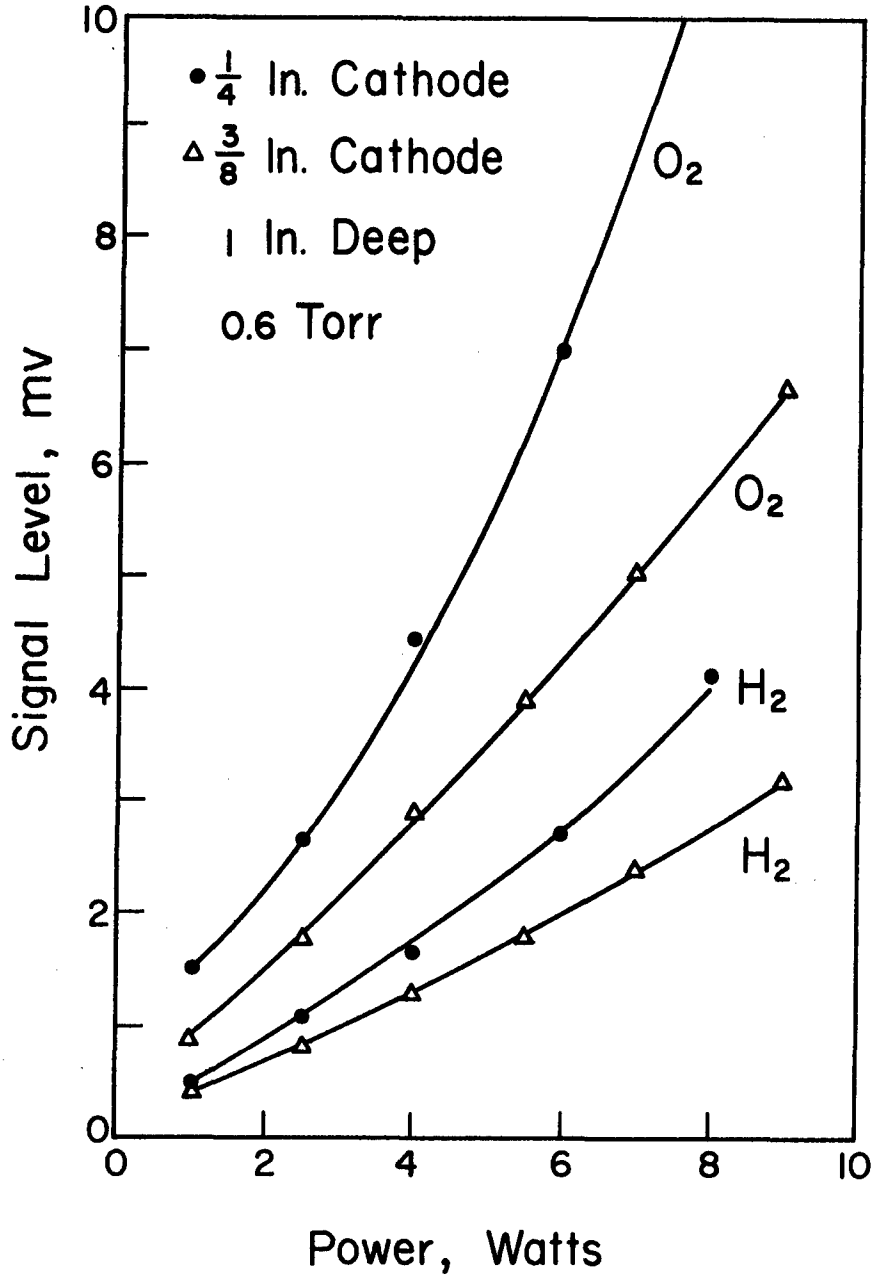


Figure 39. EFFECT OF CATHODE CAVITY DIAMETER ON SPECTRAL RESPONSE

this had essentially no effect on the output; thus possible reflections are of no significance.

## SPECTRAL RESPONSE OF SELECTED BINARY MIXTURES

A number of binary and in a few cases ternary mixtures were studied to determine the influence of one gas on the spectral response of a second as a means of establishing the feasibility of this concept in different atmospheres. These consisted of combinations of the three inert gases as well as inert gases with oxygen, nitrogen and hydrogen. In each case the range of concentrations studied were greater than one would expect to encounter in actual use.

Most of these data were obtained from the use of the spectrometers instead of from the use of interference filters.

### Helium-Oxygen

The response for the oxygen 6158.2 Å atomic line, fig. 40, relative to that for the oxygen 7771.9 Å line is much less. The oxygen 8446.4 Å line is also much more sensitive than the oxygen 6158.2 Å line, although it is near the limit of sensitivity for the S-20 response PM tube. This is not surprising since the excitation potential for the 6158.2 Å line is 12.7 eV, somewhat greater than the excitation potentials for the 7771.9 Å and 8446.4 Å lines, and its listed relative density is half that of the 8446.4 Å oxygen line. The response for the hydrogen 6562 Å doublet shown in this figure is from the moisture in the helium gas which is rated as high purity.

It should be noted that the spectral response for oxygen in helium increases as its concentration decreases. Photographs of the spectra for this region showed no band spectra or other interference that would cause this effect which should be the case if the helium was sufficiently pure. However, some argon lines were found.

The influence of pressure on the response is small for helium, fig. 41, but large for oxygen, fig. 42. At the pressure of 1 Torr the discharge could not be

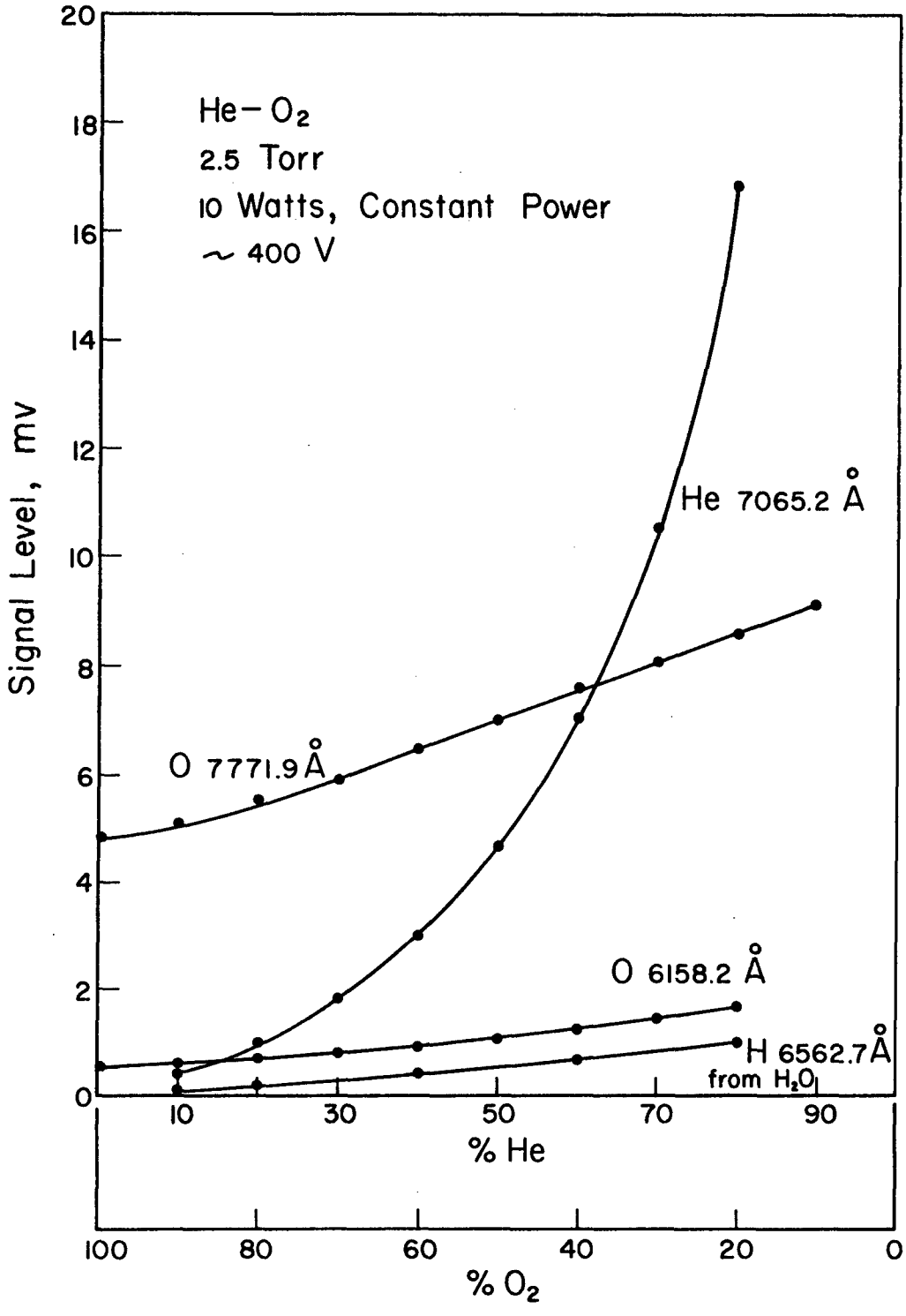


Figure 40. RESPONSE FOR $He-O_2$ BINARY MIXTURE

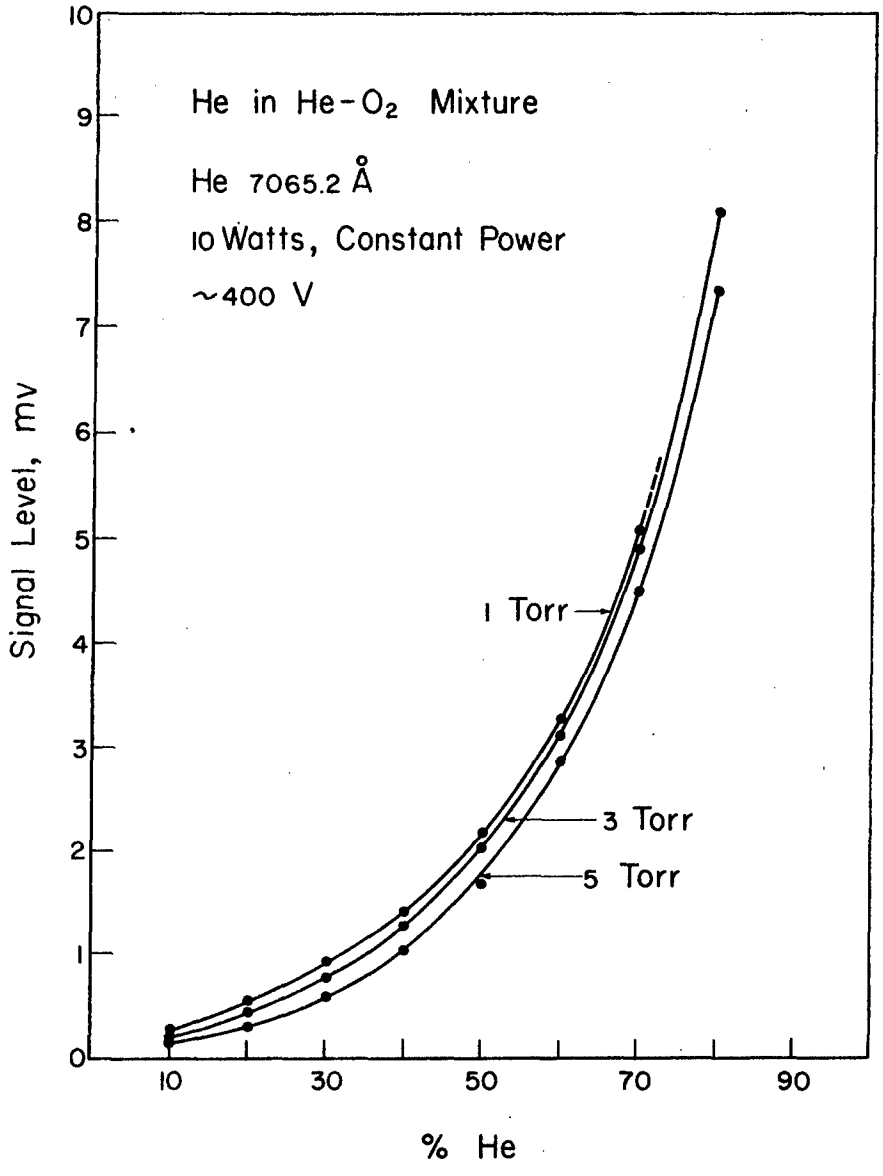


Figure 41. INFLUENCE OF PRESSURE ON HELIUM RESPONSE

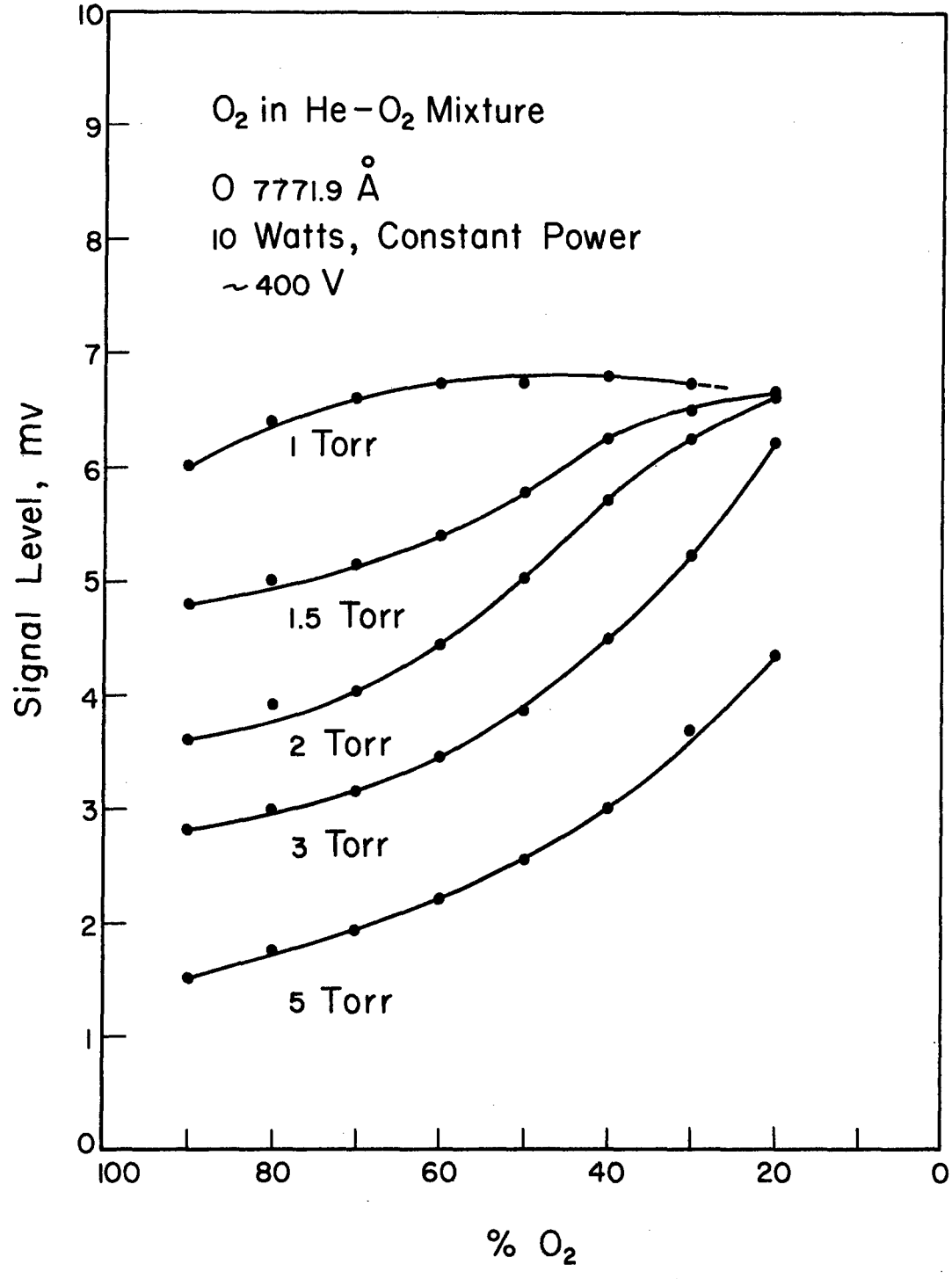


Figure 42. INFLUENCE OF PRESSURE ON OXYGEN RESPONSE

maintained at a helium concentration greater than 70%. In the 90 to 100% helium concentration range, approximately 3 to 3.5 Torr pressure was required to maintain the discharge. With good quality helium the response as a function of pressure at constant power was at its maximum at approximately 6 Torr.

Helium-Hyrdogen

Figure 43 illustrates the spectral response for the different concentrations for helium and hydrogen in binary compositions. The hydrogen response behaves in a similar manner as the oxygen in the helium, i.e., the spectral response is greater as the helium concentration increases. In addition, hydrogen also showed little sensitivity to change in its concentration at the lower pressures, e.g., 1 Torr. Spectrograms revealed no spectral interferences to produce this effect as was previously observed with oxygen and hydrogen in nitrogen.

This experiment was operated at a constant power of 10 watts. Considerable gold was found deposited on the vycor insulator after this group of experiments.

Helium-Nitrogen

The response of the nitrogen atom line 8216.5 Å for the helium-nitrogen mixtures followed the same pattern as the helium-oxygen and helium-hydrogen mixtures with respect to the influence of helium concentration and pressure.

It is of interest that the $N_2$ band at 3371 Å showed good sensitivity and a positive response with respect to its increasing concentration in helium.

Helium-Neon

The neon 6328.2 Å line strongly shows the influence of the increasing concentration of helium. The intensity of this line was relatively weak at the 100% concentration of neon. Then its spectral intensity increased very rapidly as the concentration of helium increased and the

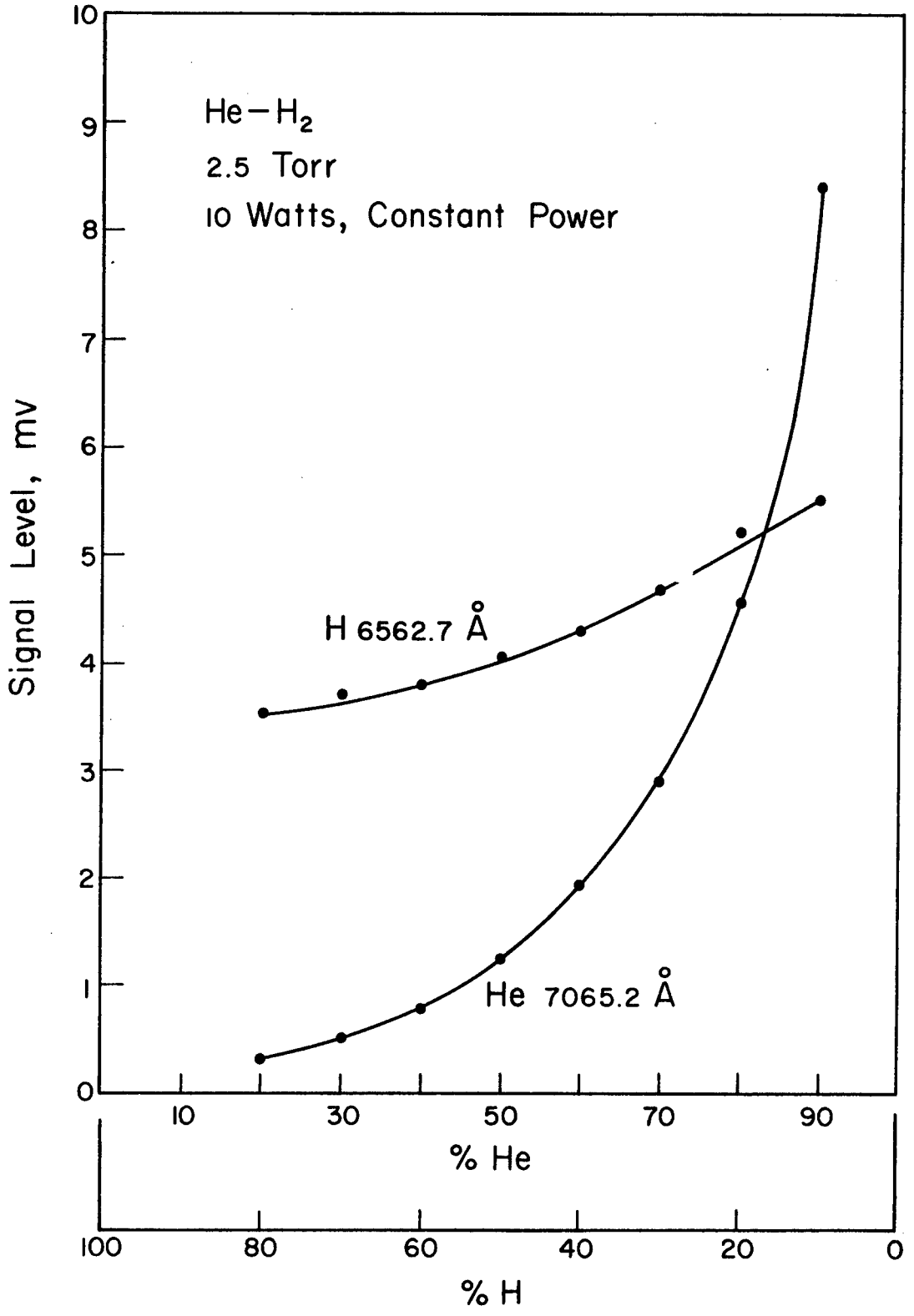


Figure 43. RESPONSE FOR $He-H_2$ BINARY MIXTURE

neon decreased, fig. 44. Two other atomic lines for neon, 7032.4 Å and 7245.2 Å, actually indicated a marked decrease in spectral intensity followed by a strong increase as its concentration continued to decrease. The readout values for these two lines were somewhat erratic, i.e., did not follow a smooth curve, but the response for both lines behaved in the same manner.

It is interesting to note that the 6328.2 Å neon line is the excited line of the helium-neon gas laser and that the 10 to 20% range is the range, and the 2.5 Torr are values associated with these gas lasers.

In each of the above cases, He-$O_2$, He-$H_2$, He-$N_2$ and He-Ne, the influence of the increasing concentration of helium is reflected in the much more efficient excitation of the element with the lower excitation potentials. It is noteworthy that at constant power operation the voltage drop across the hollow cathode increases as the helium concentration decreases.

Helium-Argon

The spectral response for argon increased in a quite linear fashion with its concentration, fig. 45. This was true for both the more intense lines such as the 7067.2 Å and the less intense lines 8006.2 and 8014.8 Å. This was not the expected response considering that the excitation and ionization potentials are in the same order as for oxygen, hydrogen and nitrogen. These values are listed in table IV.

Neon-Argon

The argon does increase as a function of concentration in decreasing neon concentrations, fig. 46. In this case the spectral response for argon was similar to that for argon in helium.

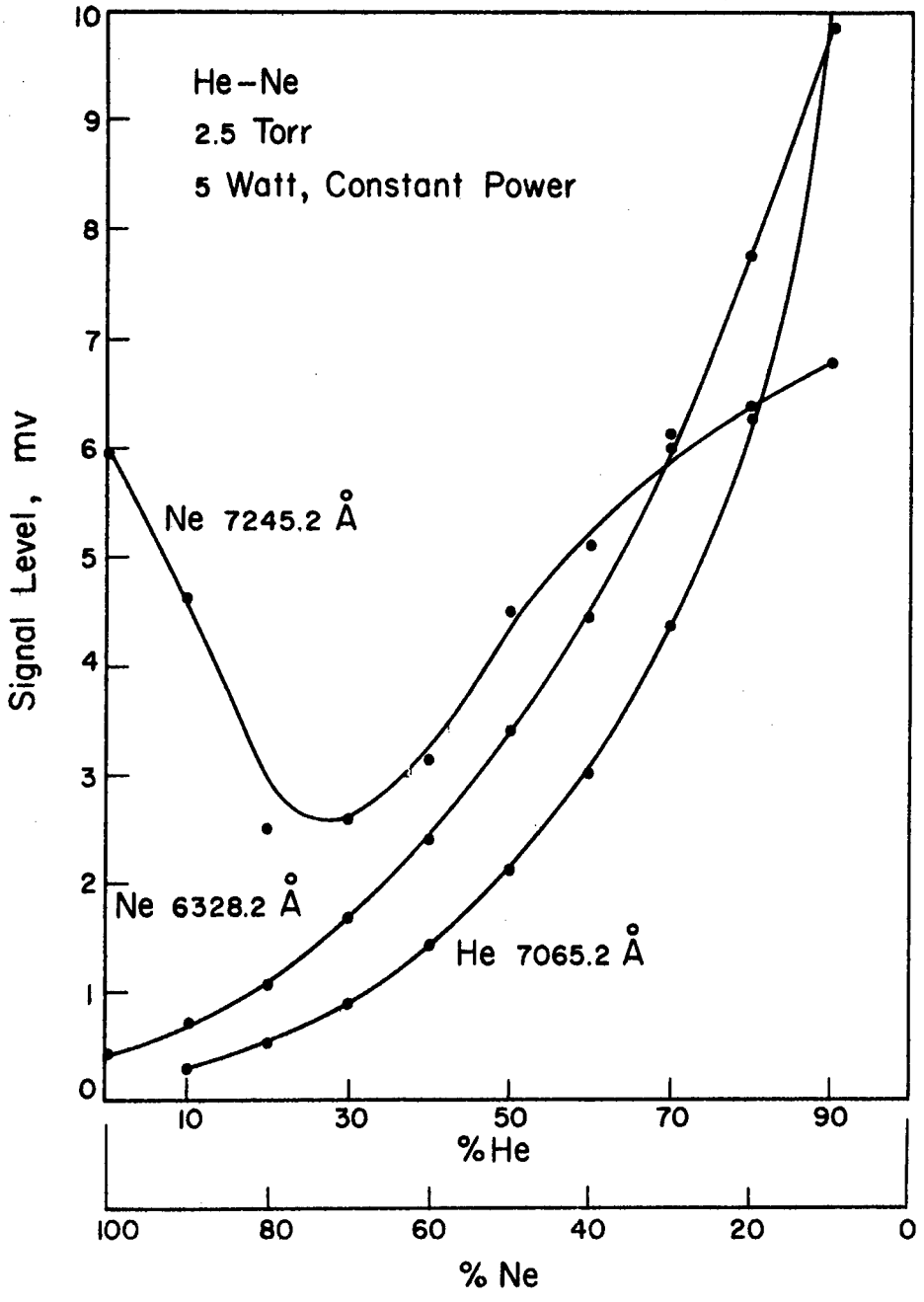


Figure 44. RESPONSE FOR He-Ne BINARY MIXTURE

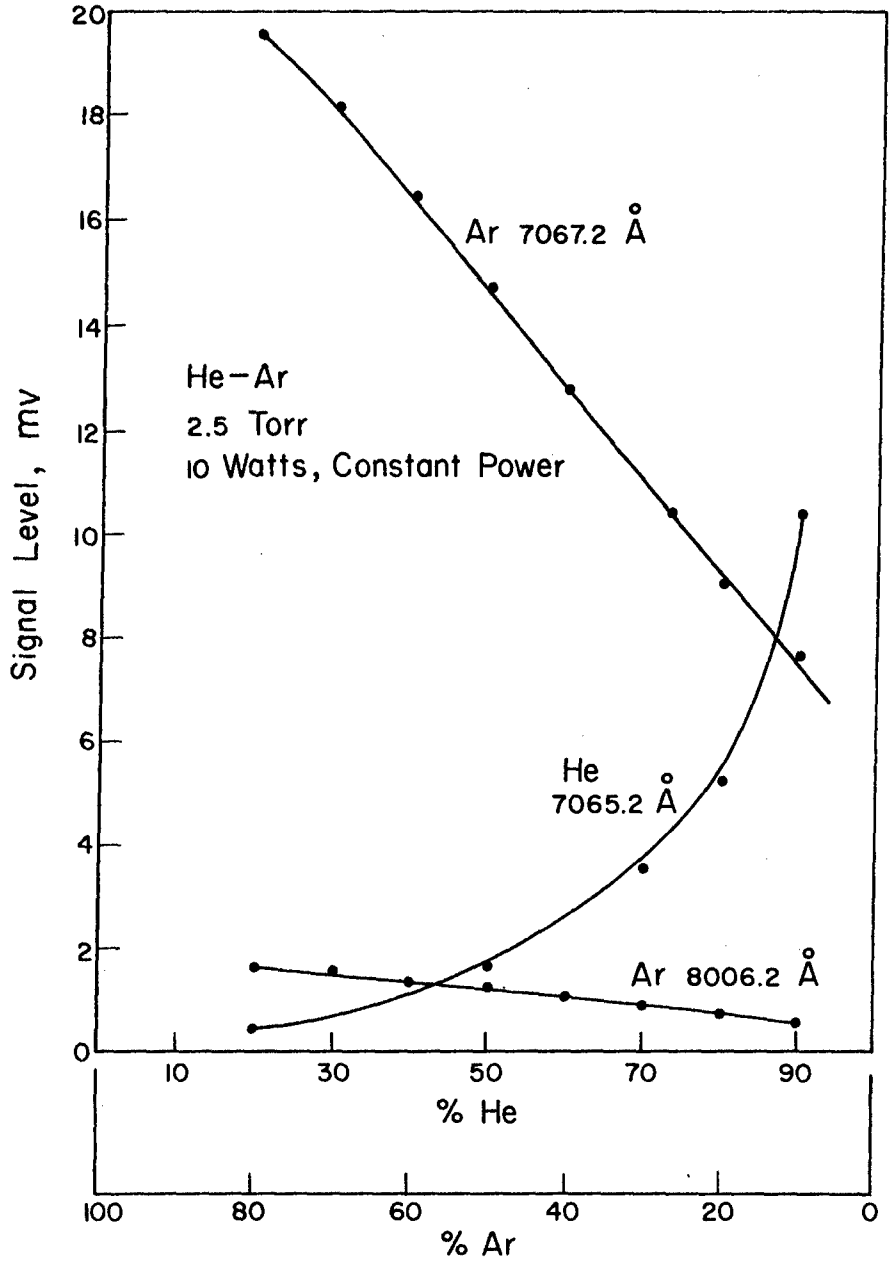


Figure 45. RESPONSE FOR He-Ar BINARY MIXTURE

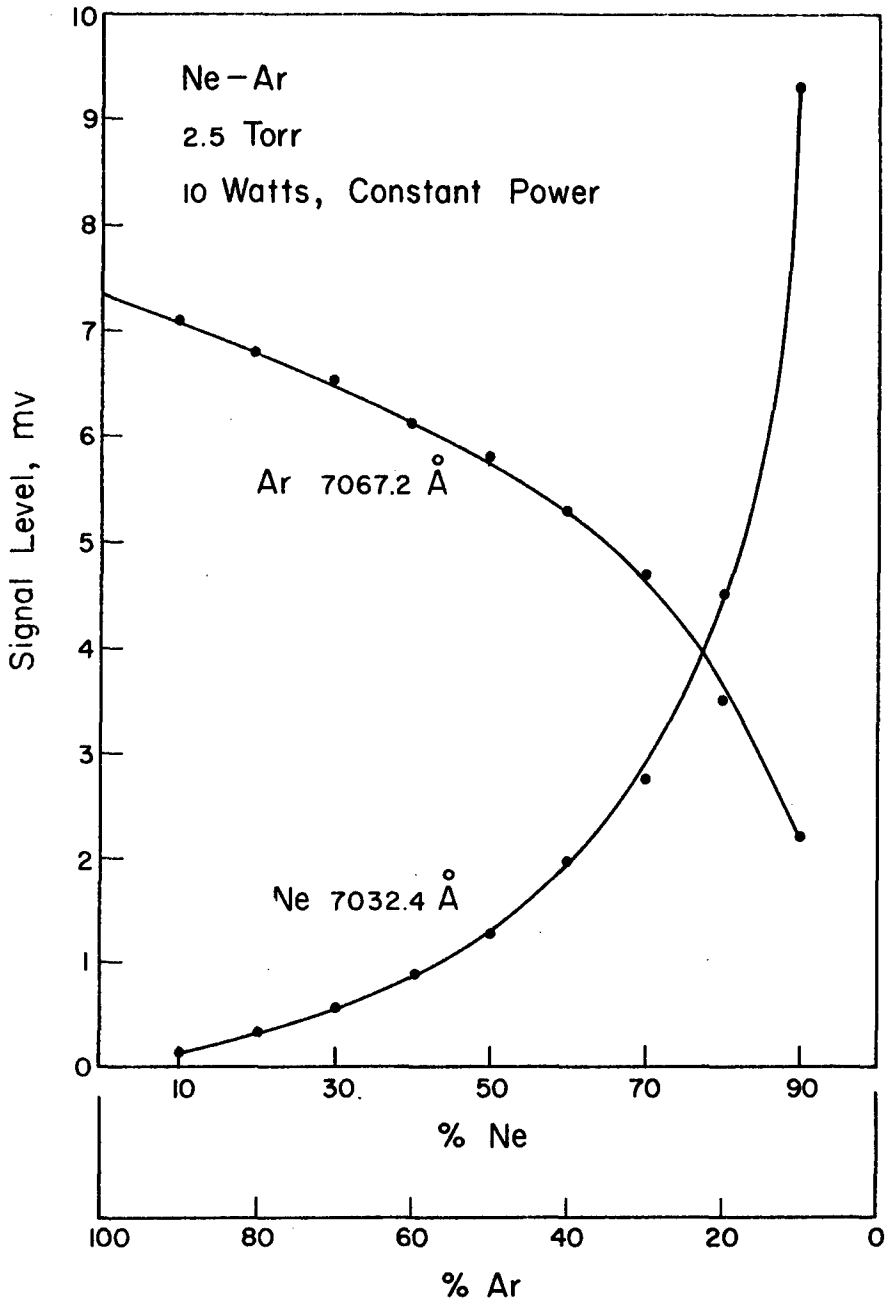


Figure 46. RESPONSE FOR Ne-Ar BINARY MIXTURE

Table IV

IONIZATION POTENTIALS OF THE SELECTED ELEMENTS AND EXCITATION POTENTIAL OF SELECTED LINES

| Element | Ionization Potential, eV | Excitation Potential, Line | eV |
|---|---|---|---|
| He | 24.46 | 7065.2 | 22.7 |
| | | 7281.4 | 22.9 |
| Ne | 21.47 | 6328.2 | -- |
| | | 7032.4 | 18.37 |
| | | 7245.1 | 18.37 |
| Ar | 15.68 | 7067.2 | 13.29 |
| | | 8006.2 | 13.16 |
| | | 8014.8 | 13.09 |
| H | 13.52 | 6562 | 12.09 |
| O | 13.55 | 7771.9 | 10.73 |
| | | 8446.4 | 10.98 |
| | | 6158.2 | 12.75 |
| N | 14.48 | 8216.5 | 11.84 |

Argon-Oxygen

Figure 47 illustrates the difference in the response from the oxygen 7771.9 Å and the oxygen 8446.4 Å line as a function of the wavelength sensitivity of the S-20 response type tube. The 8400-Å region is near the limit of the S-20 phosphor. In these cases the response of the oxygen lines is a function of concentration and, for the wide range of concentration, is reasonably linear.

Nitrogen-Oxygen

The spectral response for both the nitrogen 8216.5 Å and the oxygen 7771.9 Å lines in a binary mixture are functions of their concentration. This is illustrated in fig. 48.

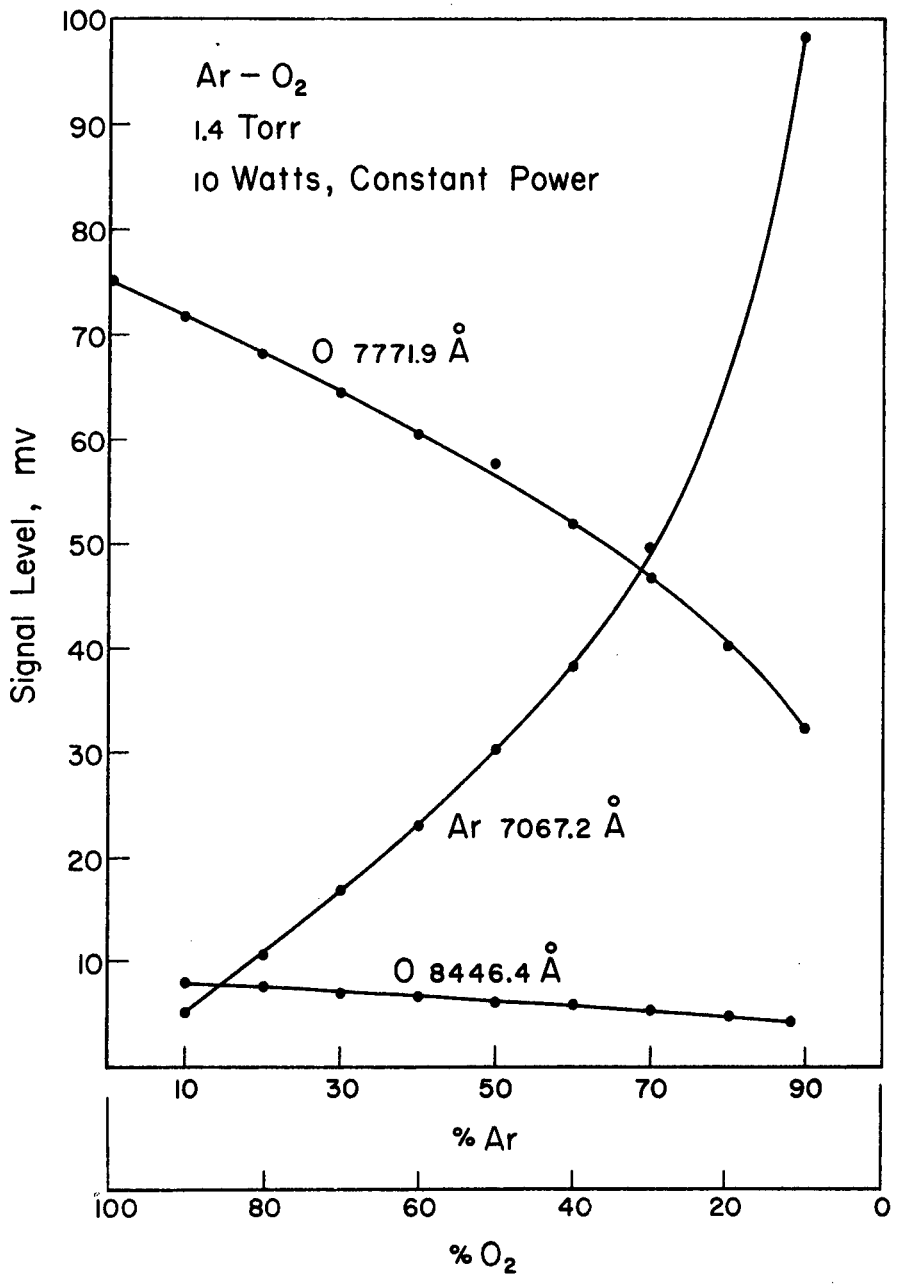


Figure 47. RESPONSE FOR Ar-$O_2$ BINARY MIXTURE

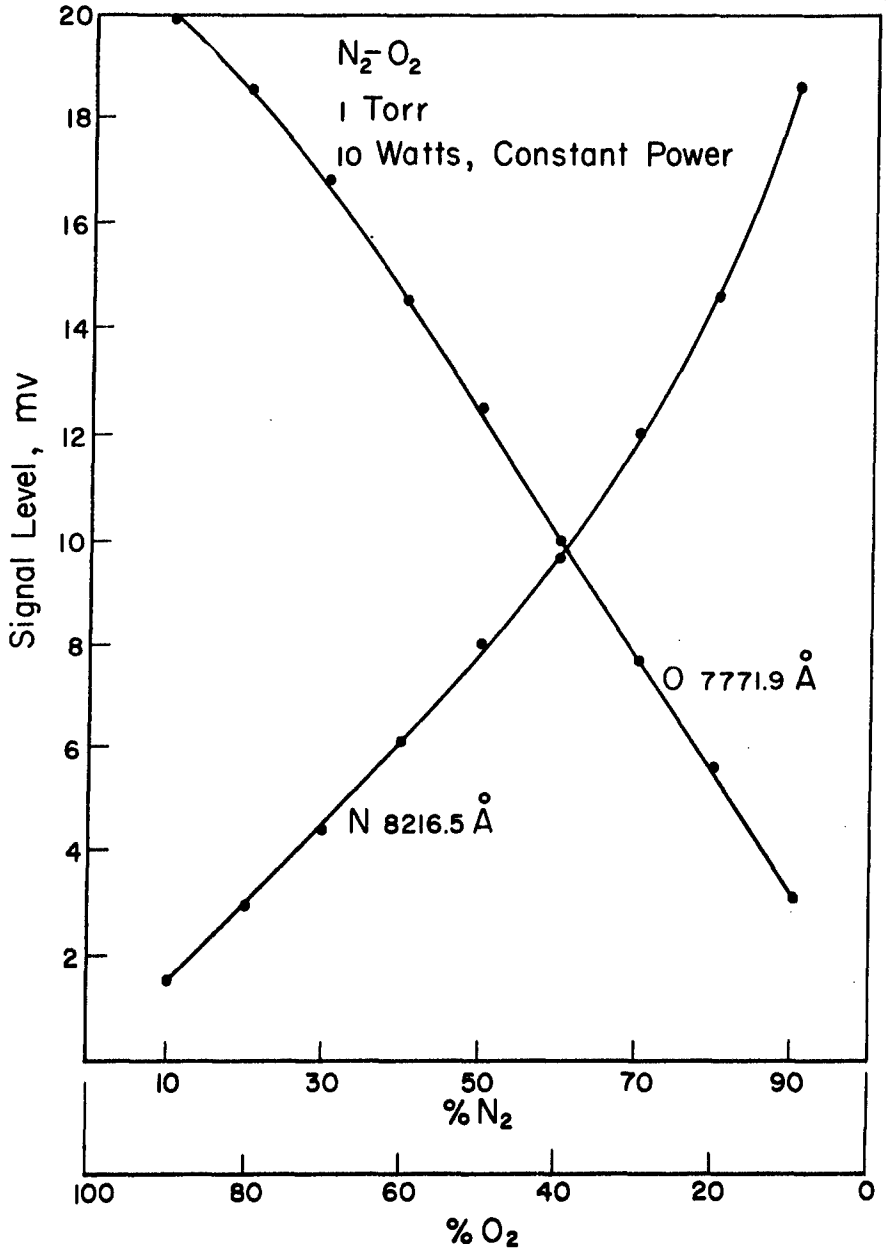


Figure 48. RESPONSE FOR $N_2$-$O_2$ BINARY MIXTURE

Discussion

The mechanism of hollow cathode excitation for a material on the cathode is the result of electronic or atomic bombardment (collisions of the first kind) and the atomic transfer of excitation energy (collisions of the second kind). As a result of the high voltage potential free electrons are accelerated from the cathode toward the anode with sufficient energy to ionize the inert rare gas atoms (carrier gas) by collisions. The secondary electrons resulting from these collisions are also accelerated toward the anode and the positive ions are accelerated toward the cathode. This intense positive ion stream of the carrier gas upon collision with the sample or cathode walls cause sputtering of sample into the discharge zone. The greater the atomic weight of the carrier gas the greater the sputtering. Then sample atoms are excited to emission through collisions of the second kind, i.e., the transfer of energy from the energetic carrier gas ions to the sample atoms. The observed emission lines from the hollow cathode are due to the carrier gas, any material that was placed on the surface of the cathode and the cathode material. In the case of solid samples, pressure is not critical.

In a discussion of the spectra for gas analysis, the total gas mixture will be considered the carrier gas. Then the number of ions formed would be determined by the strength of the high potential field, the ionization potential of each gas constituent and the concentration of each gas. If the two gases in a binary mixture have similar ionization potentials, then the number of ions formed would be essentially proportional to their concentration.

Emission may be the result of electron trapping near the cathode as well as collisions of the second kind. The probability of collisions of the second kind being an important factor can exist when one of the gases is helium because of the greater kinetic energy of its ions. The mechanism apparently is that a gas with a much lower excitation and ionization energy is much more efficiently transferred to the upper energy states, both by ionic bombardment and also second order collisions, as their concentrations become less in the presence of atoms with very high potentials. The helium ions are sufficiently energetic to excite oxygen atoms to emission through collisions.

Those binary gas mixtures in which the ionization potentials are similar, Ar(15.68 eV)-O(13.55 eV) and N(14.48 eV)-O yielded a spectral response that varied approximately proportional to their concentration, fig. 47 and 48. Each gas had little suppression effect on each other.

The spectral response for helium does show suppression in binary mixtures with oxygen, nitrogen and hydrogen. This is indicated by the shape of the helium response curve in fig. 40 and 43. In these examples there are very large differences in ionization potentials, He(24.46 eV), O(13.55 eV), N(14.48 eV) and H(1352 eV). The presence of excited helium atoms in this case are probably due to the formation of helium ions from electronic bombardment. A low concentration is indicated by the low intensity of the emission lines. However, this degree of quenching is much less than that for the d-c arc excitation or the positive column excitation in the glow discharge. In the d-c arc, the intensity of the helium lines is essentially zero until its concentration becomes greater than 75% in the presence of another gas, such as hydrogen or oxygen, with a relatively low excitation potential.

Both helium, fig. 45, and neon, fig. 46, show suppression at the high concentrations of argon as indicated by its spectral response curve. In both experiments, argon is more highly ionized due to electronic collisions and then emits as the result of trapped electrons. Apparently both helium and neon ions possess insufficient translational energy to cause additional argon excitation through collisions.

The response for neon in helium, fig. 44, is unusual in that the 7245.2 Å line initially behaves as expected for atomic lines with reasonably close excitation potentials, i.e., a decrease in intensity with decreasing concentration. The intensity of the helium 7065.2 Å line is greater than when present with gases such as hydrogen and oxygen. At this phase, apparently both gases are being ionized and excited with atomic transfer of excitation energy through collisions holding only a minor role. However, after passing through a minimum, both neon lines that were measured, the 7245.2 Å and 7032.4 Å, definitely

increased in intensity at decreasing concentration. The neon 6328.2 Å line, the wavelength of a helium-neon gas laser apparently depends in part on the laser mechanism for its excitation since it is not a very strong line under normal excitation conditions, but in fig. 44, it is quite intense.

# SECTION III

# DESIGN AND CONSTRUCTION

## MODE OF EXCITATION AND OPTICAL DESIGN

An optical instrument was designed and developed to monitor the emission spectra of air type atmospheres in which nitrogen and oxygen were the major components, and hydrogen and carbon dioxide were the minor components. The source of light was hollow cathode excitation of the gas mixtures. The instrument was of the continuous direct readout design and was a small lightweight laboratory model that may be used for further experimentation.

The instrument consists of essentially four major parts; the light source, the optical block in which the selected emission spectra is isolated, photo-receptive device to detect the emitted light, and the electronic and power system for the readout and the excitation source, respectively. Figures 49 and 50 illustrate exploded views of the first three components. These components are shown mounted in the chassis case arranged in the same order, fig. 51. The view of the front panel is illustrated in fig. 52.

### Hollow Cathode Excitation

The hollow cathode mode of excitation was selected over the other types of glow discharges and over arcs or plasmas because of its (1) low power requirements, (2) excellent stability, (3) the brilliance and spectral intensities of the higher energy species associated with the negative and cathode glow of the glow discharge which can be concentrated by making the cathode into a tube, (4) the lack of the lower energy band spectra found in the positive column of the glow discharge, and (5) operation at moderate pressures.

The design of the hollow cathode source was similar to that by Werner et al. (ref. 6). This design was

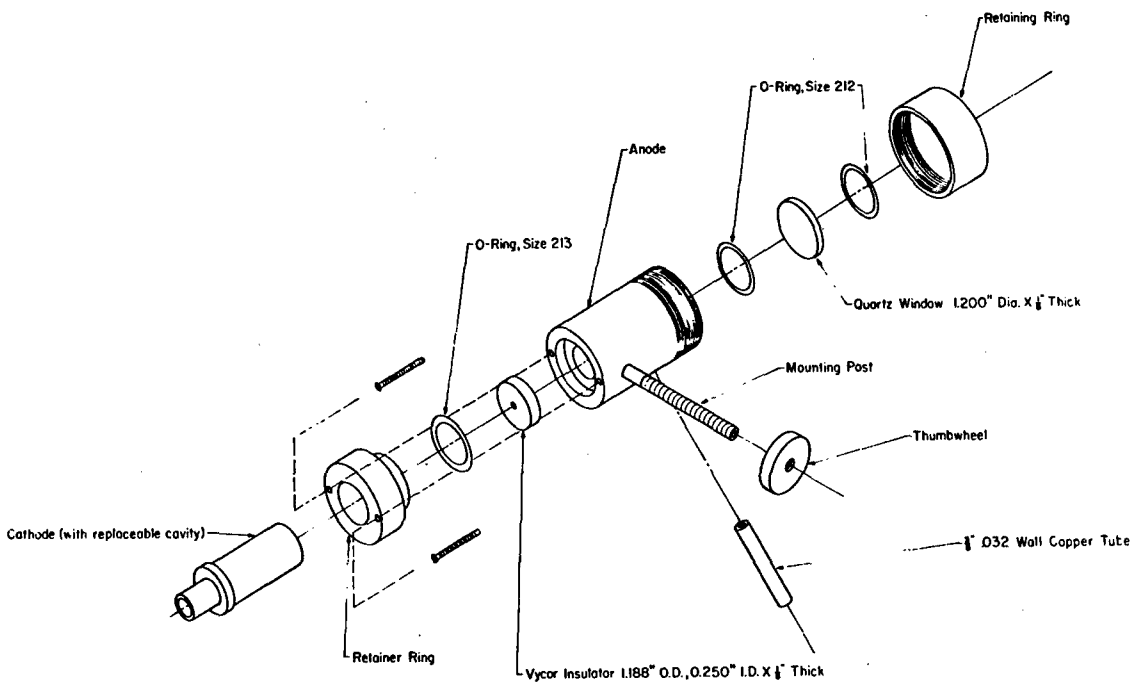


Figure 49. EXPLODED VIEW OF LIGHT SOURCE

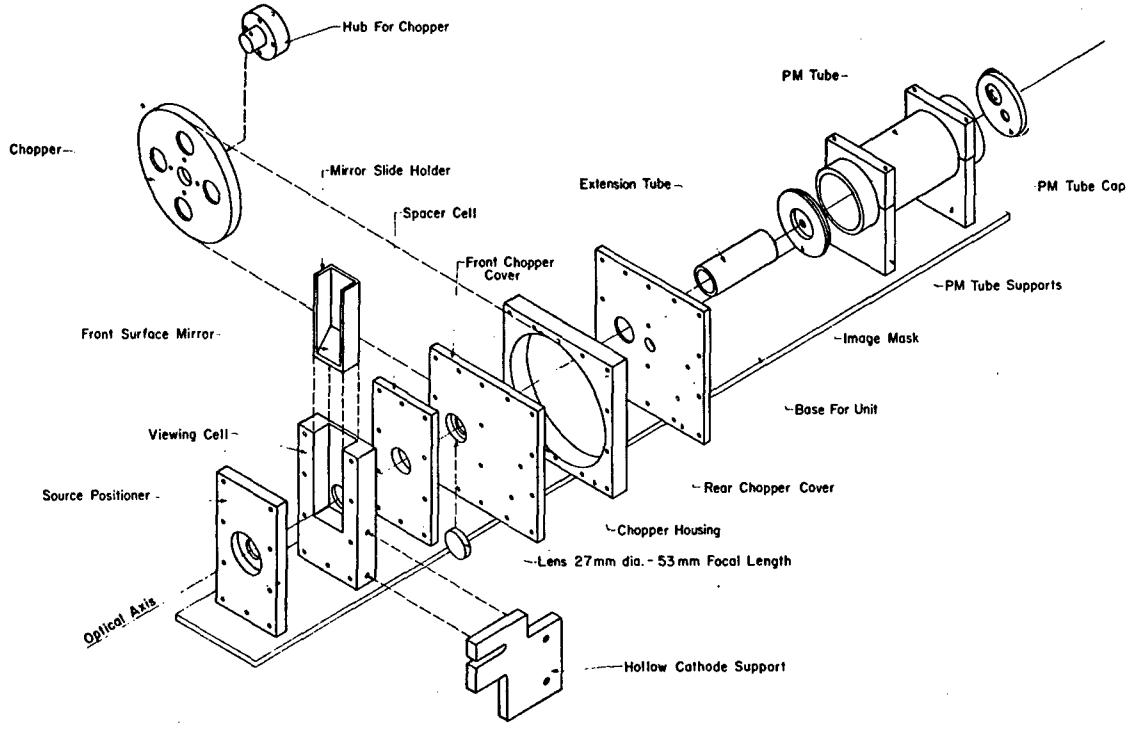


Figure 50. EXPLODED VIEW OF OPTICAL BLOCK AND PM TUBE

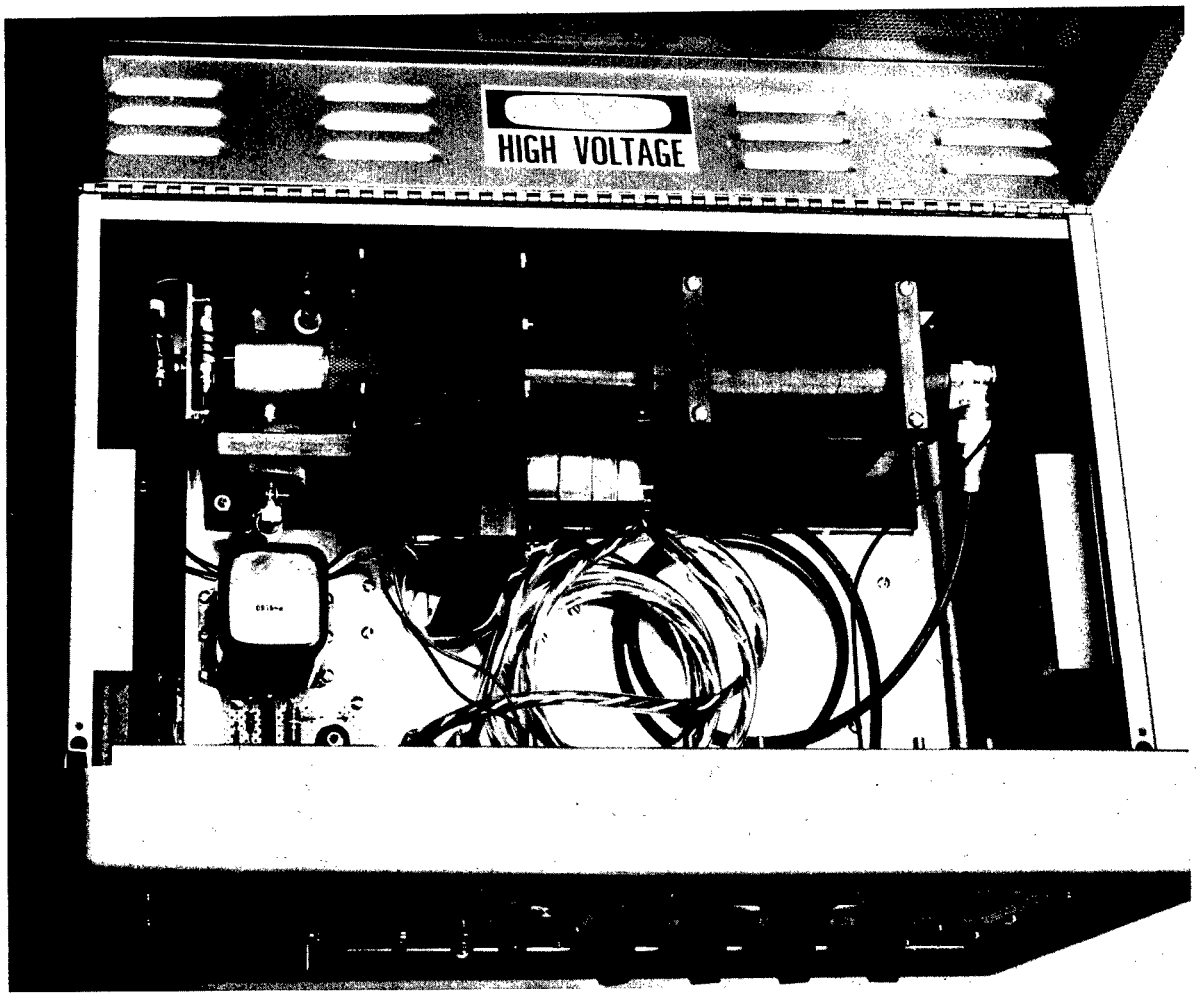


Figure 51. OPTICAL COMPONENTS, TOP VIEW OF MONITOR

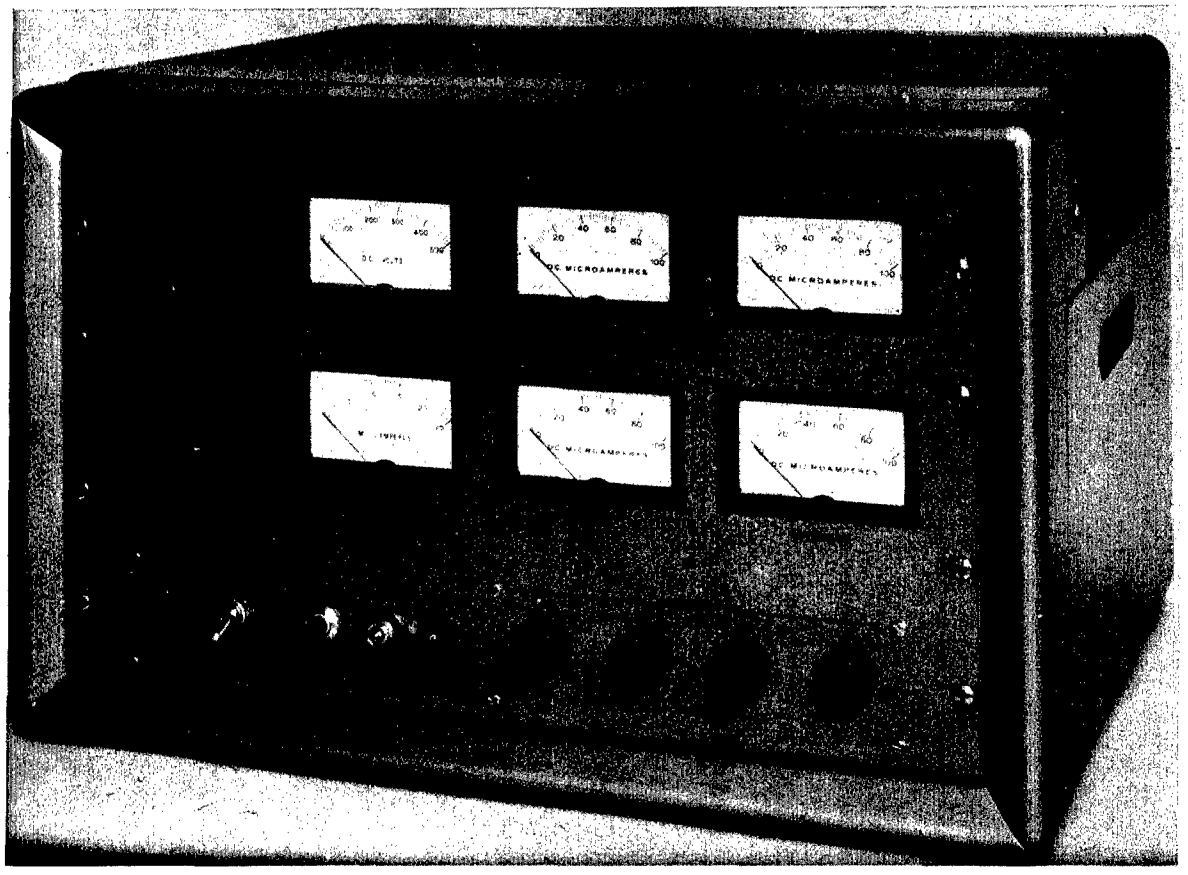


Figure 52. FRONT PANEL OF MONITOR

chosen because of its relatively simple design and ease in which the cathode could be replaced.

The details of the source as it was developed for this instrument are shown in fig. 49. The anode is 2 in. in length with an inside diameter of 5/8 in. The air is taken in at the front near the window and flows back through the separator-insulator to the cathode. At this point the gas spreads before the cathode to eight openings and is pumped from the rear. A drawing of the cathode is shown in fig. 53. The hollow cathode is lined with gold foil. The narrow space, 0.015 in. offset, between the cathode and the insulator to permit the passage of the gas to the small exhaust tubes, was intended to create a pressure drop in this region. This resulted in a more stable discharge and prevented the discharge from dropping back into the exhaust tubes, since the discharge favors the higher pressure of the cathode cavity to the much lower pressure of the exhaust tubes. The above design was developed because the conventional cathode did not appear to possess the reproducibility and stability desired.

The inside dimensions of this cathode were 1/4 in. in diameter and 1/2 in. deep. The optimum depth is approximately 1/2 in., fig. 38. The 1/4 in. depth was slightly less sensitive with respect to given concentration-power-pressure conditions than the 1/2 in. which in turn was better than the smaller diameters.

The 1/4-in. diameter cathode was somewhat more intense than the 3/8 in. at the same pressure and power conditions and the emission output for the 1/8 in. cathode was somewhat more intense than the 1/4 in. cathode, however the latter was much more difficult to start and maintain, especially in a helium type atmosphere.

The lens-mask system to remove most of the anode glow was incorporated into the instrument. Its position in the instrument is shown in fig. 50. The 27-mm diameter lens with a 53-mm focal length was mounted in the front face plate of the filter wheel housing and the mask was placed before the face of the photomultiplier tube. The light path arrangement is illustrated in fig. 54.

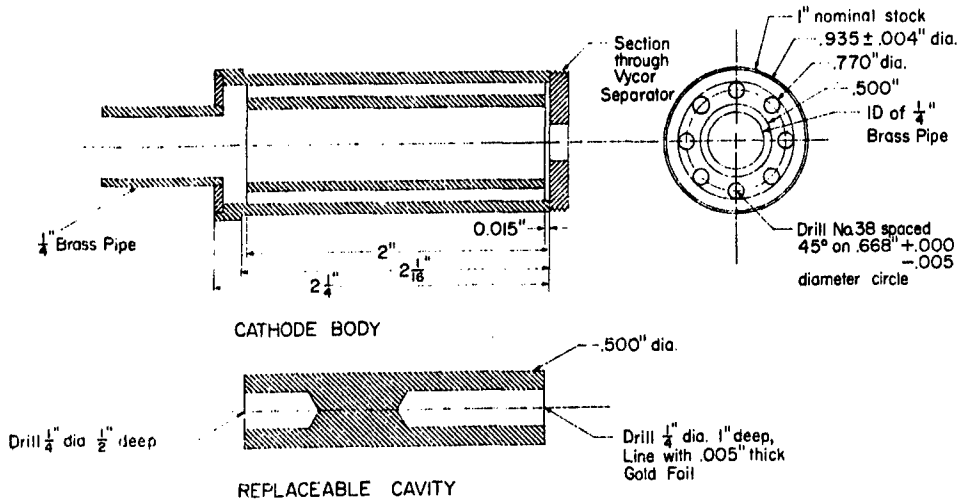


Figure 53. DETAILS OF THE CATHODE

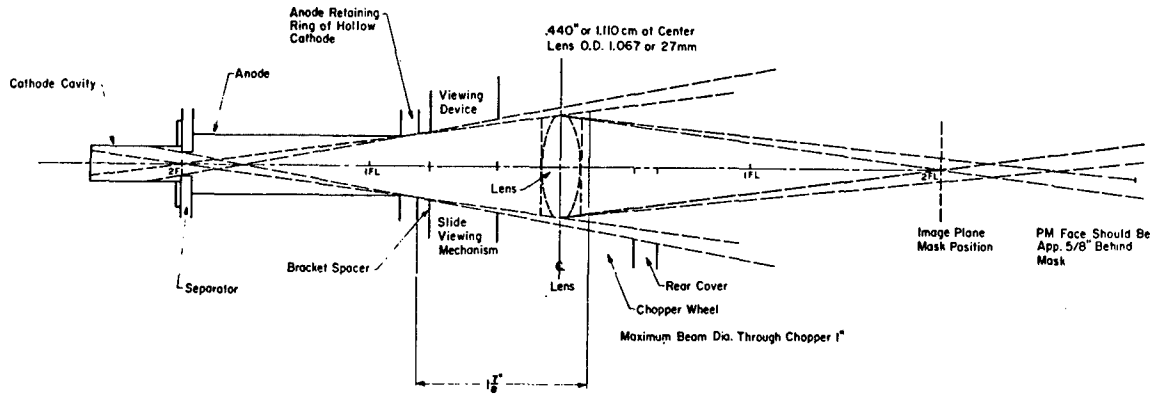


Figure 54. LIGHT PATH DIAGRAM FOR MASKING ANODE GLOW

Aluminum is considered an excellent cathode material (ref. 9) because of its low work function and because of the chemical stability of its surface even with moisture. Werner et al. (ref. 6) also used aluminum cathodes in their monitoring of the A.E.C. $Li^6$-$Li^7$ program. However, these or other workers apparently had not been concerned with atmospheres containing oxygen.

The intensity of the emission spectra continued to decrease with use under the same power and gas composition conditions. The interior was found to be coated with a black layer of finely divided material that was found to be chiefly aluminum oxide. The voltage across the cathode increased as the oxide layer developed. Gold was selected as a substitute since it does not form an oxide. Gold foil inserts were used in the cathode and the anode.

The anode fits into the optical housing and can be removed by simply loosening the two knurled lock nuts and lifting the source from its mounts.

## Isolation of Spectra

Two approaches were considered for the basic optical design, 1) the use of a grating to diffract the light, and 2) the use of interference filters at the selected wavelengths.

The advantage of the grating is that it offers greater versatility in line or band selection for monitoring since photo-receptive devices with maximum sensitivity at different wavelengths are possible. The disadvantage is that the instrument would be larger and include several photomultiplier tubes. A very small instrument of this type is possible if a special grating had been designed and purchased and used in a unit with the new small size photomultiplier tubes. In the longer wavelength, these are still not commonly used and so are relatively expensive.

A basic study of the spectra showed that the numerous and intense nitrogen and nitrogen related bands obscured all other possible spectra such as the $O_2^+$ band system in the 2900- to 6000-Å region. Although nitrogen was the

dominant element, no good clear band was sufficiently isolated to make it superior to the 8216.5-Å line.

When the supposedly strong $CO_2^+$ bands at 2883 Å and 2896 Å did not develop with the aluminum hollow cathode, the carbon 9094.9-Å line group was selected to monitor the carbon dioxide.

The selection of hydrogen 6562.7-Å, oxygen 8446.4-Å, nitrogen 8216.5-Å and carbon 9074.9-Å lines made possible the use of a single S-1 response photomultiplier tube, since it will cover the total region of interest. This in turn made the use of interference filters more feasible. The selected interference filters were mounted in a four-channel rotating chopper or filter wheel. Details of the wheel are given in fig. 55, and its position and the housing relative to the instrument's parts is shown in fig. 50. The wheel was driven by a Amphenol Borg Model 1003-45Y, 300 rpm synchronous motor which corresponds to 5 cycles per second. Each channel is on 70° of each revolution. Thus the a-c signal is superimposed on dark current, any drift, etc.

This section also includes a viewing cell that is essentially a dark slide with a small mirror at a 45° angle, fig. 50. In the up position it does not block the optical path. It may be lowered to examine the discharge when such problems are suspected. The lens was placed after this slide so as to avoid apparent distortion when viewing the discharge.

## Readout System

The single photomultiplier readout system was direct and continuous. The response using the four-channel filter wheel, as displayed on an oscilloscope, is illustrated in fig. 56. The peak heights from left to right represent 15% oxygen, 80% nitrogen, 3% hydrogen and 2% carbon dioxide. The spikes represent the response from the switching diodes. These spikes show the switching points which trigger the gating circuit in relation to the signal received by the photomultiplier tube. The gating circuit is triggered from a light sensitive diode in the rear chopper cover aimed at a small light bulb in the front of the chopper cover. This bulb is visible in fig. 51. Small holes drilled in the periphery of the

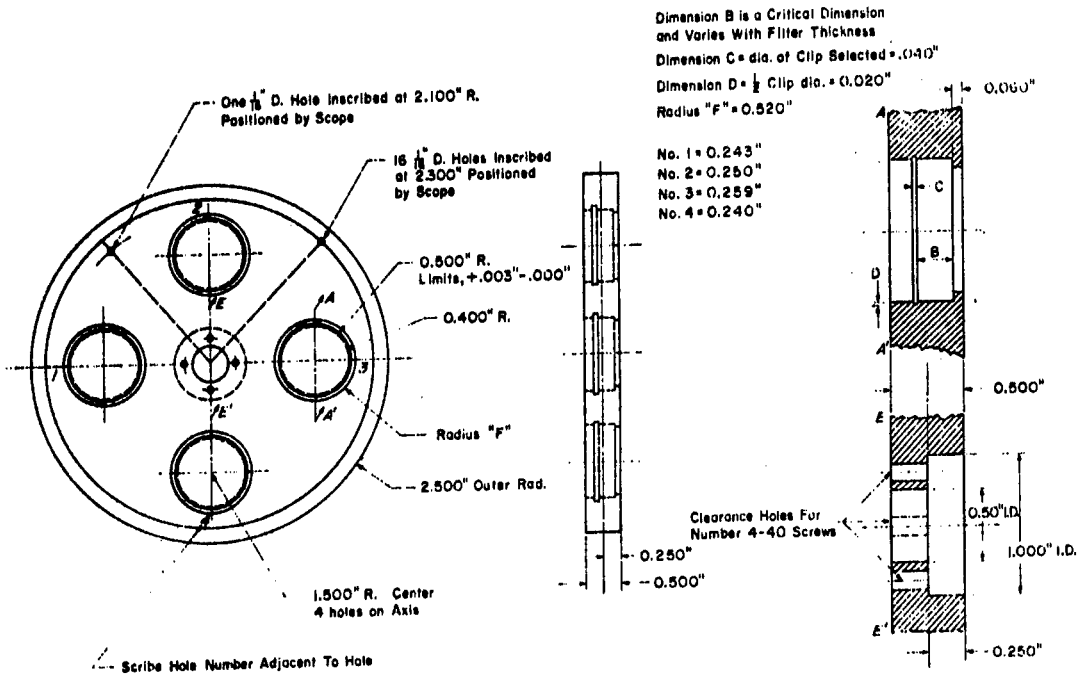


Figure 55. DETAILS OF ROTATING FILTER WHEEL

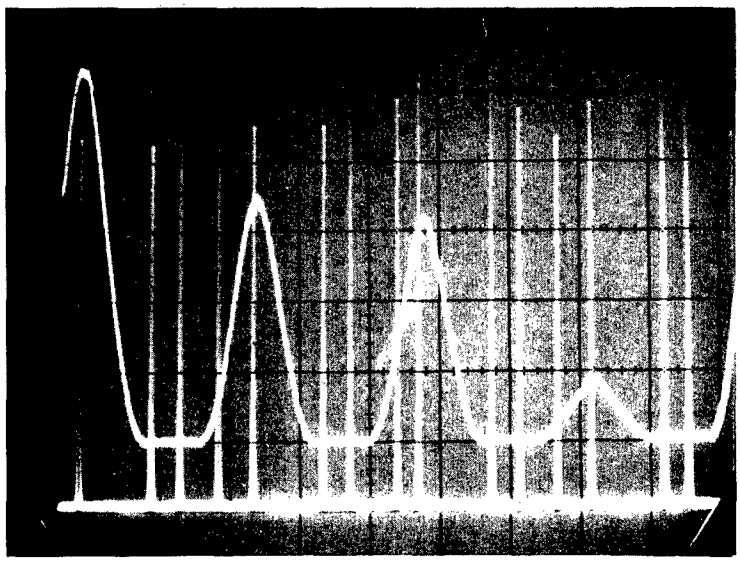

Figure 56. OSCILLOSCOPE DISPLAY; FOUR-CHANNEL FILTER WHEEL READOUT

filter wheel permit the trigger light to pass at the proper time intervals.

The switch point occurring as the signal begins to increase causes the gating circuit to feed the signal to the integrator and proper meter driver card.

At maximum amplitude the signal shuts off until the next point on the base line is reached. At this time the dark current of the photomultiplier is fed into a reference circuit by the gating circuit until the following point again shuts it off. There is no signal stored until the next switch point moves into position, thus completing the cycle. Four such cycles occur during each revolution. One revolution is shown in fig. 56.

## ELECTRONICS DEVELOPMENT

### Basic Design Considerations

The electronics portion of the system involves the conversion of the optical interference filter outputs to electrical signals, their amplification and presentation on separate output meters.

The implementation of the electronics function could take several forms depending upon the S/N at the optical detector output, the response time required of the system and the size requirements placed upon the system. A system design providing a maximum S/N and a minimum response time would employ a high frequency optical chopper at the hollow cathode followed by beam splitters and four parallel interference filters each followed by a detector, tuned amplifier, synchronous detector and meter driver. Here the high frequency chopping allows narrow band amplification and thus maximum S/N at the expense of the additional equipment.

A second approach is possible which also provides maximum S/N but at the expense of the system response time. In this approach a high frequency chopper is also employed but only a single narrow band amplifier and synchronous detector is required. In this case the four

interference filters are incrementally rotated between hollow cathode and the detector with each filter transmitting continuously for a duration of 1 to 5 seconds. The four meter drive circuits at the output would be switched in synchronism with their respective filters. This, however, requires a rather complicated mechanical drive system.

A third system approach, which was employed in the system, involves a compromise. Here the mechanical complexity is minimized as well as the amount of electronic equipment at the expense of S/N. In this approach the four interference filters are mounted in a wheel and rotated at 300 rpm. The detector and amplifier output is thus a continuous signal composed of consecutive voltage samples proportional to the concentrations of $N_2$-$O_2$-$H_2$-$CO_2$-$N_2$-$O_2$-$H_2$-$CO_2$-etc. The amplifier output is then multiplexed to the $N_2$, $O_2$, $H_2$ and $CO_2$ meter driver circuits in synchronism with the above time varying voltage signal. Although the amplifier cannot be as sharply tuned at the lower frequencies involved to maximize the S/N, the signal levels are of sufficient magnitude to enable satisfactory system operation for the concentration range in which this equipment is being designed.

System Design

The system operation can be visualized by means of the system block diagram of fig. 57. The optical detector employed is the RCA 7102 photomultiplier which possesses an S-1 photocathode enabling the detection of the carbon line at 9094.9 Å. A solid state silicon detector was also investigated due to the advantage of eliminating the high voltage PM power supply. However, the PM tube was selected over the silicon diode due to the additional gain it possesses and the ease of varying the gain by means of the PM supply voltage which provides a versatile laboratory instrument. The PM supply voltage is variable over the range from 800 to 1200 VDC which provides for operation of the tube in the region of minimum equivalent anode dark current input and thus maximum S/N. This range of supply voltage provides for a 300 to 1 gain range for the PM tube which should be sufficient for most applications.

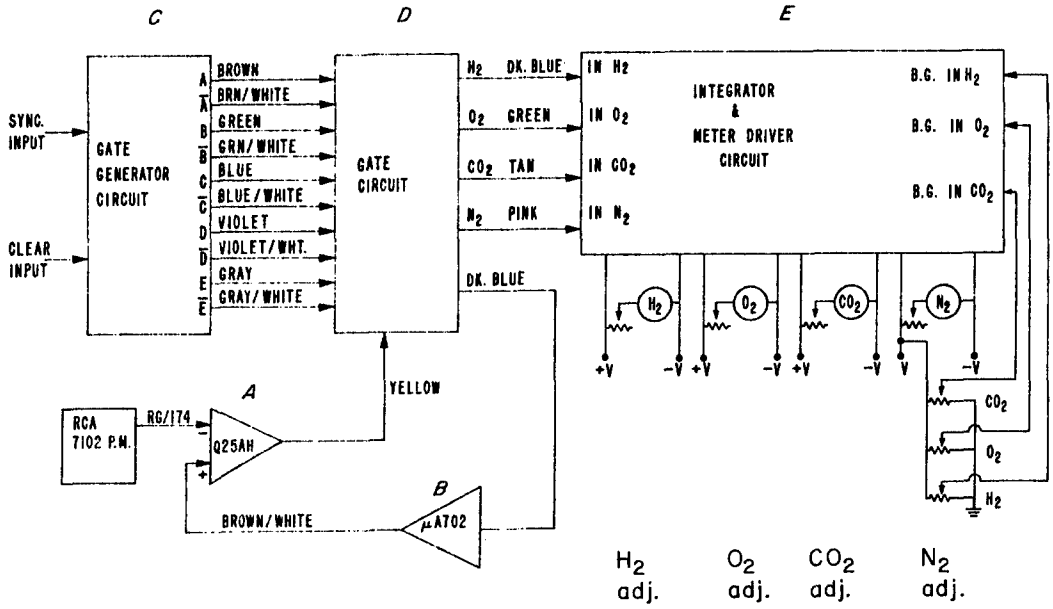


Figure 57. ELECTRONICS; BLOCK DIAGRAM OF SYSTEM

The output of the photomultiplier, as seen in fig. 57, is fed into Q25AH, a high input impedance differential operational amplifier. This amplifier performs three functions in the system; 1) it performs an impedance transformation from the 2.2 MΩ output impedance of the PM tube load resistor to a few hundred ohms to drive the integrator circuitry; 2) it provides an additional gain of 5 providing an output voltage up to approximately 8 volts for a maximum system dynamic range; and 3) it provides for dark current subtraction via its second input. In conjunction with dark current variations any d-c drift in the amplifier output is also automatically compensated. This function is performed by means of the gate circuit and the amplifier μA702. The gate circuit periodically samples the "dark" output of the PM tube-Q25AH amplifier combination and transmits the voltage to the μA702 amplifier. This voltage is low pass filtered, amplified, and transmitted to the alternate input of the Q25AH differential amplifier providing a closed loop system.

The functional operation of the gate generator and gate circuits is most easily visualized from fig. 58, the system timing diagram. As the name suggests, the timing diagram displays the relative timing of the outputs of the PM tube, the gate generator, and gate circuits. The synchronization of the gate circuit to the PM output is maintained with the synchronous and clear inputs to the gate generator. These signals are generated by means of lamps, photodiodes and holes positioned in the periphery of the filter wheel, as illustrated by figs. 50, 51 and 55. The gating holes were positioned by manually rotating the filter wheel and observing the static output of the PM tube. The synchronous holes were positioned at the peaks of the filter outputs, at points approximately 1/2 the peak value on the leading edge of the filter outputs and at the beginning and end of the dark output areas. A single clear hole was positioned on the trailing edge of the $CO_2$ output pulse. The gate generator consists of a five-stage binary scaler made up of flip-flops A through E. As seen from the timing diagram, the flip-flop outputs make a transition from one state to another when the input to the stage goes from a high to a low voltage. As seen from fig. 58, the clear pulse serves only to gate the E flip-flop to the unit since the flip-flop states may assume any state when the power is turned on. In the

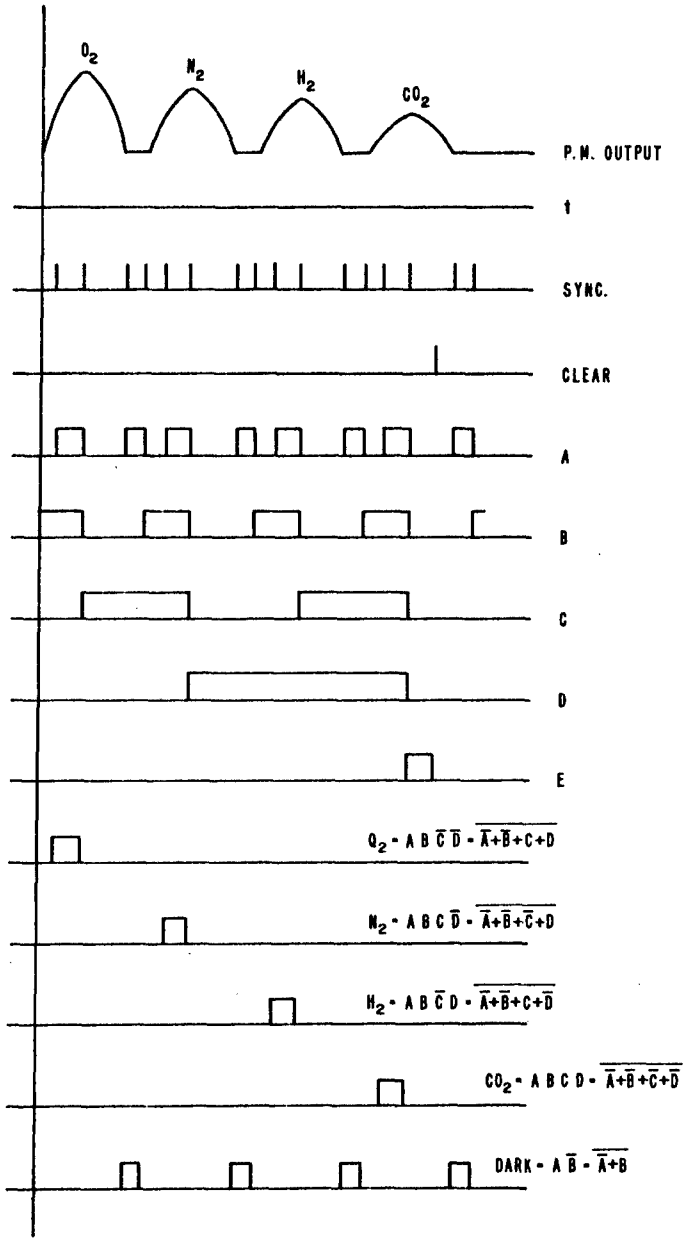


Figure 58. SYSTEM TIMING DIAGRAM

present system, the E flip-flop does not serve any function but was included to enable easy expansion of the system up to eight interference filters. The expansion of the system to 5, 6, 7, or 8 filters merely requires adding the gating circuits and meter drivers with a minimum change in the present circuitry. The gating functions required to provide sequential outputs to the integrators are seen in the lower five lines of the timing diagram, fig. 58. The corresponding logic equations determine the diode positions in the gating generator circuit of fig. 61. As seen from the timing diagram, fig. 58 and fig. 61, "NOR" logic is used to provide the gating functions with the minimum amount of circuitry. Thus the function of the gate circuit is to multiplex the PM output to the appropriate integrators in synchronism with the interference filter wheel.

The final block, E, in the diagram of fig. 57 consists of four integrator and meter driver circuits for the $N_2$, $O_2$, $H_2$, and $CO_2$ meters. These circuits store the peak voltages derived from their respective interference filters and provide sufficient drive for the output meters. A second amplifier is employed in each channel which derives its input from a potentiometer across the power supply. This allows zeroing the meters as they are connected as voltmeters across the output of the two amplifiers. This second amplifier and differential output meter connection also allows injection of signals from a given channel, say $N_2$, to subtract from the other channels. This may be used to compensate for interference due to the emission band structure of a particular gas which passes through the interference filter of another gas.

## Circuit Description

### Signal Amplifier

Figure 59, part A, is the circuit diagram for the signal amplifier which is denoted A in the photograph, fig. 60. The input amplifier consists of a Philbrick Q25AH integrated circuit operational amplifier. The amplifier gain is set at 5 as determined by the 2.2 MΩ input resistance and 10 MΩ feedback resistor while the bandwidth extends from d-c to 200 cps as determined by

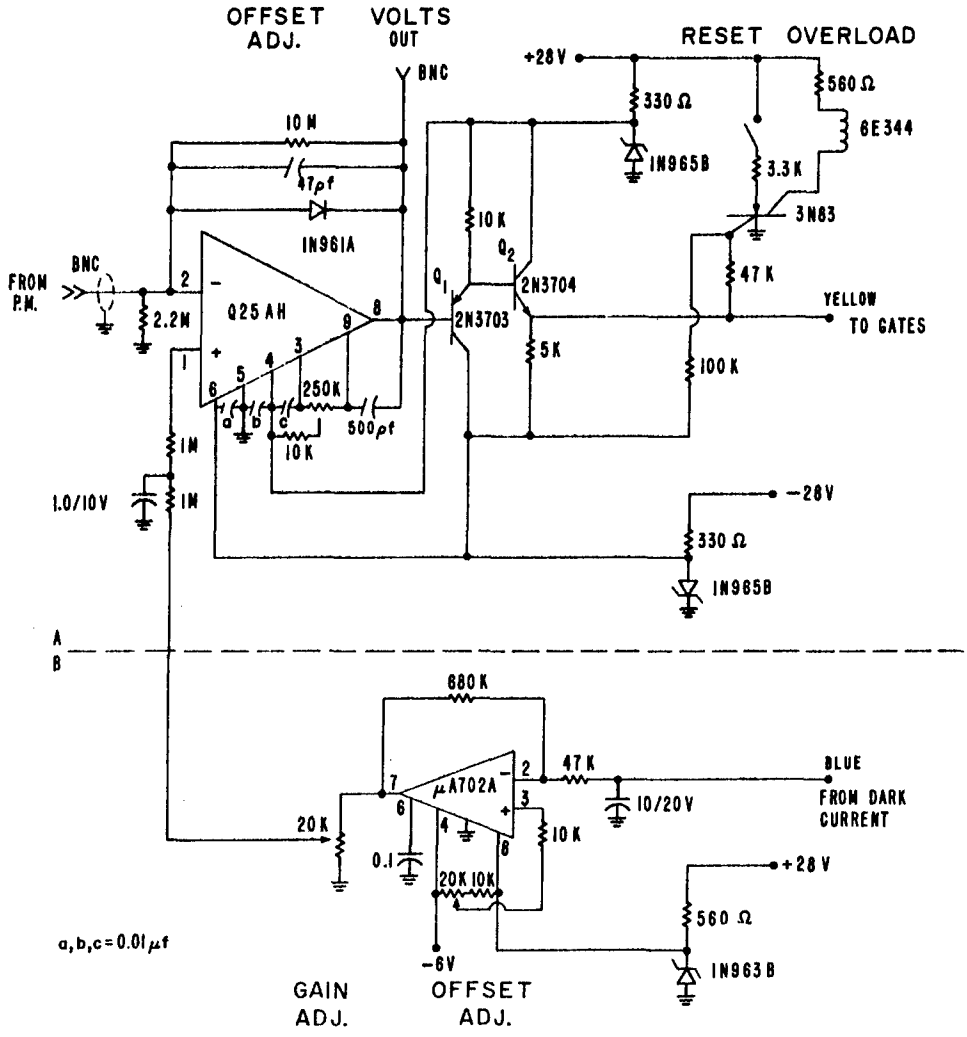


Figure 59. SIGNAL AMPLIFIER AND DARK CURRENT COMPENSATION

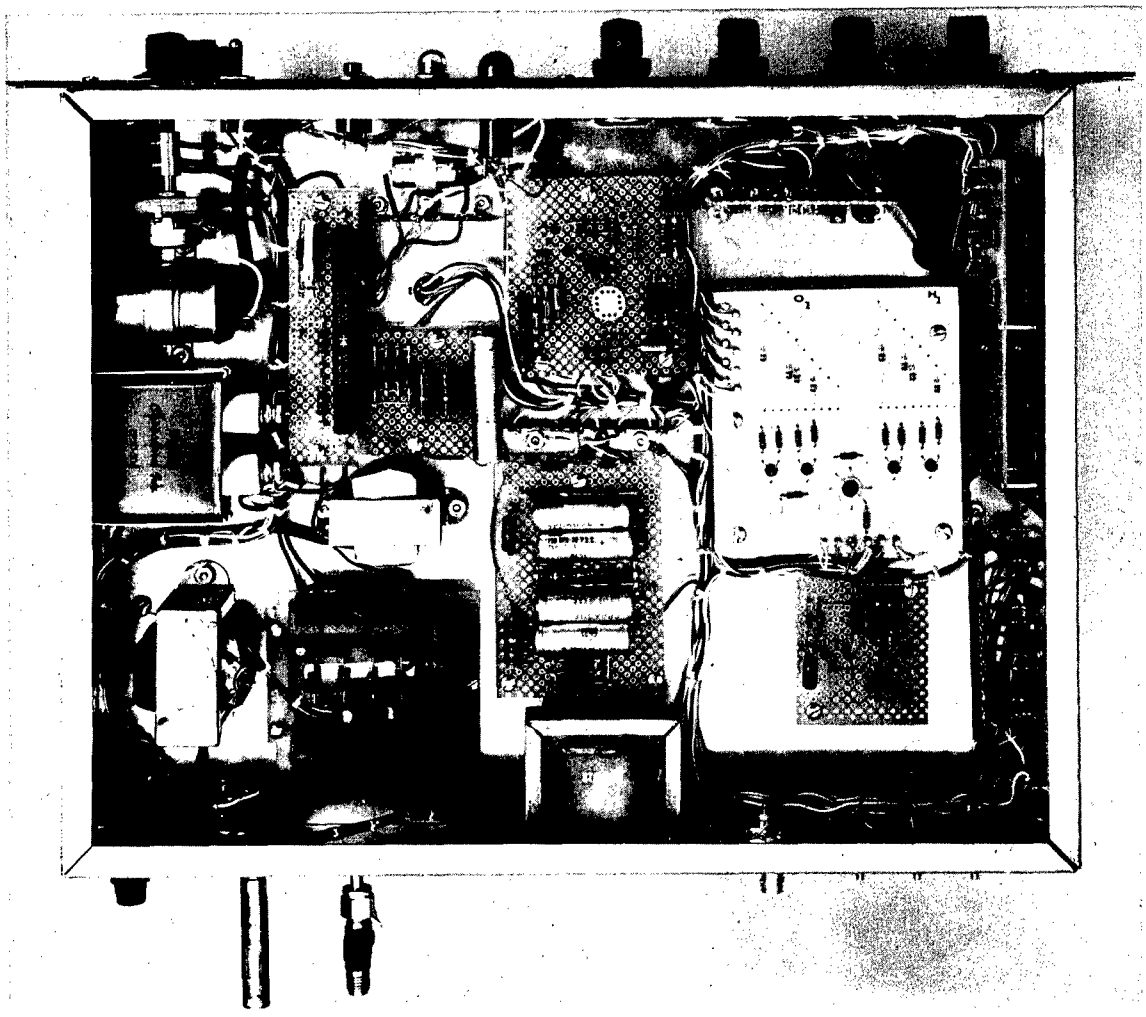

Figure 60. ELECTRONICS LAYOUT; BOTTOM VIEW

the 10 MΩ and 47 Pf in the feedback path. Initial offset voltage adjustment is performed by means of the 250K potentiometer OFFSET ADJ. A 10 voltage zener diode is employed in the feedback path for protection of the amplifier. At the output of the Q25AH amplifier a pair of emitter follower amplifiers consisting of $Q_1$ and $Q_2$ are employed to provide a low drive impedance to the integrator circuits. The use of a PNP transistor followed by an NPN transistor provides compensation for the $V_{BE}$ voltage offsets and thus the drive voltage lies close to the amplifier output voltage. Because of the wide range of possible signal levels, a threshold circuit and lamp OVERLOAD are included in the circuit. The threshold circuit consists of $Q_3$, a silicon controlled switch, which goes into its conducting state when the voltage at the gate, as determined by the 47K and 100K resistors, exceeds the threshold voltage. After the threshold has been exceeded, $Q_3$ remains in the conducting state independent of the gate voltage. Depression of the switch RESET interrupts the holding current and switches $Q_3$ into the off state.

Since a direct coupled signal amplifier is employed, a second amplifier is used to invert the dark current output of the signal amplifier and inject this signal into the positive input of the signal amplifier. This amplifier is denoted "B" in fig. 60 and its circuit diagram is seen in fig. 59B. Here a Fairchild integrated circuit operational amplifier is employed with a maximum gain of approximately 14 as determined by the 47K input resistor and the 680K feedback resistor. Initial offset adjustment is obtained via the potentiometer OFFSET ADJ. The dark voltage pulses from the gate circuit are integrated via the 10μf capacitor at the amplifier input. The amplifier output is low pass filtered by a tee section consisting of two 1MΩ resistors and a 1.0μf capacitor.

Gating Generator

The gating generator circuit is denoted "C" in fig. 60 while its circuit diagram is seen in fig. 61. The synchronous and clear gating signals are derived from the filter wheel from Texas Instruments H-38 silicon photo-duo-diodes which are illuminated by General Electric Type 253 prefocused bulbs. Upon illumination, the

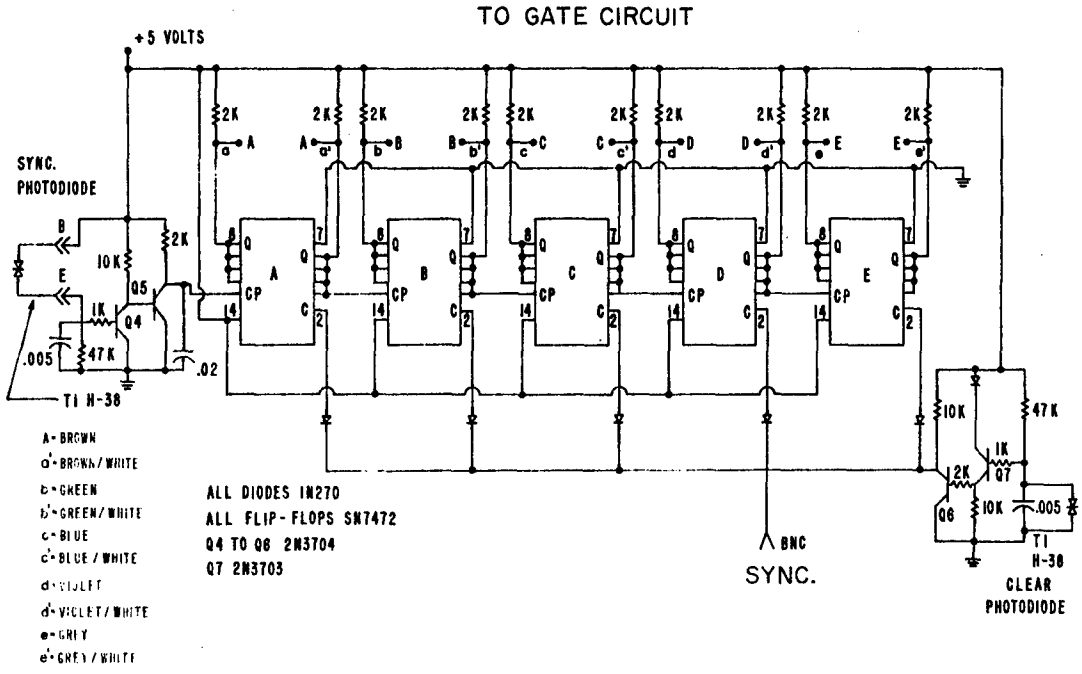


Figure 61. GATE GENERATOR CIRCUIT

synchronous photodiode's impedance falls delivering sufficient current to the base of $Q_4$ to drive it into saturation. Since the $V_{CE}$ of $Q_4$ in saturation is below the cutoff $V_{BE}$ of $Q_5$, transistor $Q_5$ stops conducting, causing the collector voltage to rise toward the supply voltage. At the end of the illumination period, $Q_4$ is again cut off and $Q_5$ returns to its normal saturation state, thus delivering a positive pulse to the clock (CP) input of flip-flop A. The operation of the clear gate circuit is inverted with respect to the synchronous circuit. Here illumination of the clear photodiode sinks the base current of $Q_7$, turning it on and thus supplies sufficient base current to $Q_6$ to drive it into saturation. Thus, during illumination the clear inputs to the flip-flops are driven to the $V_{CE_{SAT}}$ level of $Q_6$ and set the flip-flops to logical 0 (low output on Q terminals). The flip-flops employed in the circuit are Texas Instruments type SN 7472 J-K master-slave units. The integrated circuit flip-flops contain three input "AND" gates for both the J and K inputs, and thus terminals 3, 4, and 5 are tied together to form the J input while 9, 10, and 11 form the K input. The J-K flip-flops are wired to perform a toggle function by tieing J to $\overline{Q}$ and K to Q. In this mode the flip-flop changes state when the clock input (CP) makes a transition from a high voltage input to a low voltage input. Thus a five-stage binary scaler is formed by tieing the CP input of each stage to the preceding stage $\overline{Q}$ input.

Gate Circuit

The gate circuit is denoted "D" in fig. 60 and consists of a tier of three printed circuit cards. The circuit diagram associated with the gate circuit is seen in fig. 62. The operation of each of the five gate circuits is identical with the timing determined by the diode connections to the binary scaler. If, for example, we consider the top gate circuit of fig. 62, transistor $Q_8$ is in saturation if any or all of leads $\overline{A}$, $\overline{B}$, C and D are at the high or +4 volt state. In this state, current through the 820Ω resistor forward biases the emitter-base junction of $Q_{13}$ causing the $Q_{18}$ gate voltage (G) to set near +12V. The $Q_{18}$ source voltage(s) equals the output voltage of the signal amplifier and thus ranges between

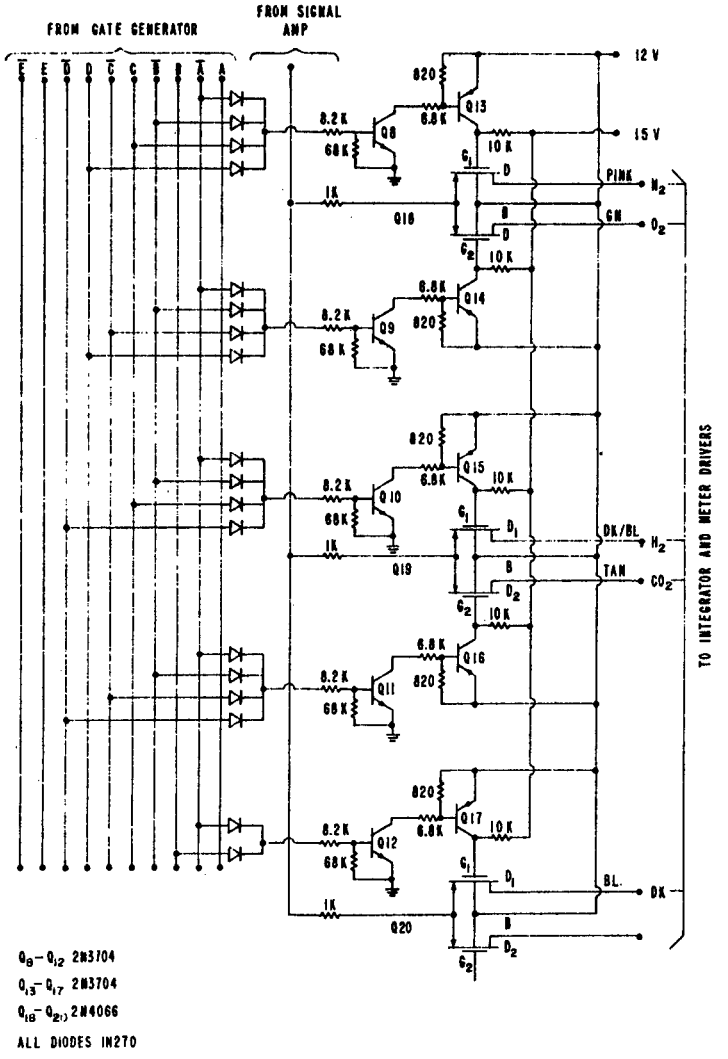


Figure 62. GATE CIRCUIT

0 and +10 volts. Therefore, the gate-source voltage, $V_{GS}$, is positive during this state. Since the switching device is a P-channel MOS Field-Effect transistor, the source-drain path is open during this period. If now one considers the state when $\overline{A}$, $\overline{B}$, C and D are all in the low or 0.2 volt stage then $Q_8$ and $Q_{13}$ are both in the non-conducting state and thus the gate voltage (G) is at -15 V. The gate-source voltage, $V_{GS}$, is in the range between -15 and -25 volts (depending on $V_S$) and $Q_{18}$ is in the conducting state with a resistance in the order of 300 Ω. The remaining four gate circuits function in a similar manner with the timing sequence of the timing diagram of fig. 58.

Integrator and Meter Driver

The integrator and meter driver circuitry comprise a double tier of printed circuit cards denoted E in fig. 60. The circuit diagram of a typical circuit is seen in fig. 63. An RC integrator is employed consisting of a 10$\mu$f capacitor and a 200K resistor. The integrator voltage drives a high input impedance emitter follower consisting of $Q_{21}$ and $Q_{23}$. The input transistor is required to only supply the base drive to $Q_{23}$ and thus minimizes the current drain from the RC integrator. A similar pair of transistors are employed which derive their input from a potentiometer d-c BAL and from a background input B.G. IN. The output meter is connected to monitor the differential voltage between collector of $Q_{23}$ and that of $Q_{24}$. This allows for initial balance and for background subtraction due to band interference from the $N_2$ channel. The circuit of fig. 63 was modified to that of fig. 64 for the $N_2$ channel. This was found necessary since at low $N_2$ concentrations the $+V_{out}$ voltage goes negative due to the 0.7 volt $V_{BE}$ drop of transistor $Q_{21}$. The circuit of fig. 64 compensates for the $V_{BE}$ drop allowing the output voltage to fall within 50 mv of the input voltage.

Power Supply

The system power supply circuit diagrams are seen in fig. 65 and 66. The supplies employ off-the-shelf transformers rather than a single multi-tap unit due to their

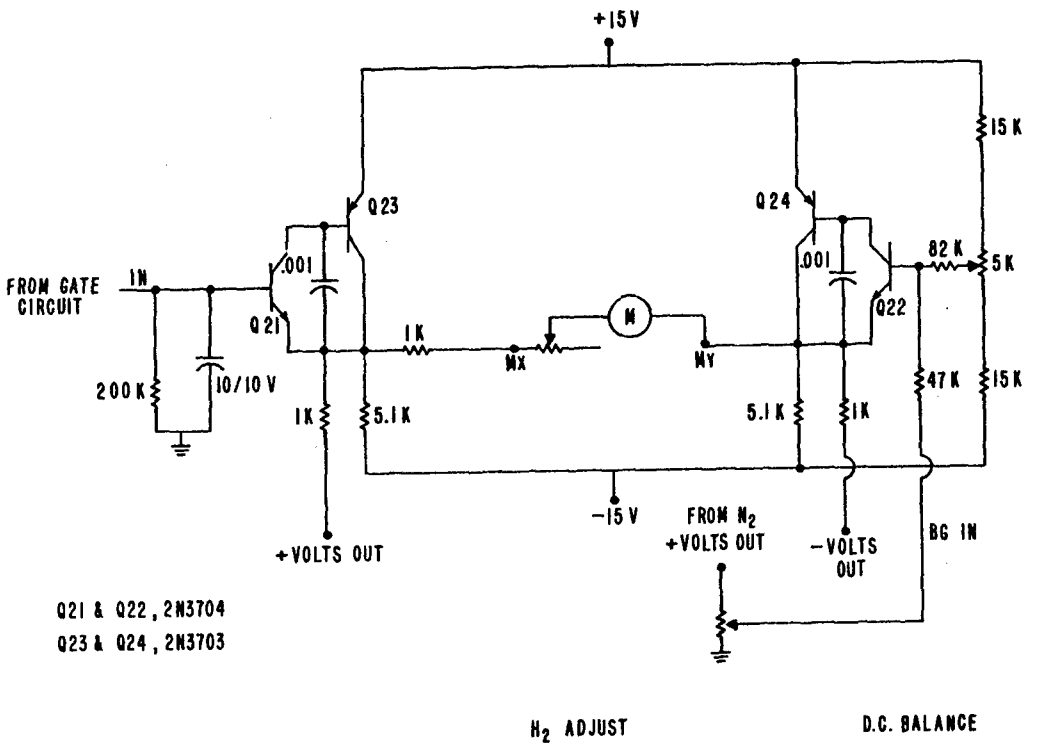


Figure 63. TYPICAL INTEGRATOR AND METER DRIVE CIRCUIT

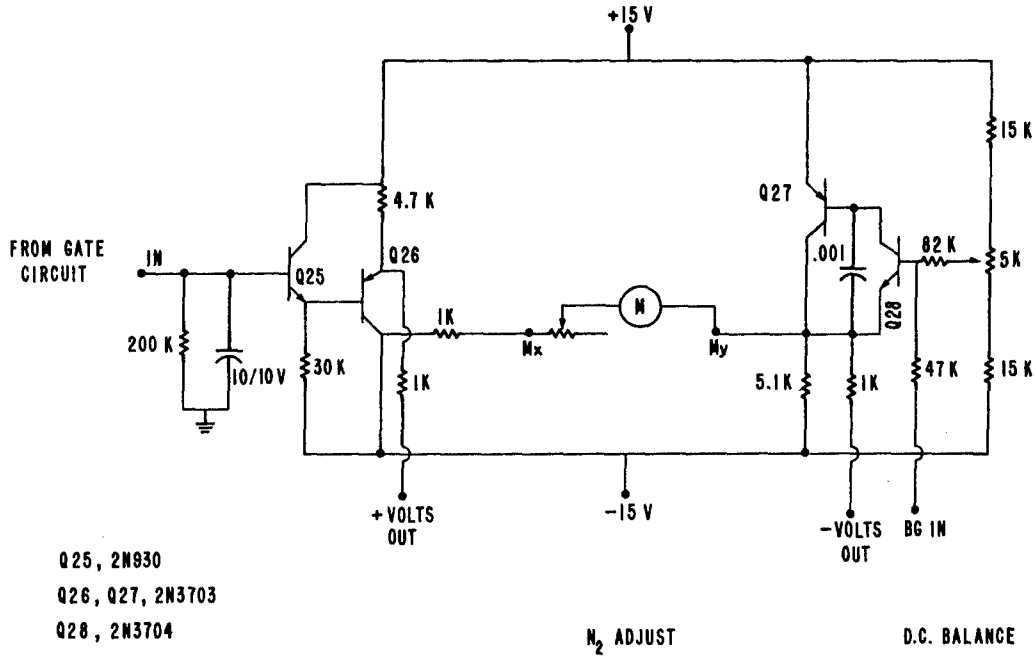


Figure 64. NITROGEN INTEGRATOR AND METER DRIVE CIRCUIT

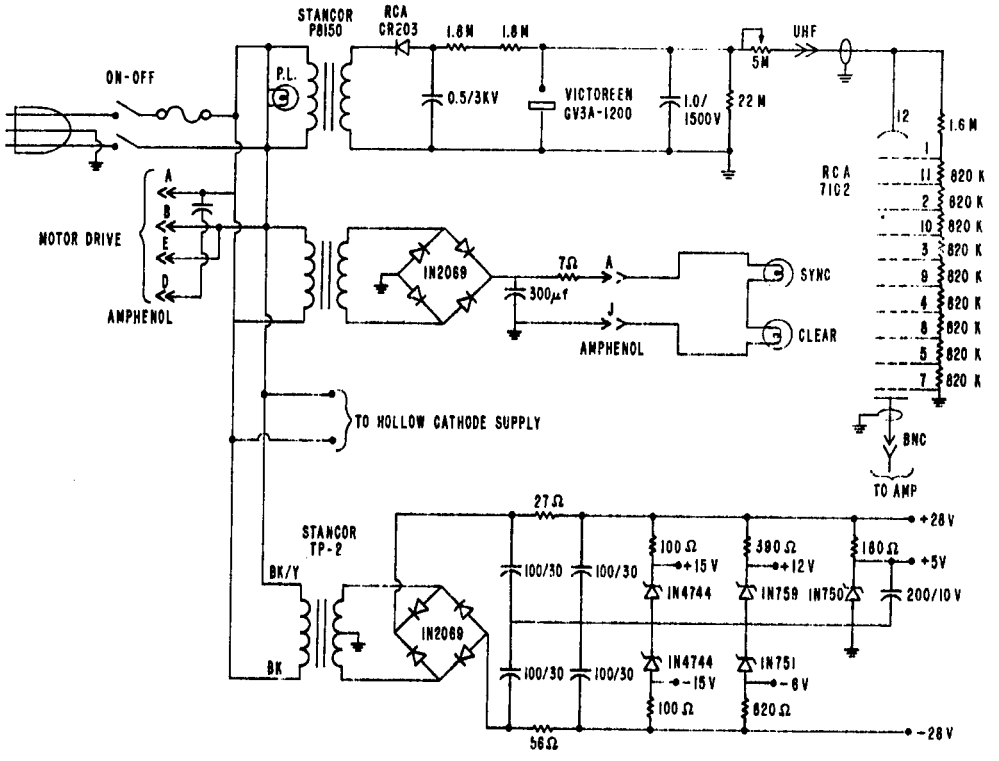


Figure 65. ELECTRONICS POWER SUPPLY

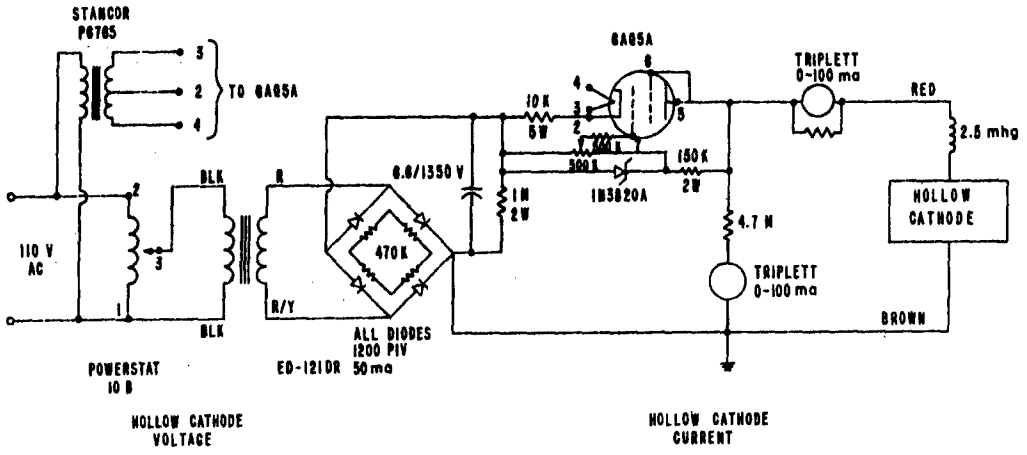


Figure 66. HOLLOW CATHODE POWER SUPPLY

availability in the breadboard model. The PM power supply, denoted F in fig. 60, is a half-wave rectifier followed by a pi-section filter. The supply is regulated by a Victoreen 1200 volt cyrotron tube whose voltage deviates by only 10 V for a 100$\mu$a change in tube current. The PM voltage adjustment is obtained via a series of 5M$\Omega$ potentiometer P.M. ADJ. The elecronics power supplies, denoted G in fig. 60, are derived from a full-wave rectifier which is filtered to minimize the 120 cps ripple. The +15, -15, +12, +5, and -6 volt supplies employ zener diode regulation to provide stable system operation over the normal range of line and load variations. The hollow cathode supply, denoted H in fig. 60, consists of a variac driving a stepup transformer which in turn drives a full-wave bridge rectifier. The bridge output, adjustable from approximately 0 to 900 volts, is constant current regulated with a 6AQ5A pentode. The current regulator portion of the circuit is mounted on vector board above the chassis.

# APPENDIX

The following detail drawings refer to figure 50.

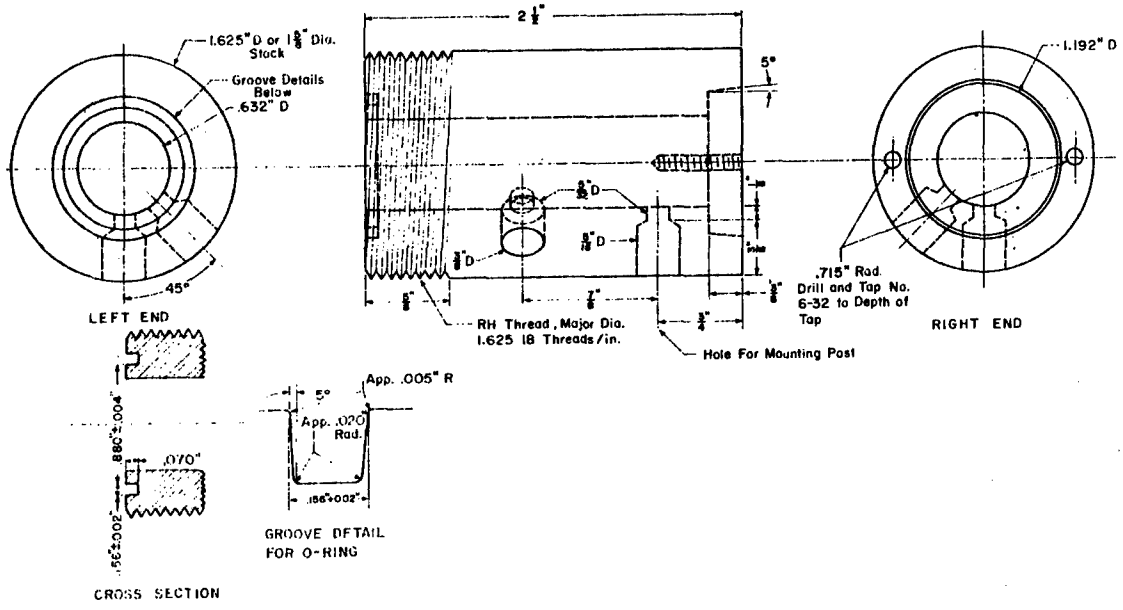


Figure 67. GOLD LINED BRASS ANODE

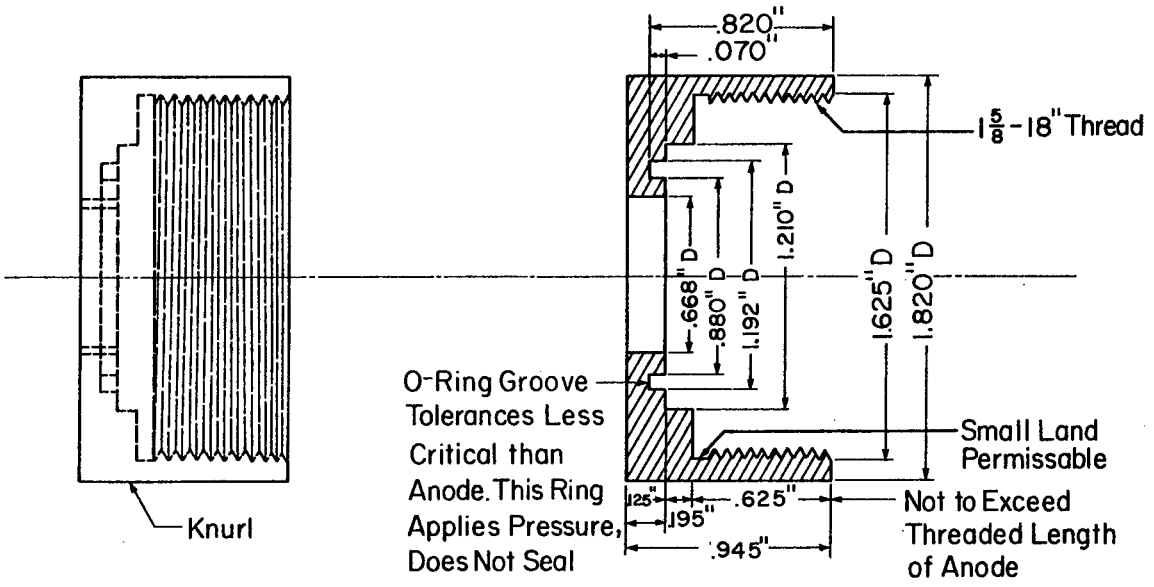


Figure 68. BRASS ANODE RETAINING RING

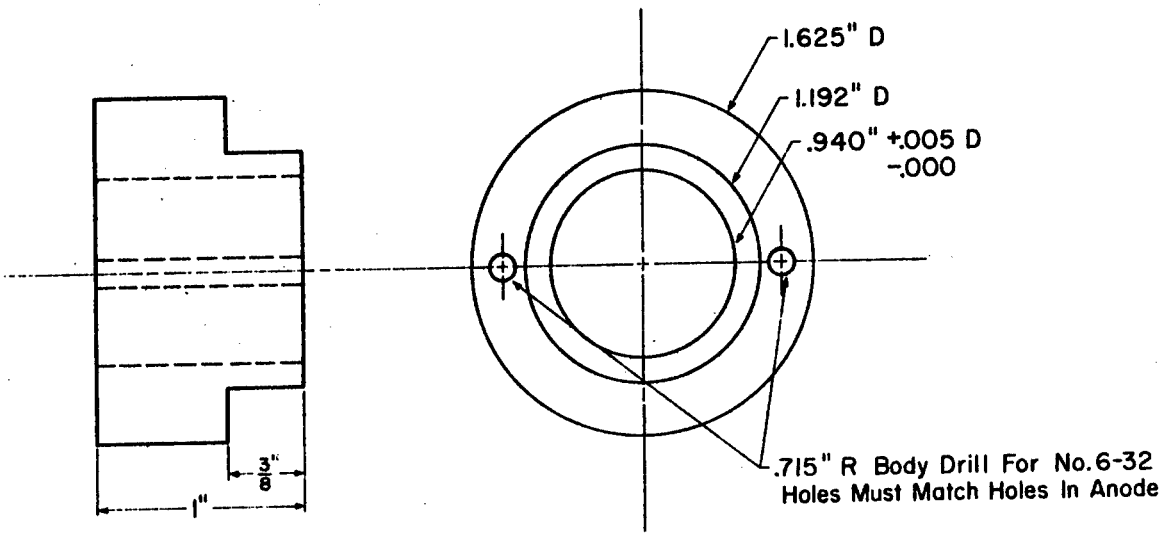


Figure 69. BAKELITE RETAINER RING

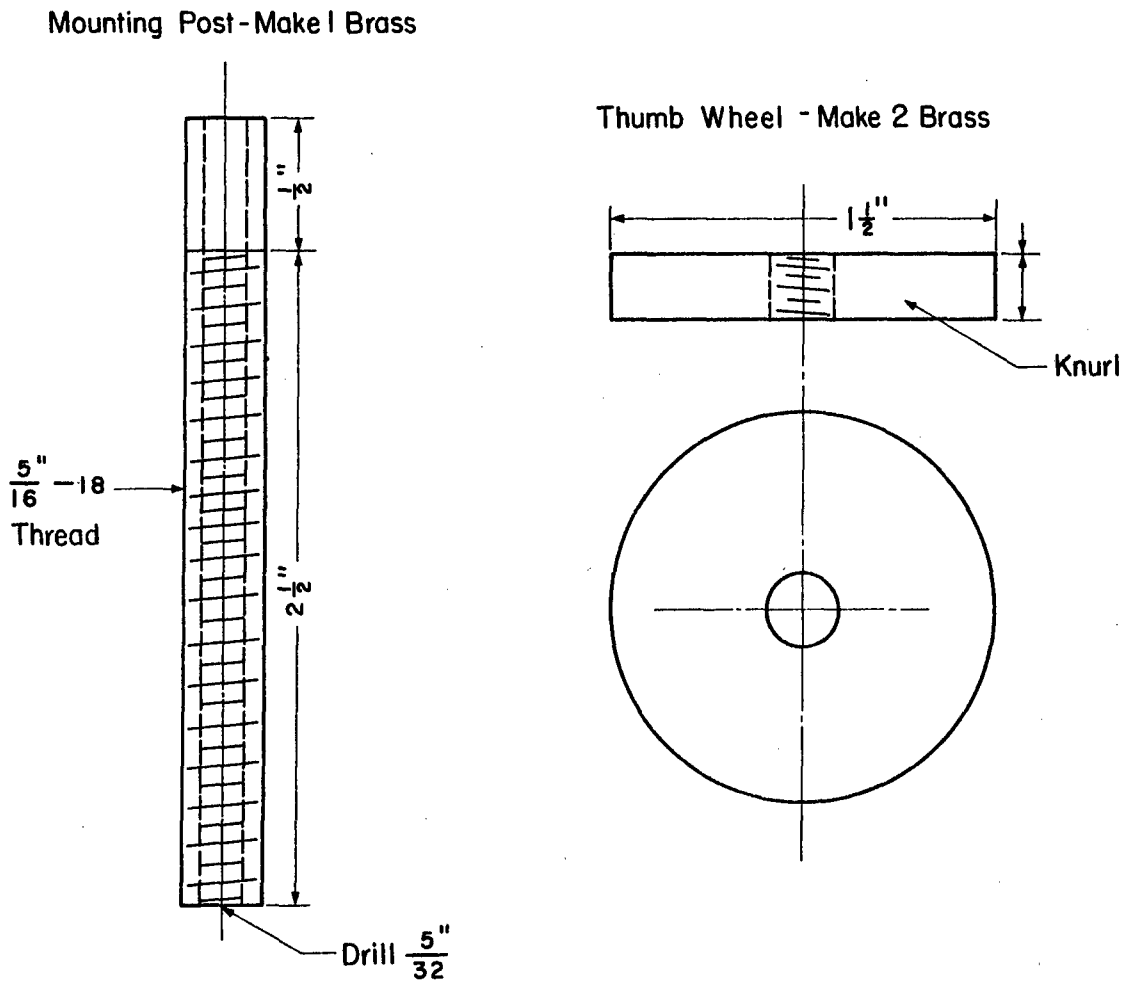


Figure 70. MOUNTING POST AND THUMBWHEEL

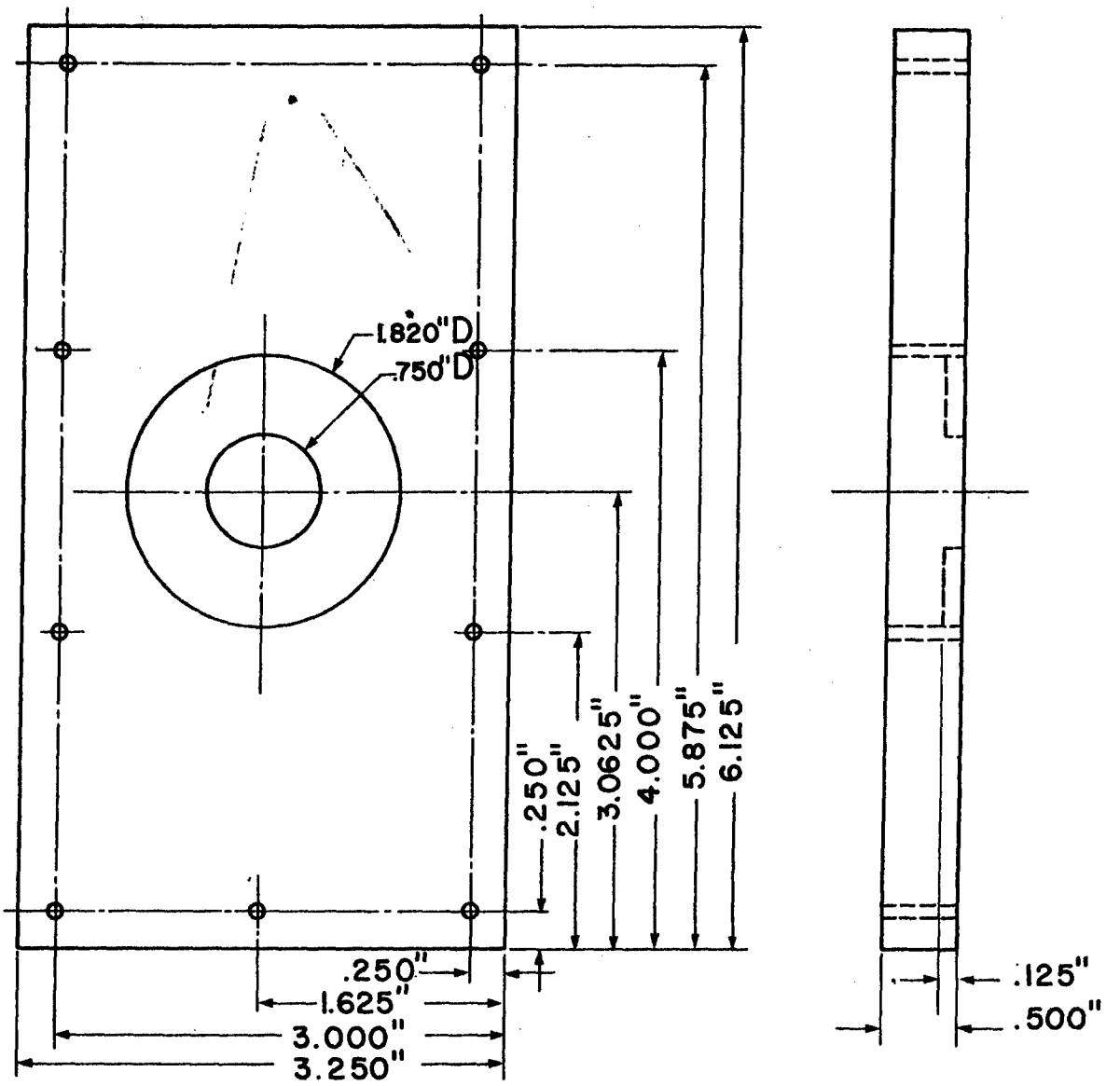


Figure 71. BAKELITE SOURCE POSITIONER

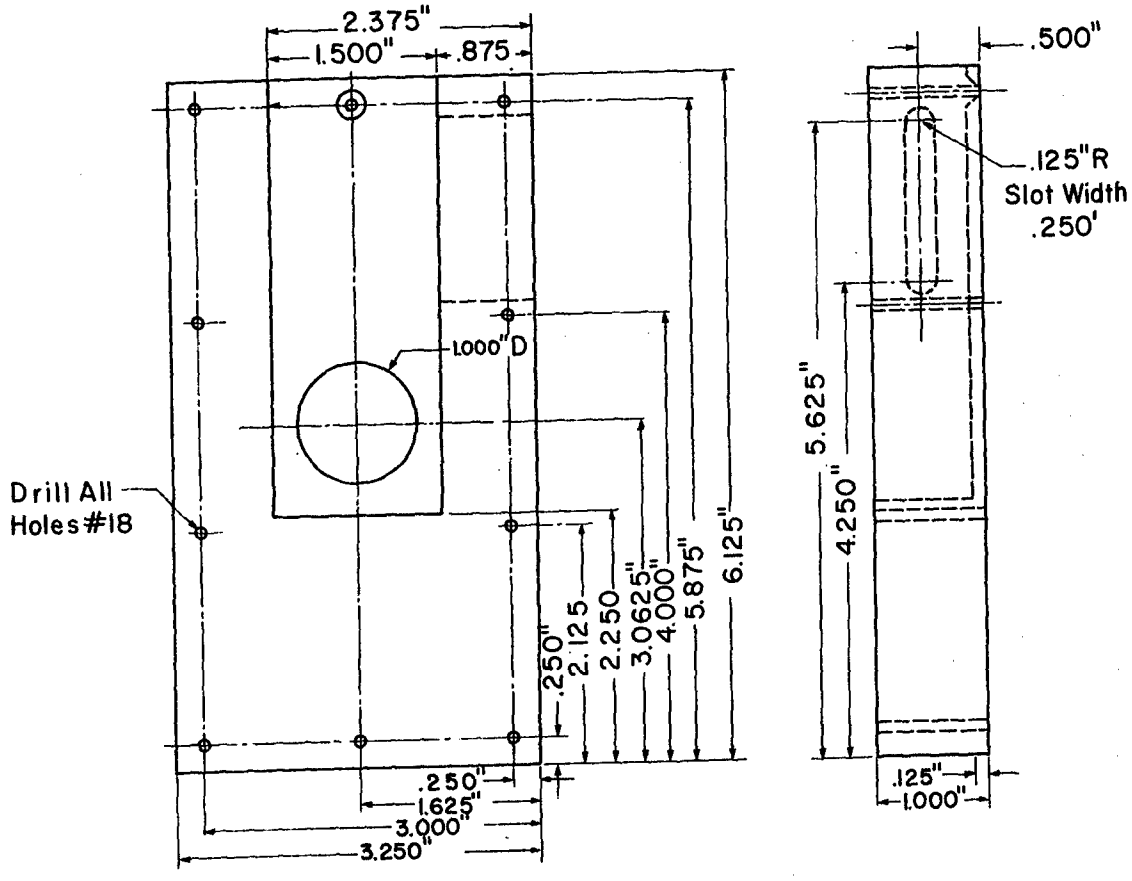


Figure 72. VIEWING CELL

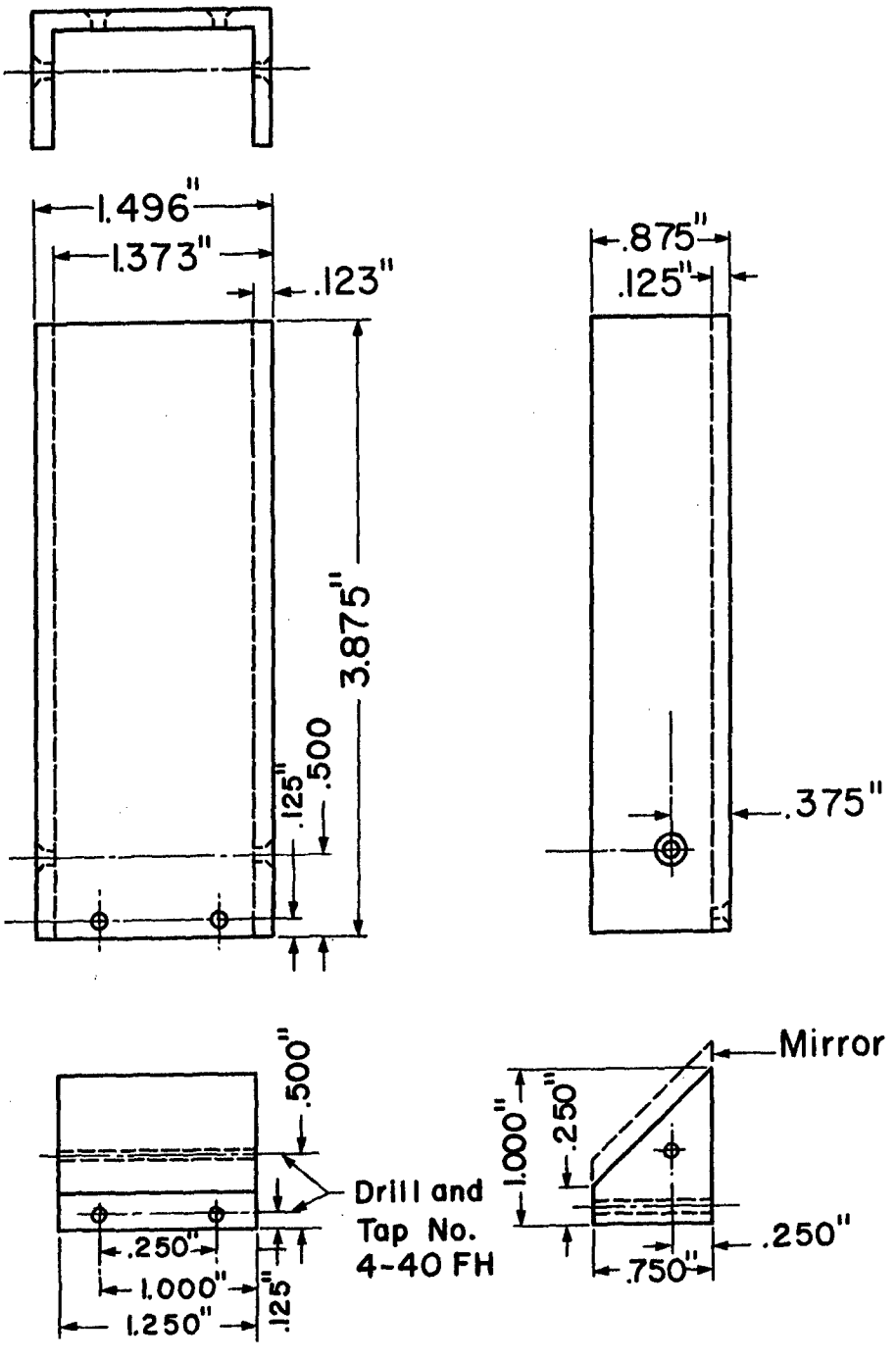


Figure 73. MIRROR SLIDE HOLDER

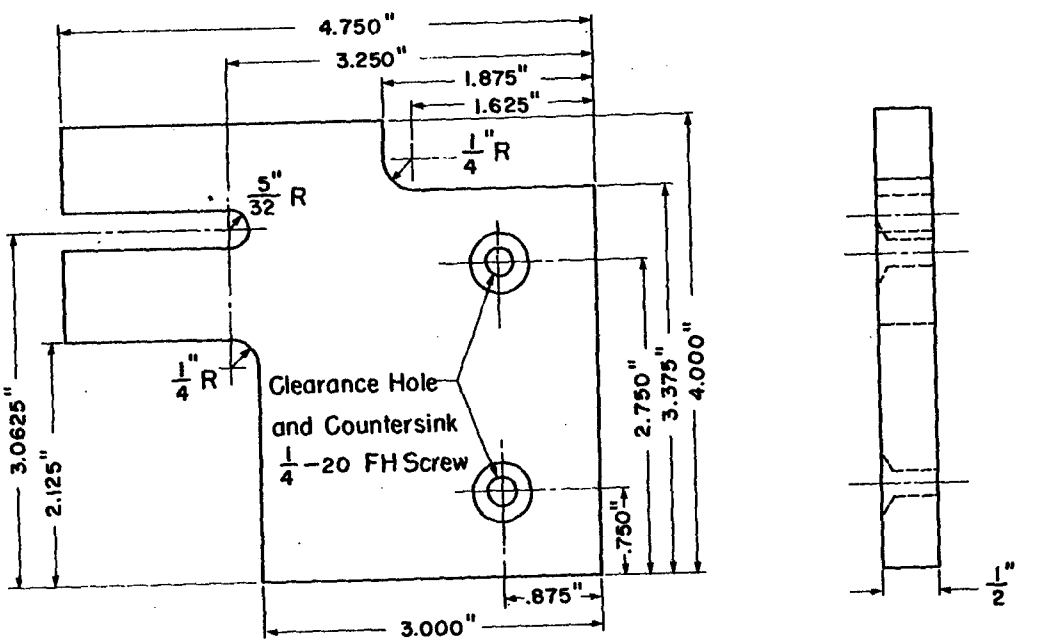


Figure 74. BAKELITE HOLLOW CATHODE SUPPORT

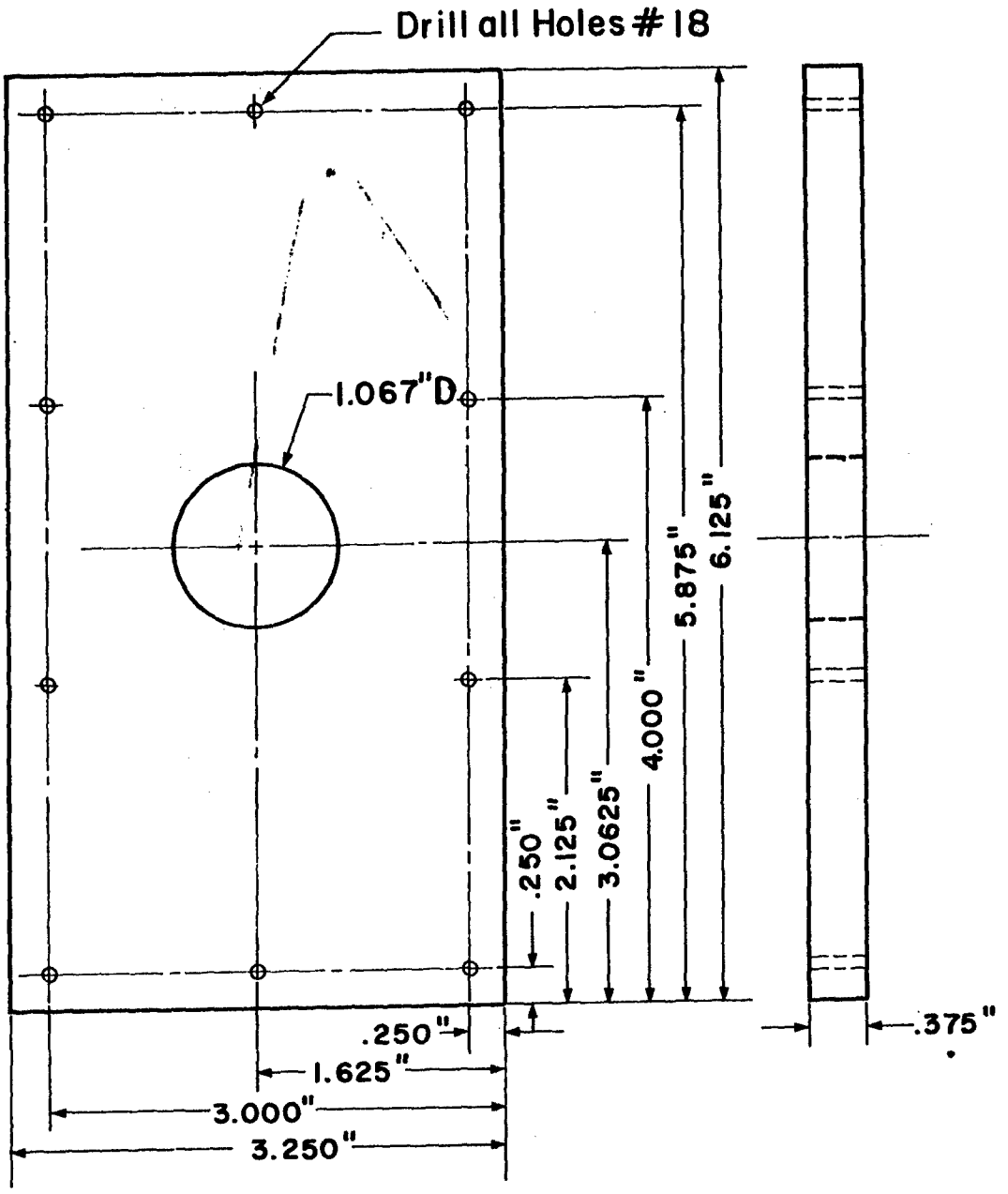


Figure 75. SPACER CELL

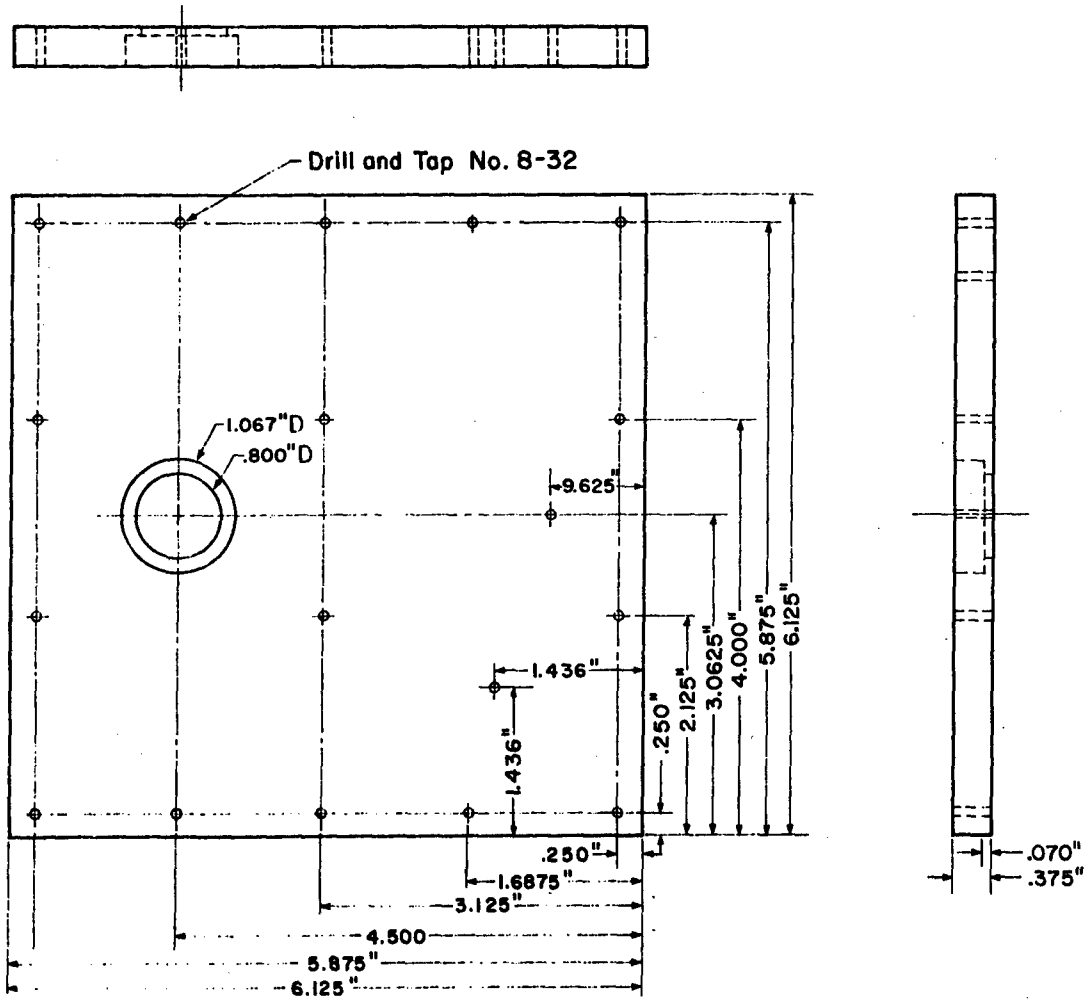


Figure 76. FRONT CHOPPER COVER

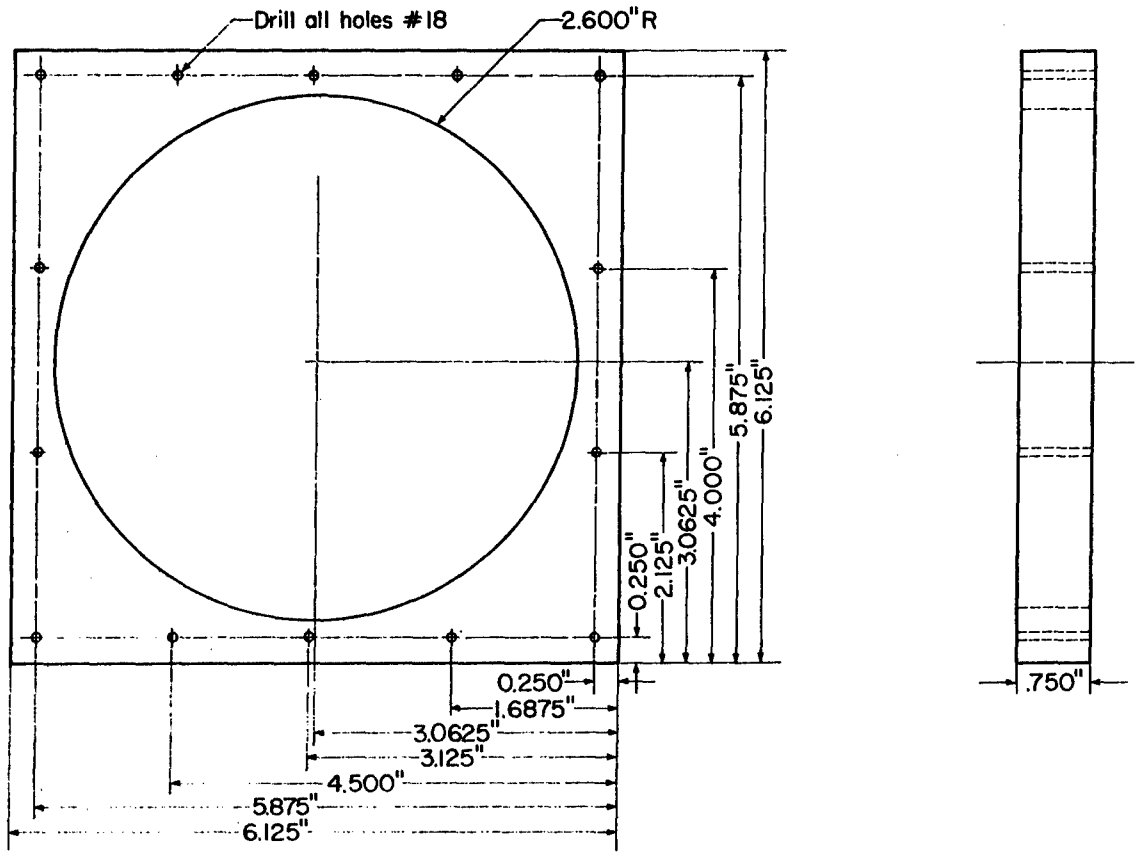


Figure 77. FILTER WHEEL - CHOPPER HOUSING

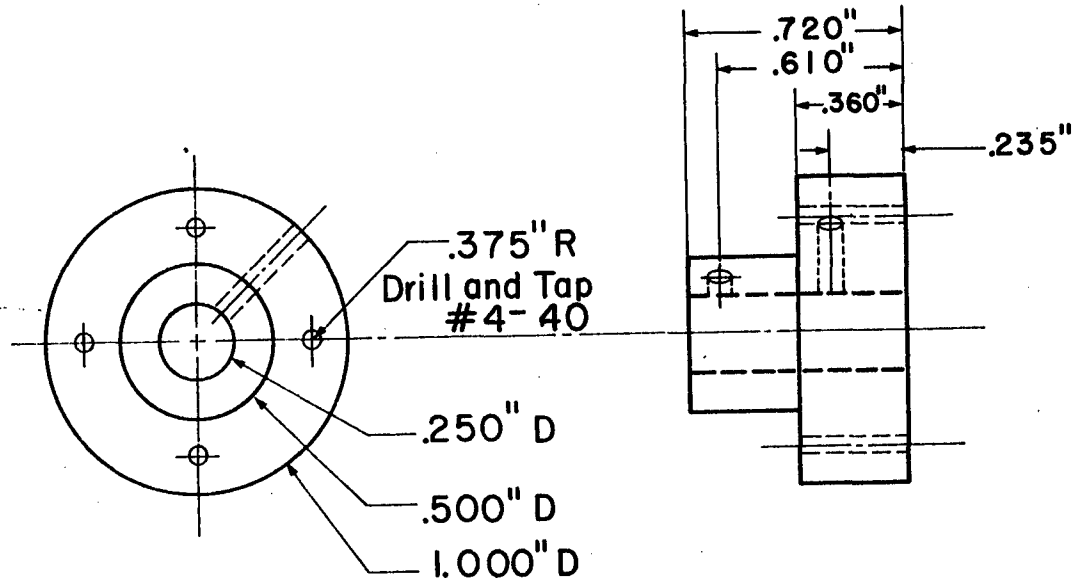


Figure 78. CHOPPER HUB

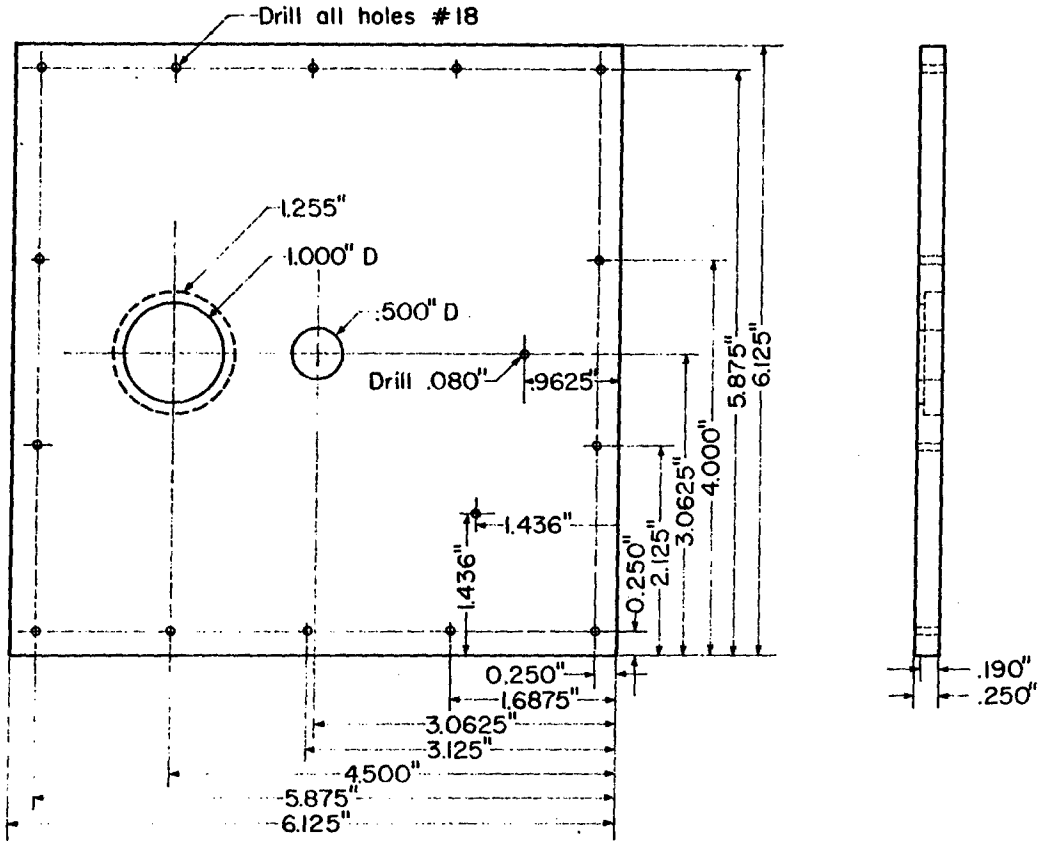


Figure 79. REAR CHOPPER COVER

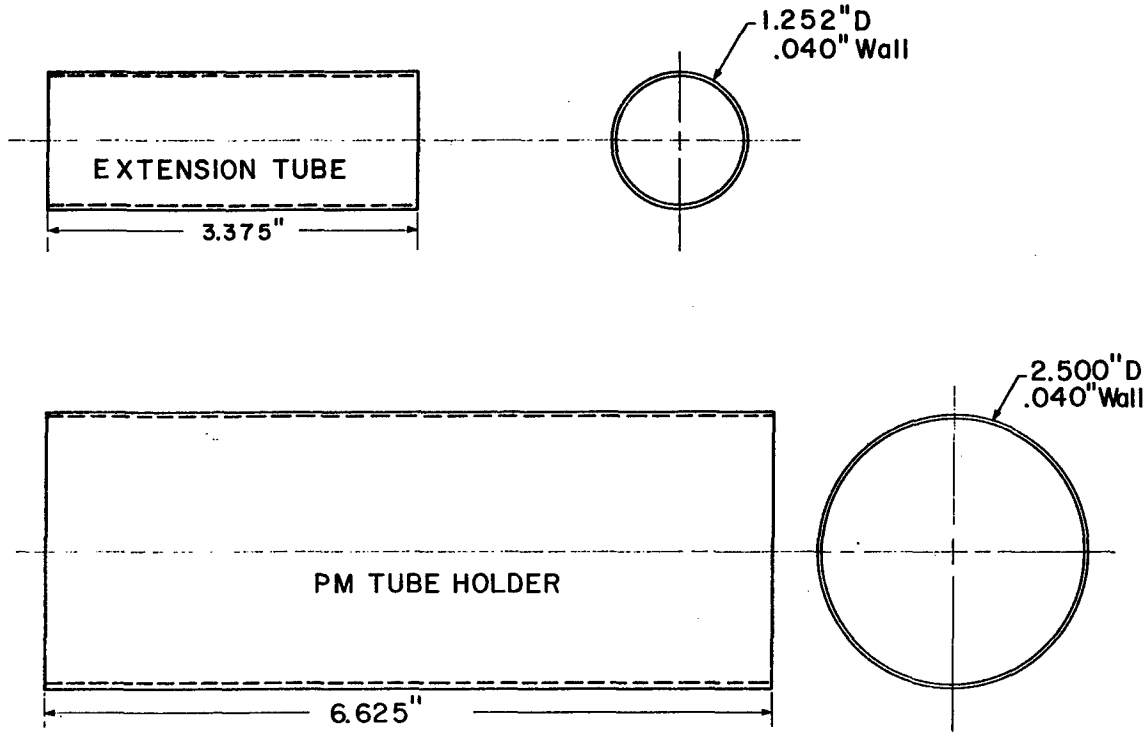


Figure 80. EXTENSION TUBE AND PM HOLDER

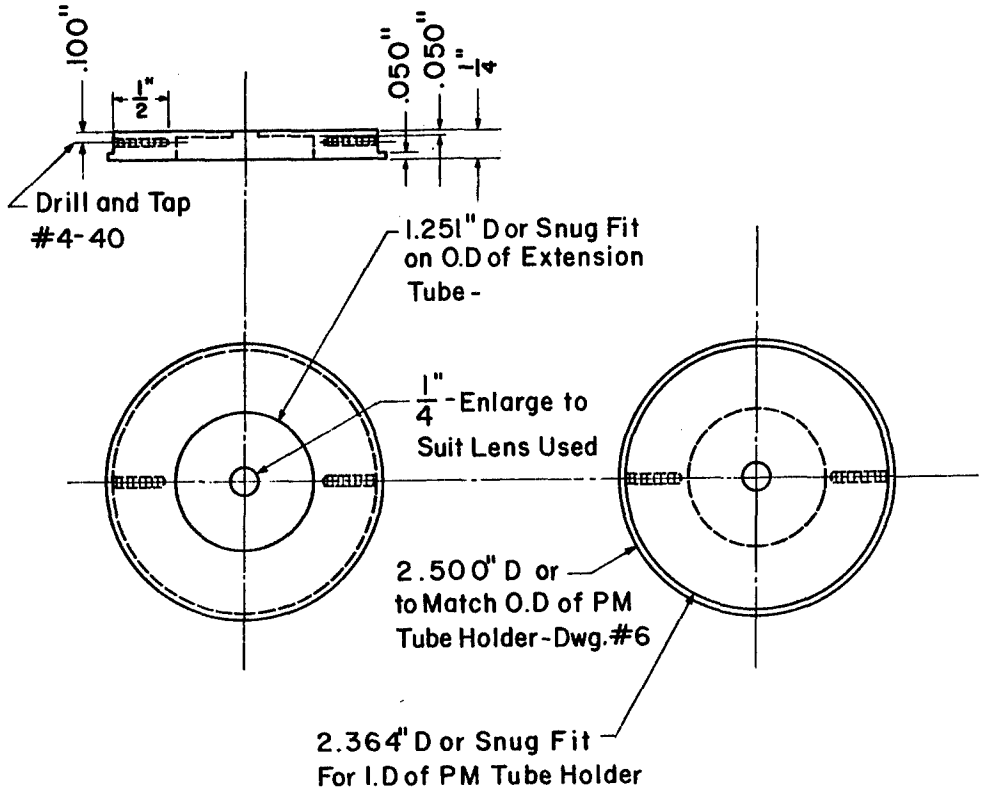


Figure 81. IMAGE MASK

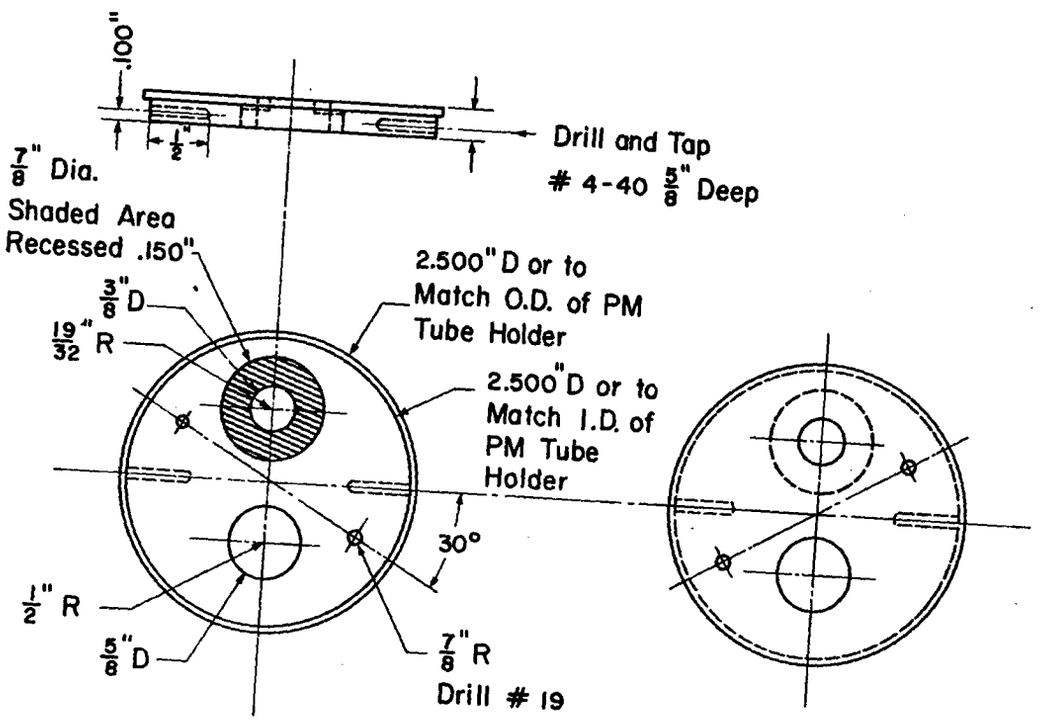


Figure 82. PM TUBE CAP

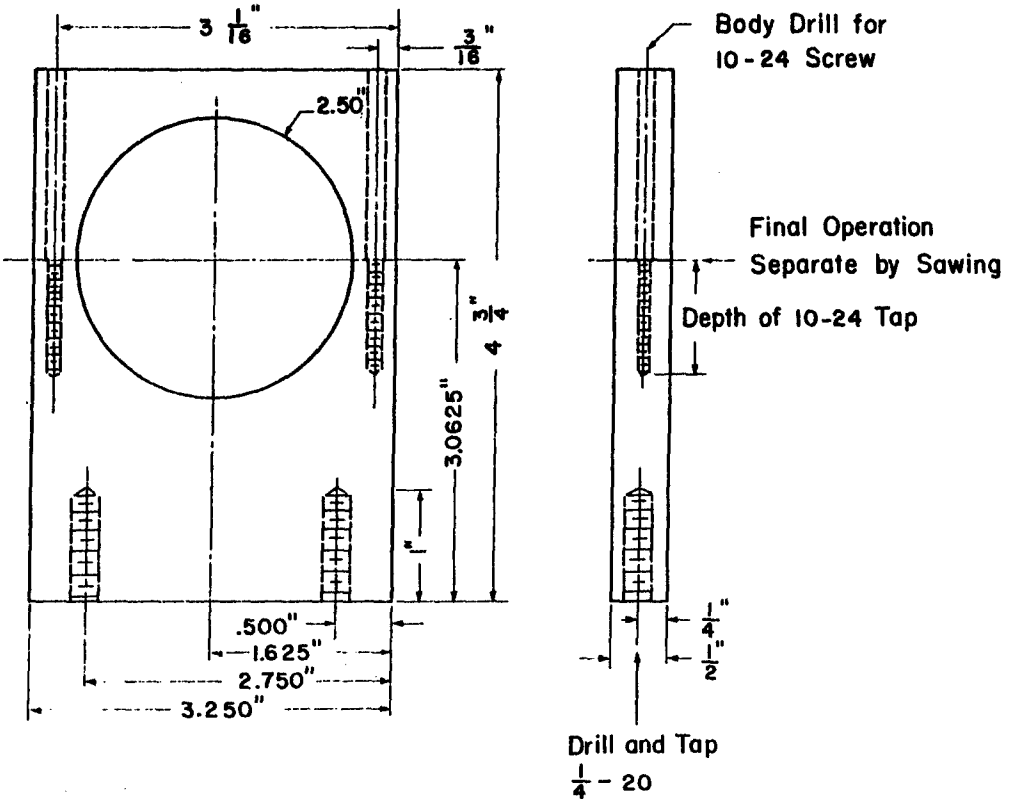


Figure 83. PM TUBE SUPPORT

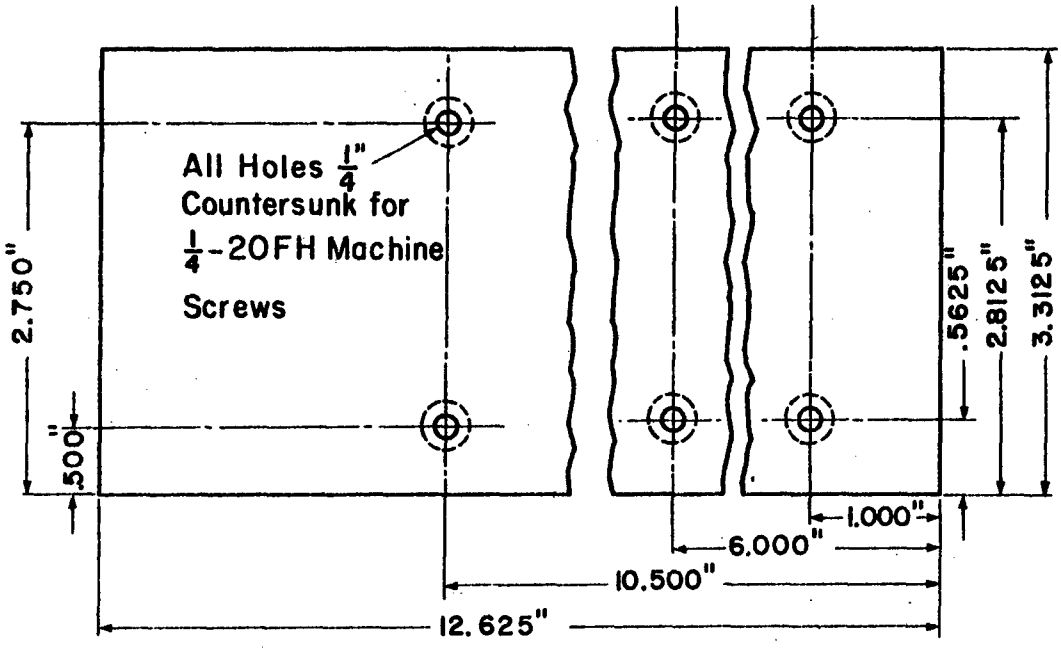


Figure 84. BASE FOR ASSEMBLY

## REFERENCES


1. G. Herzberg, Spectra of Diatomic Molecules, D. van Nostrand Co., Inc., Princeton, N.J., 1950.

2. R. W. B. Pearse and A. G. Gaydon, The Identification of Molecular Spectra, John Wiley & Sons, New York, C1962.

3. V. Raziunas, W. A. Loseke and E. L. Grove, "Application of the Stallwood Jet and d-c Arc to the Analysis of Air Contamination in Inert Gases," Appl. Spectry., 20, 395 (1966).

4. E. L. Grove, V. Raziunas and W. A. Loseke, "Spectrographic Monitoring of Inert-Gas Shields for Atmospheric Contaminants," Welding Journal, 29, 282 (1964).

5. E. L. Grove, Technical Summary Report, Jan. 1966, IITRI-U6010-18, Design, Development and Fabrication of a Portable Spectrometer-Type Monitor, Contract NAS8-11723, George C. Marshall Space Flight Center, NASA-Huntsville.

6. G. K. Werner, D. D. Smith, S. J. Ovenshine, O. B. Rudolph and J. R. McNally, "Further Investigations in the Spectro-Isotopic Assay Technique for Lithium," J. Opt. Soc. Am., 45, 202 (1955).

7. R. S. Braman, Interim Technical Report, IITRI-U6042-1, Application of Hollow Cathode and Microwave-Stimulated Emission Techniques to Detection, Contract No. DA-44-009-AMC-1576(T), U.S. Army Engineering Research and Development Laboratories.

8. Contract No. NAS5-11501, "Investigation of Hollow-Cathode Excitation Source for Water Vapor Measurements," Goddard Space Flight Center.

9. D. H. Arroe and J. E. Mach, "Hollow Cathode Source Design for High Resolution Spectroscopic Studies with Small Samples," J. Opt. Soc. Am., 40, 386 (1950).

Security Classification

**DOCUMENT CONTROL DATA - R & D**

*(Security classification of title, body of abstract and indexing annotation must be entered when the overall report is classified)*

| 1. ORIGINATING ACTIVITY (Corporate author) | 2a. REPORT SECURITY CLASSIFICATION |
|---|---|
| IIT Research Institute<br>10 West 35th Street<br>Chicago, Illinois 60616 | UNCLASSIFIED<br>2b. GROUP<br>N/A |

3. REPORT TITLE

DEVELOPMENT OF A LABORATORY MODEL GAS ANALYZER USING EMISSION TECHNIQUES

4. DESCRIPTIVE NOTES (Type of report and inclusive dates)

Final Report, 1 November 1965-25 August 1967

5. AUTHOR(S) (First name, middle initial, last name)

Ewart L. Grove

| 6. REPORT DATE | 7a. TOTAL NO. OF PAGES | 7b. NO. OF REFS |
|---|---|---|
| April 1969 | 133 | 9 |

| 8a. CONTRACT OR GRANT NO. | 9a. ORIGINATOR'S REPORT NUMBER(S) |
|---|---|
| AF 33(615)-3271 | |
| b. PROJECT NO. 6373 | IITRI-U6033-20 |
| c. Task No. 637302 | 9b. OTHER REPORT NO(S) (Any other numbers that may be assigned this report) |
| d. Work Unit No. 637302023 | AMRL-TR-68-130 |

10. DISTRIBUTION STATEMENT

This document has been approved for public release and sale; its distribution is unlimited.

| 11. SUPPLEMENTARY NOTES | 12. SPONSORING MILITARY ACTIVITY |
|---|---|
| | Aerospace Medical Research Laboratory, Aerospace Medical Div., Air Force Systems Command, Wright-Patterson AFB, OH 45433 |

13. ABSTRACT An instrument using emission spectroscopic techniques was designed and developed for monitoring the major components in air-type atmospheres. The essential components consist of a hollow cathode excitation source, four interference filters mounted in a filter wheel, a single photomultiplier tube and an electronic circuit, controlled by switching diodes and a gating circuit to record the response for each gas on individual meters. Hollow cathode was selected because of the spectral brightness of high energy species, lack of low energy species associated with positive column discharge and low power requirements. Aluminum cathodes rapidly lost sensitivity and did not excite the 2883 A and the 2896 CO2(+) bands. Gold, which does not form the oxide, was satisfactory as a cathode lining. The region from about 2900 to 6000 A was very dense with overlapping bands, any selected wavelength was masked. The lines selected were hydrogen 6562.8 A, oxygen 8446.4 A, nitrogen 8216.5 A, and carbon for carbon dioxide 9094 A lines. The influence of power, pressure and other gases were studied. Satisfactory responses were obtained in the 2-watt range. Wide concentrations of gases such as oxygen and nitrogen have little influence on each other. However, gases with wide differences in excitation potentials such as helium and oxygen do influence the spectral response of each other. The helium emission is suppressed, but to a much lesser degree than for thermal modes of excitation. In helium the line intensities of oxygen and hydrogen increased as the concentration of these gases decreased, but the intensity of helium lines increased with increasing concentration. Other gases were studied.

**DD FORM 1 NOV 65 1473**

Security Classification

| 14. KEY WORDS | LINK A | | LINK B | | LINK C | |
|---|---|---|---|---|---|---|
| | ROLE | WT | ROLE | WT | ROLE | WT |
| Emission spectroscopy | | | | | | |
| Hollow cathode excitation | | | | | | |
| Excitation | | | | | | |
| Interference filters | | | | | | |
| Spectral intensity | | | | | | |
| Negative and cathode glow | | | | | | |